The Dissertation Committee for Pornpun Vivithanaporn Certifies that this is the approved version of the following dissertation:

CELLULAR MECHANISMS THAT MODULATE KAINATE RECEPTOR TRAFFICKING AND ASSEMBLY

Committee:

Geoffrey T. Swanson, Supervisor

Lisa A. Elferink

John Marshall

Kenneth M. Johnson

Xiaodong Cheng

Dean, Graduate School

CELLULAR MECHANISMS THAT MODULATE KAINATE RECEPTOR TRAFFICKING AND ASSEMBLY

by

Pornpun Vivithanaporn, B.Sc.

Dissertation

Presented to the Faculty of the Graduate School of Biomedical Sciences

The University of Texas Medical Branch

in Partial Fulfillment

of the Requirements

for the Degree of

Doctor of Philosophy

The University of Texas Medical Branch

June, 2007

Acknowledgements

I want to express my utmost gratitude to my mentor, Dr. Geoffrey Swanson for his wonderful mentoring, patience and continuous support. During my five years in his lab, I had chances to explore many aspects of research in protein trafficking. Under his considerable guidance, I developed my skills not only in scientific knowledge but also presentation and writing skills. I wish one day I can be as good a mentor and successful scientist as him. I would like to thank all my committee members: Dr. Kenneth Johnson, Dr. Xiaodong Cheng, Dr. Lisa Elferink and Dr. John Marshall for their insightful comments and advices throughout my dissertation project.

I would like to recognize help from all past and present members of the Swanson laboratory. In particular, I thank Dr. Sheng Yan who taught me basic experimental techniques when I started as a rotation student and his preliminary work on kainate receptors interactions with 14-3-3 proteins. I am grateful to Dr. James Sanders and Leanne Lash, who provided friendship, thoughtful comments, and support with my research. I thank Helene Lyons-Swanson for her technical assistance.

This research was supported by a Young Investigators Award from the National Alliance for Research on Schizophrenia and Depression and National Institute of Mental Health Grant R03 MH65289 to Dr. Geoffrey Swanson. I would like to acknowledge Dr. Leoncio Vergara, Dr. Teng-Leong Chew and Paul Cheresh for their technical support in confocal microscopy.

I would like to express my appreciation to my family. All of my success is a result of my parent's encouragement, understanding and their believing in me. Lastly, I would like to thank all my friends in Galveston and Chicago, who made me personal life enjoyable through out my five years in Graduate school.

CELLULAR MECHANISMS THAT MODULATE KAINATE RECEPTOR TRAFFICKING AND ASSEMBLY

Publication No._____

Pornpun Vivithanaporn, Ph.D.

The University of Texas Medical Branch, 2007

Supervisor: Geoffrey T. Swanson

Kainate receptors (KARs) in the mammalian brain play a variety of physiological roles that require selective assembly, intracellular trafficking, and synaptic targeting. Cytoplasmic and non-cytoplasmic determinants that modulate KAR expression at the plasma membrane have been recently characterized. The intracellular trafficking determinants are presumed to bind to chaperone proteins, but these proteins have not been identified for any KAR subunit. Here we identified two chaperone proteins that associated with the carboxy terminus but differently regulated the localization of KA2 receptors. We found that coatomer protein complex I (COPI) subunits interacted with KA2 subunits at the arginine-based ER retention/retrieval motif and these associations were decreased in heteromeric GluR6a/KA2 receptors. Disruptions of COPI and KA2 associations by alanine mutations at the arginine-rich domain and elimination of COPI vesicles were correlated with the increased expression at the plasma membrane of KA2 receptors, indicating that COPI proteins regulated the ER localization of receptors. KA2 receptors also co-precipitated with three isoforms of 14-3-3 proteins; only the KA2 and 14-3-3γ association was correlated with higher plasma membrane expression of receptors. In addition to identifying cytoplasmic chaperone systems, we were interested in understanding the nature of a recently described trafficking checkpoint in non-cytoplasmic regions. Mutations in domains typically involved in glutamate binding and ion permeation disrupt expression of KARs at the plasma membrane. A conformational change of receptors after glutamate binding is proposed to permit egress of KARs from the ER. We mutated critical amino acid residues in the extracellular linker domain of GluR6a subunits and found that desensitization rates were only weakly correlated with

plasma membrane expression levels. Alteration of these residues impaired other stages of receptor biosyntheis including assembly and degradation of mutated receptors. We found that mutations at the transduction linker collectively altered subunit assembly, degradation, desensitization and a post-assembly stage. Our characterizations of chaperone proteins and mechanisms that regulate intracellular trafficking provide a better understanding of cellular controls in the early stages of KAR biosynthesis.

Table of Contents

List of Tables

List of Figures

List of Abbreviations

AMPA	α-amino-3-hydroxy-5-methyl-4-isoxazolepropionic acid
ANOVA	a one-way analysis of variance
BiP	binding protein
CHO	Chinese hamster ovary
CNS	central nervous system
COPI	coatomer protein complex I
CTD	carboxy terminal domain
DMEM	Dulbecco's modified Eagle's medium
eGFP	enhanced green fluorescent protein
EGTA	ethyleneglycol bis(2-aminoethyl ether)-N,N,N'N'-tetraacetic acid
ELISA	Enzyme-linked immunosorbent assay
EPSC	excitatory postsynaptic current
ER	endoplasmic reticulum
ERAD	ER-associated degradation
GABA	gamma-aminobutyric acid
GFP	green fluorescent protein
GluR	glutamate receptor
HEK	human embryonic kidney
HEPES	4-(2-hydroxyethyl)-1-piperazineethanesulfonic acid
HRP	Horseradish peroxidase
iGluR	ionotropic glutamate receptor
IB	immunoblot
IP	immunoprecipitate
IPSC	inhibitory postsynaptic current
KA	kainate
KAR	kainate receptor
K_D	dissociation constant

LBD	ligand binding domain
LTP	long-term potentiation
mGluR	metabotropic glutamate receptor
MHC	major histocompatibility
mRNA	messenger RNA
NMDA	N-methyl-d-aspartate
NTD	amino terminal domain
PAGE	polyacrylamide gel electrophoresis
PBS	phosphate-buffered saline
PC	preclear
PDZ	postsynaptic density 95/disc large/zonula occludens-1
PSD	postsynaptic density
SAP	synapse associated proteins
SDS	sodium dodecyl sulfate
VSVG	vesicular stomatitis virus glycoprotein
WB	Western blot

CHAPTER 1: INTRODUCTION

1.1 SPECIFIC AIMS

Kainate receptors (KARs), a subfamily of ionotropic glutamate receptors (iGluRs), participate in excitatory synaptic transmission and may be involved in the pathogenesis of neurological diseases. A variety of subunit compositions of KARs are found in different types of neurons and are targeted to specific synaptic sites. Subcellular localization and targeting of receptors is controlled by diverse sequences in each KAR subunit that act as sites for chaperone protein associations or post-translational modifications. Several discrete cytoplasmic determinants of KAR localization recently have been characterized, but the chaperone proteins that regulate KAR trafficking are unknown. Non-cytoplasmic domains of KAR subunits also have a role in receptor trafficking; they appear to be engaged at a checkpoint for receptor export out of the endoplasmic reticulum (ER), in addition to their roles in the agonist binding, receptor gating, and subunit assembly. However, the mechanism underlying this quality-control process is not understood. Our studies will elucidate intracellular mechanisms responsible for trafficking of two distinct KAR subunits that exhibit either retention in the ER (KA2) or robust plasma membrane expression (GluR6a). An understanding of the cellular mechanisms that control the biosynthesis of KARs will facilitate construction of a model describing the regulation of biosynthesis, trafficking and targeting, which are important determinants of KAR function at both excitatory and inhibitory synapses.

Specific aim 1: Determine chaperone systems involved in KA2 receptor trafficking

KA2 subunits are efficiently retained in the ER when expressed alone, and this retention results from the presence of an arginine-rich sequence in the cytoplasmic tail of the subunit protein. The cellular chaperones that interact with these sequences are unknown. We theorize that the coatomer complex I (COPI) chaperone system, a prominent

retention/retrieval mechanism, acts as a retrograde pathway for ER retention of KA2 receptors, whereas 14-3-3 proteins may promote cell surface expression. COPI and 14-3-3 proteins were shown recently to control surface expression of several receptors and ion channels in a competitive fashion. I will test the protein-protein interactions of KA2 receptors with COPI and 14-3-3 proteins, and identify their binding sites in the KA2 subunit. The role of COPI and 14-3-3 proteins in the modulation of KA2 trafficking will be determined by correlation between the degree of interactions and the surface expression level of receptors.

Specific aim 2: Determine the role of the M3-S2 transduction linker in GluR6a receptor biosynthesis.

Homomeric GluR6a KARs express highly at the plasma membrane. Mutations in domains that control receptor function, such as gating and ligand-binding domains, cause GluR6a receptors to be sequestered in the ER. These observations have led to the hypothesis that a functional checkpoint exists for ER egress and this checkpoint is analogous structurally to the glutamate-bound desensitized state. Desensitization is a well-characterized biophysical phenomenon in iGluRs with a distinct receptor conformation from that associated with activated and unliganded states. The proposed correlation between desensitization and trafficking from the ER is based on relatively limited number of altered receptors. We aim to elucidate the role of a critical linker domain, which likely transduces binding energy into channel gating in the early quality control step of GluR6a receptor trafficking and assembly. We will generate mutants of GluR6a receptors that have various desensitization rates and measure the plasma membrane expression of these mutants to determine if a correlation exists between the rate of desensitization and receptor trafficking. Furthermore, we will determine if altered trafficking is accompanied with other changes in receptor biosynthesis.

1.2 GLUTAMATE RECEPTORS

Glutamate is the predominant excitatory amino acid in the central nervous system (CNS). Glutamate receptors are subdivided into ionotropic and metabotropic receptors based on their structure and mechanism of action. IGluRs are ligand-activated cation channels, which mediate the majority of fast excitatory synaptic transmission. IGluRs are divided into three subtypes according to their sequence homology and pharmacology. These receptors are named after the agonists that activate them: N-methyl-D-aspartate (NMDA), α-amino-3-hydroxy-5-methyl-4-isoxazole propionic acid (AMPA), and kainate receptors (Dingledine et al., 1999; Mayer and Armstrong, 2004). These three types of iGluRs appear to serve different functions in the CNS, with the roles played by KARs being only recently characterized (Lerma, 2003).

In contrast, metabotropic glutamate receptors (mGluRs) provide modulation of synaptic transmission in synapses of the CNS by regulating glutamate and gamma-aminobutyric acid (GABA) release through G-protein coupled signaling pathways. MGluRs are separated into three groups based on their sequence similarity, signal transduction mechanism, and selective agonists. Group I mGluRs, including mGluR1 and mGluR5, activate phospholipase C and phosphoinositide hydrolysis, which subsequently stimulates the release of calcium ion from the ER and the accumulation of cyclic AMP. Group II (mGluR2-3) and Group III (mGluR4, 6-8) inhibit adenylate cyclase and cyclic AMP formation, but are activated by different selective agonists. In addition, mGluRs can couple directly to cation channels, including potassium and calcium channels (Conn and Pin, 1997; Hermans and Challiss, 2001).

1.3 IONOTROPIC GLUTAMATE RECEPTOR TOPOLOGY

IGluRs are composed of four individual subunits that form a cation-selective ion channel differentially permeable to sodium (Na^+), potassium (K^+), calcium (Ca^{2+}) and magnesium (Mg^{2+}) ions. Each subunit of iGluRs can be thought of as a modular protein with at least

four distinct domains based on the sequence region and function (Figure 1.1). The extracellular amino-terminal domain (NTD, in green) of iGluR subunits plays a role in tetrameric receptor assembly and modulation of channel gating in NMDA receptors. The ligand-binding domain (LBD, in red) is composed of two discontinuous extracellular sequences (denoted S1 and S2) separated by the membrane domain. The tertiary structure of S1 and S2 regions forms a clamshell-like structure and is linked to the NTD and the ion channel pore by short linker domains. Agonists such as glutamate (Glu, in yellow) bind to the LBD at the cleft between two lobes. The LBD of iGluRs participates in many functions that include ligand binding, receptor oligomerization, and control of channel gating. The membrane (M, in blue) domain consists of three transmembrane segments (M1, M3, and M4) and a re-entrant pore loop (M2). The membrane domain forms the ion channel pore and determines the ion selectivity and gating properties of receptors. RNA editing of glutamine (Q) to arginine (R) codons in the pore loop region of some AMPA and kainate receptors changes ion selectivity of the channel proteins from Ca^{2+} permeable to Ca^{2+} impermeable. Finally, the carboxy-terminal domain (CTD) of iGluRs is intracellular and contains trafficking motifs, which interact with various chaperone proteins to regulate receptor trafficking and targeting, and sites of modulation by second messenger systems (Schoepfer et al., 1994; Madden, 2002; Bredt and Nicoll, 2003; Mayer and Armstrong, 2004).

1.4 KAINATE RECEPTOR FAMILY

Kainate receptors are a subtype of iGluRs. The sequence similarities of KARs to AMPA and NMDA receptors are 40% and 20%, respectively (Dingledine et al., 1999). There are five different gene products in the KAR family, which is subdivided into two groups based on sequence homology and affinity for the marine toxin kainate (Figure 1.2). KARs can be formed both homomeric and heteromeric assemblies of subunits. GluR5, -6 and -7 subunits have a relatively lower affinity for kainate, with dissociation constant (K_D) values in the range of 50-100 nM, and can assemble to form functional homomeric

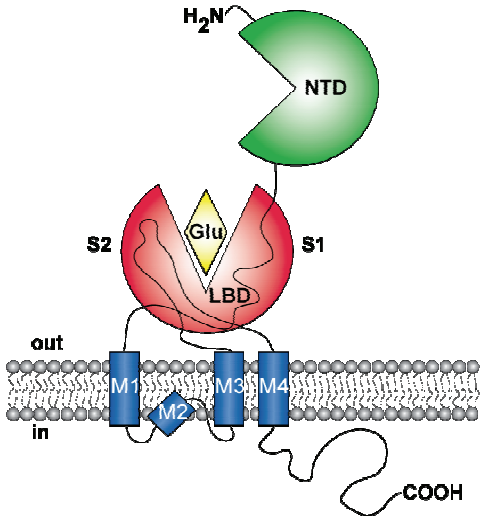

Figure 1.1: Illustration of domain structures in an ionotropic glutamate receptor subunit.
See text for details.

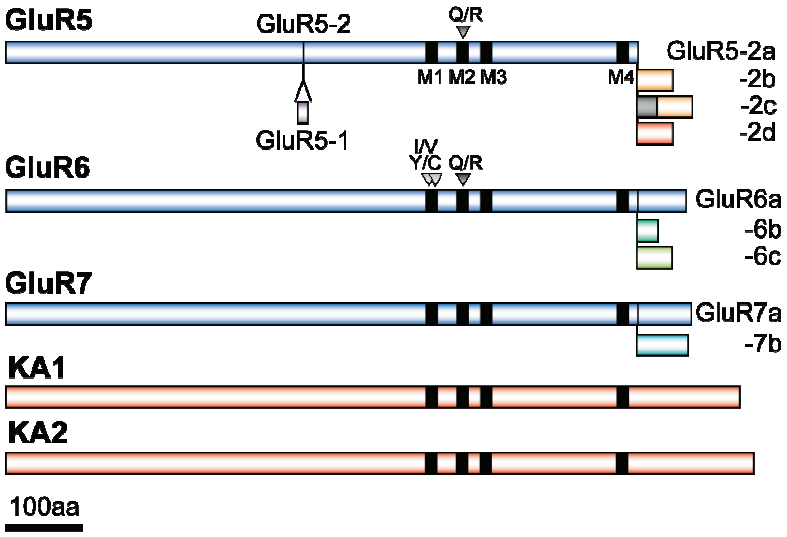

Figure 1.2: Schematic representation of kainate receptor subunit sequences and their mRNA splice variants.
Kainate receptors consist of GluR5-7 and KA1-2 subunits. The scale of illustrations is relative to the primary amino acid sequence. The black bars represent the four membrane domains, triangles indicate RNA editing sites, and alternate splice isoforms are as indicated.

receptors (Egebjerg et al., 1991; Bettler et al., 1992; Sommer et al., 1992). Q/R (glutamine/arginine) site editing of GluR5 and GluR6 subunit mRNAs changes the calcium ion permeation, the current-voltage relationship and the single channel properties (Dingledine et al., 1999). Two additional mRNA editing sites, I/V (isoleucine/valine) and Y/C (tyrosine/cysteine), in the first transmembrane domain of GluR6 subunits slightly affect the calcium ion permeability (Kohler et al., 1993). In addition, GluR5-7 subunit mRNAs undergo alternate splicing at both N-terminal and C-terminal ends, resulting in several splice variants. GluR5-7 subunits can co-assemble with other subunits and other isoforms to form heteromeric receptors with diverse functional properties (Schiffer et al., 1997; Cui and Mayer, 1999; Paternain et al., 2000). The KA1 and KA2 subunits have a higher affinity for kainate, with K_D values of 5-15 nM (Werner et al., 1991; Herb et al., 1992). Transfected cells expressing homomeric KA1 and KA2 receptors do not exhibit currents; however, heteromeric receptors between these two subgroups of KARs, such as GluR6a/KA2 receptors, can be activated by agonists and exhibit distinct functional properties compared to homomeric KARs (Herb et al., 1992). The heteromeric assembly and alternate splicing of KAR mRNA create a variety of subunit compositions and diverse functional properties of KARs (Lerma, 2003).

In the CNS, KAR mRNAs are highly expressed in nearly every type of neuron in the CNS, including in the hippocampus, amygdala, cerebellum, and dorsal root ganglia. KARs are expressed at both presynaptic and postsynaptic membranes and have distinct subunit compositions at different synapses (Huettner, 2003). Postsynaptic KARs contribute to excitatory postsynaptic currents (EPSCs) only in a subset of glutamatergic synapses. These include CA1 interneurons and CA3 pyramidal neurons in the hippocampus (Castillo et al., 1997; Cossart et al., 1998), Purkinje cells in the cerebellum (Renard et al., 1995), Off bipolar cells in the retina (DeVries and Schwartz, 1999), and interneurons and pyramidal cells in the amygdala (Braga et al., 2004). The KAR-mediated EPSC has slower rise and decay times than AMPA-mediated EPSCs, and contribute to a lesser degree to the mossy fiber EPSC than AMPA receptors (Castillo et

al., 1997). KARs on presynaptic membranes mediate both excitatory and inhibitory synapses by inhibiting the evoked release of glutamate and GABA, respectively (Chittajallu et al., 1996; Clarke et al., 1997; Rodriguez-Moreno et al., 1997). In addition, presynaptic KARs act as facilitatory autoreceptors (Contractor et al., 2001; Schmitz et al., 2001). Recently, KARs were reported to control neuronal excitability through G-protein coupled receptors (Rozas et al., 2003; Melyan et al., 2004). In the past decade, the development of various generations of selective KAR agonists and antagonists, KAR specific antibodies, and KAR knockout mice have revealed several physiological roles for KARs in fast synaptic transmission, modulation of presynaptic transmission, and potential involvement in diseases such as epilepsy, ischemia, pain, and migraine (Huettner, 2003; Lerma, 2003).

1.5 FUNCTIONAL PROPERTIES AND STRUCTURE OF KAINATE RECEPTORS

Glutamate binding to iGluRs leads to channel opening (gating) and cation permeation. Activation of KARs and other iGluRs is terminated either by unbinding of agonist, known as *deactivation*, or by inactivation of receptors in the continued presence of agonists, known as *desensitization*. Glutamate-evoked KAR currents desensitize rapidly and nearly completely on a millisecond time scale, and the rate of desensitization varies with the receptor subunit composition. After removal of agonists, the recovery from the desensitized state of kainate receptors is relatively slow compared to AMPA receptors and occurs over a seconds time scale. Desensitization of KARs can be attenuated by the lectin concanavalin A, which interacts with several N-linked oligosaccharides (Dingledine et al., 1999; Lerma et al., 2001). Desensitization of iGluRs occludes ion fluxes through receptors and thereby inactivates receptor function. As a result, desensitization is thought to play a role in the regulation of shape, amplitude, duration, and frequency of receptor currents at some, but not all synapses (Jones and Westbrook, 1996).

Crystallization of the GluR2 AMPA ligand-binding core with kainate showed that the S1 and S2 primary sequences of the LBD form two lobular domains called D1 and D2, which are connected by a "hinge" region and which are separated by a cleft. Kainate binds to the LBD within this cleft and interacts with several amino acid residues from both the D1 and D2 domains (Armstrong et al., 1998). Glutamate binding triggers a rotation of the domains around the central hinge region to enclose agonists in the cleft. The extent of cleft closure in AMPA and KA ligand-binding domain is correlated with ligand activity. Full agonists, such as glutamate, trigger more lobe rotation than partial agonists such as kainate, while antagonists stabilize the relatively "open" structure observed in the unliganded (*apo*) state of the ligand-binding core (Armstrong and Gouaux, 2000; Mayer et al., 2006). Further studies showed that ligand-binding cores of GluR2 subunits assemble as dimers. Point mutations that stabilize interactions across the dimer interface, or allosteric modulators, that have similar effect, block receptor desensitization; conversely, mutations that disrupt dimer interfaces promote desensitization of glutamate-evoked currents (Partin et al., 1996; Stern-Bach et al., 1998; Sun et al., 2002). Biochemical and functional studies, together with the crystallization of the LBD of AMPA and kainate receptors, led to structural models for the biophysical phenomena of activation and desensitization. Ligand binding energy from the cleft closure between D1 and D2 domains is transduced through the linker to the pore domain, resulting in the receptor activation and opening of the associated ion channels. The agonist-bound "closed" conformation is relatively unstable and consequently inter-subunit contacts are rearranged, resulting in a nonconducting state known as the desensitized conformation (Armstrong and Gouaux, 2000; Sun et al., 2002; Mayer and Armstrong, 2004).

1.6 KAINATE RECEPTOR TRAFFICKING: CYTOPLASMIC DETERMINANTS

The classically defined biosynthetic-secretory pathway of plasma membrane proteins, including kainate receptors, begin with translation and subunit assembly in the ER,

vesicular transport from the ER to the Golgi, transit through the Golgi stacks, and export out of the Golgi to the plasma membrane (Alberts et al., 2002). Homomeric receptors of GluR5-7 kainate subunits are expressed at the plasma membrane to varying degrees (Pinheiro and Mulle, 2006). Alternate splicing in the intracellular carboxy terminus of GluR5-7 mRNAs greatly affects the intracellular trafficking of these subunits (Figure 1.3). GluR5a and GluR5b receptors express at low levels at the plasma membrane of COS-7 cells and cultured hippocampal neurons, whereas GluR5c receptors with the insertion of 29 amino acids in C-termini exhibit no detectable receptors at the cell surface and are retained in the ER (Jaskolski et al., 2004). GluR6a and GluR7a receptors have distinct C-termini from GluR6b and GluR7b receptors, and are expressed on the plasma membrane to a greater degree than GluR6b and GluR7b receptors in COS-7 cells and cultured hippocampal neurons (Jaskolski et al., 2004; Jaskolski et al., 2005b). KA2 subunits are retained in the ER as homomeric receptors but can be present at the plasma membrane when co-assembled with GluR5-7 subunits in HEK293 and COS-7 cells (Herb et al., 1992; Ren et al., 2003a). The intracellular localization of KA1 receptors is unknown. The similarity of C-terminal sequences between KA1 and KA2 subunits suggests that homomeric KA1 receptors are probably localized in the ER (Figure 1.3).

Trafficking and targeting of iGluRs from biosynthesis to their site of action are controlled by trafficking motifs in the carboxy-terminal domain, which interact with various chaperone proteins (Collingridge et al., 2004). ER localization of GluR5b, GluR5c, GluR7b and KA2 receptors is mediated by arginine-based motifs (RXR) in the C-termini (Ren et al., 2003a; Ren et al., 2003b; Jaskolski et al., 2004; Jaskolski et al., 2005b). Similarly, arginine-based motifs have been identified as novel ER-retention signals in potassium channels (Zerangue et al., 1999), $GABA_B$ receptors (Margeta-Mitrovic et al., 2000) and NMDA receptors (Scott et al., 2001). Among others, KA2 receptors have an additional arginine-based ER retention signal in the first intracellular loop between membrane domain 1 and 2 (Nasu-Nishimura et al., 2006). On the other hand, GluR6a and GluR7a receptors express highly at the plasma membrane of COS-7 cells and cultured

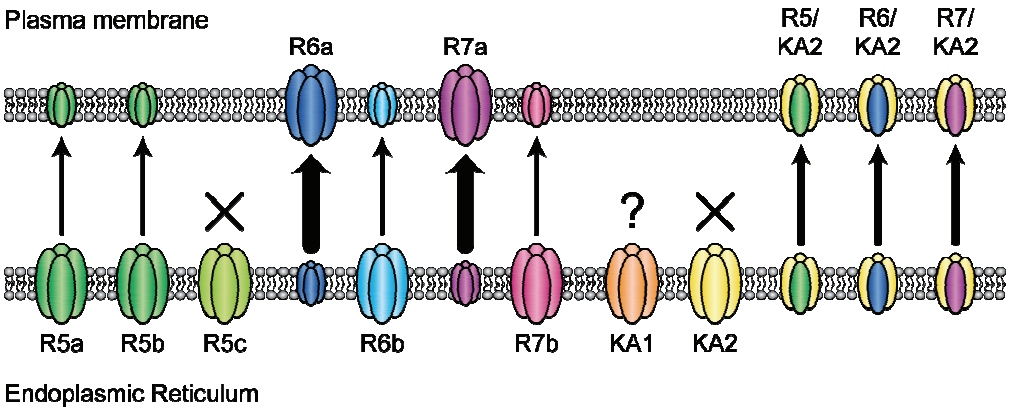

Figure 1.3: Intracellular trafficking and localization of kainate receptor subunits.
Homomeric kainate receptors are expressed at the cell surface in varying degrees. Heteromeric receptors of GluR5-7 with KA2 subunits transit to the cell surface. The scale of receptors and arrows is generally relative to the level of receptors present in each membrane. Adapted from Pinheiro and Mulle, *Cell Tissue Res*, 2006.

hippocampal neurons because they contain a forward trafficking motif, CQRRLKH, in the C-terminus (Yan et al., 2004; Jaskolski et al., 2005b).

The C-termini of some KAR subunits contain postsynaptic density 95/disc large/zonula occludens-1 (PDZ) binding sites. PDZ binding proteins are scaffolding and chaperone proteins and play a central role in localization of iGluRs at synapses and modulation of synaptic transmission (Kim and Sheng, 2004). GluR5, GluR6 and KA2 receptors interact directly with several PDZ binding proteins, including post-synaptic density (PSD)-95/ synapse associated protein 90 (SAP90), SAP97, SAP102, syntenin, protein interacting with C-kainase (PICK)-1 and glutamate receptor interacting protein (GRIP) (Garcia et al., 1998; Mehta et al., 2001; Hirbec et al., 2003). KARs show differential associations with PDZ binding proteins. For example, GluR6 subunits bound to the PDZ1 domain of SAP97 to a lesser degree than SAP90, whereas KA2 subunits bound to an Src homology

3 (SH3) domain of SAP97 with a higher affinity than SAP90 (Mehta et al., 2001). In addition, GluR6 receptors indirectly associate with cadherin/catenin adhesion protein complexes (Coussen et al., 2002). These chaperone proteins play a role in receptor targeting and clustering at the synapse and regulate KAR function. Interestingly, elimination of PDZ binding sites did not interfere with trafficking of GluR5 and GluR6 receptors to the plasma membrane (Ren et al., 2003b; Yan et al., 2004). Although several chaperone proteins interacting with C-termini have been identified, there is limited knowledge about chaperone proteins interacting with other KAR trafficking motifs, such as the CQRRLKH forward trafficking domain.

A large proportion of retrograde trafficking of misfolded or unassembled proteins and ER-resident proteins from the *cis*-Golgi back to the ER is mainly mediated by vesicles coated with coatomer protein complex I (COPI) chaperone proteins. COPI proteins consists of 7 distinct subunits: α, β, β', γ, δ, ε, and ζ. All subunits of COPI act together to form a complex to create COPI-coated vesicles (Lowe and Kreis, 1998; Duden, 2003), and a defect in any one subunit disrupts Golgi structure and transport between ER and Golgi. For example, CHO(ldlF) cells contain a temperature-sensitive (ts) mutation of the ε-COP subunit. At a non-permissive temperature (39.5^{o}C), the degradation rate of ε-COP in CHO(ldlF) cells is very rapid and the capability to form COPI vesicle coats is lost, resulting in the failure of COPI function (Guo et al., 1994; Guo et al., 1996). On the other hand, some Golgi glycosylation enzymes and Shiga toxin, which lack definite COPI-binding motifs, can slowly transport from the Golgi back to the ER via a COPI-independent pathway (Storrie et al., 2000).

COPI retrieves its target proteins by binding to various retention motifs. In soluble proteins, the lysine-aspartate-glutamate-leucine (KDEL) sequence signals the retrieval of proteins to the ER via the KDEL receptor recruiting COPI complexes. The canonical consensus binding site of COPI in integral membrane proteins is a di-lysine motif (KKXX). The α, γ, and δ subunits of COPI are reported to directly bind with di-lysine

containing proteins (Duden, 2003; Lee et al., 2004). Recently, several arginine-based ER retention motifs of membrane proteins have been identified as non-canonical binding sites for COPI in nicotinic acetylcholine receptors (Keller et al., 2001) and potassium channels (O'Kelly et al., 2002; Yuan et al., 2003). Previous data from our laboratory in collaborative studies with Dr. John Marshall (Brown University) indicated that the ER retention of KA2 subunits was controlled by the polyarginine domain at residues 862-866 (R862-866) (Ren et al., 2003a), which we propose is a binding site for COPI.

COPI mediated ER retention/retrieval of integral proteins can be occluded by steric hindrance following heteromeric assembly of $GABA_B$ receptors and MHC class II β-subunit (Margeta-Mitrovic et al., 2000; Khalil et al., 2003), by associations with PDZ binding proteins in NMDA receptors (Standley et al., 2000), or by associations with 14-3-3 proteins in potassium channels (O'Kelly et al., 2002; Yuan et al., 2003). 14-3-3 proteins regulate several cellular processes including signal transduction, cell-cycle control, and protein translocation to the plasma membrane. The 14-3-3 protein family in mammals consists of β, ε, γ, η, σ, τ and ζ isoforms, which have high sequence homology. All 14-3-3 isoforms have three major types of consensus binding sites: $RSXS^{p}XP$, $RXXXS^{p}XP$, and $(S/T)^{P}X_{1-2}$-COOH, where S^{P} and T^{P} denotes a phosphoserine and a phosphotyrosine (Dougherty and Morrison, 2004; Coblitz et al., 2006), but these consensus sequences exhibit degeneracy (Jeanclos et al., 2001; O'Kelly et al., 2002). Most interactions between 14-3-3 isoforms and their target proteins depend on the phosphorylation of specific serine or threonine residues. However, 14-3-3 proteins bind to some proteins, such as exoenzyme S and exoenzyme A20 in a phosphorylation-independent manner (Yaffe, 2002). Competition between COPI and 14-3-3 proteins in the regulation of intracellular trafficking can be either phosphorylation dependent (O'Kelly et al., 2002) or phosphorylation independent (Yuan et al., 2003). Recently, the 14-3-3γ isoform was reported to bind GluR6a kainate receptors (Coussen et al., 2005). At low stringency KA2 is predicted to contain a 14-3-3 binding site at a site overlapping the arginine-rich ER retention signal (RKTSRSRRRRR, residues 856-862). In addition, serine and threonine

residues in this predicted binding site of KA2 sequence are potential phosphorylation sites of protein kinase A (PKA) and protein kinase C (PKC) (Obenauer et al., 2003). The overlap of this putative 14-3-3 associated domain suggests that these proteins compete with COPI complex proteins for binding to the KA2 subunit (Figure 1.4). We therefore tested the hypothesis that COPI and 14-3-3 proteins play a central role in KA2 kainate receptor trafficking.

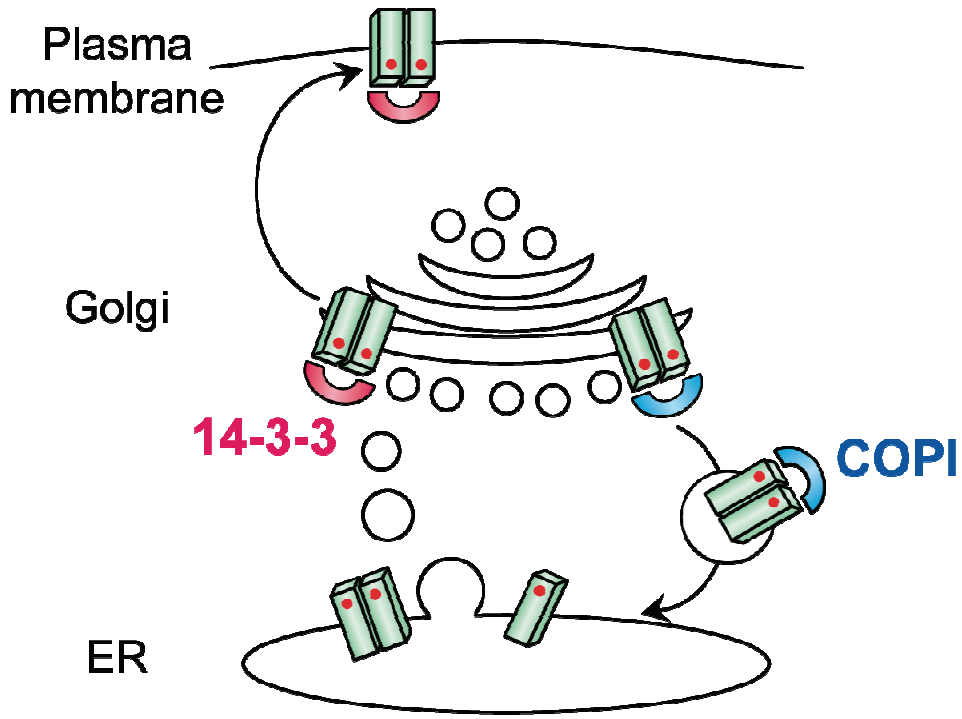

Figure 1.4: A model of KA2 receptor trafficking regulated by COPI and 14-3-3 proteins.
The square represents a subunit of KA2 proteins, and the red dot indicates the arginine-based ER retention signals. Assembled KA2 receptors are transported out of the ER to the Golgi. If the arginine-based motifs are masked and KA2 receptors interact with 14-3-3 proteins (red color), 14-3-3 proteins promote the transit of KA2 receptors to the cell surface. If the COPI complex (blue color) binds to the arginine-based domains, KA2 receptors are retrieved to the ER. Model is adapted from Michelsen et al, *EMBO Rep*, 2005.

1.7 KAINATE RECEPTOR TRAFFICKING: NON-CYTOPLASMIC DETERMINANTS

Recently, it has been reported that cellular trafficking and targeting of glutamate receptors are not only regulated by their trafficking determinants in the cytoplasmic tail, but are also modulated by the membrane domain and the extracellular ligand binding domain. Mutations of amino acid residues in the pore domain responsible for receptor gating in *Caenorhabditis elegans* GLR-1 AMPA receptors (Grunwald and Kaplan, 2003) and mammalian GluR2 AMPA receptors (Greger et al., 2002) interfere with receptor expression at the plasma membrane. Changes in critical residues disrupting ligand binding of *C. elegans* GLR-1 AMPARs (Grunwald and Kaplan, 2003), GluR6 KARs (Mah et al., 2005), and KA2 KARs (Valluru et al., 2005) reduce or eliminate plasma membrane localization. Furthermore, mutations of amino acid residues in ligand binding domains involved in the regulation of receptor desensitization in GluR2 AMPARs (Greger et al., 2006) and GluR6 KARs (Fleck et al., 2003; Priel et al., 2006) affected the level of plasma membrane expression. A point mutation in AMPA receptors that disrupted receptor desensitization led to ER retention of receptors, whereas a point mutation that favors receptor entry into the desensitized state seemed to promote the cell surface expression of receptors (Greger et al., 2006). This data led to formulation of a model in which tetrameric receptors bind glutamate in the ER and shift into a conformation analogous to the desensitized state, which then acts as a checkpoint for iGluR proteins to exit the ER (Mah et al., 2005; Valluru et al., 2005; Greger et al., 2006; Priel et al., 2006) (Figure 1.5).

We were interested in testing this model for KARs by generating a series of mutants with a variety of desensitization properties. Changes in a variety of domains, including the inter-subunit and inter-domain residues in the S1 and S2 regions, alter desensitization properties of AMPA and KA receptors (Fleck et al., 2003; Greger et al., 2006; Priel et al., 2006; Zhang et al., 2006). In contrast to AMPARs, a single point mutation at the GluR6 dimer interface is not sufficient to eliminate desensitization of KARs (Fleck et al., 2003).

Desensitization of KARs can be blocked either by mutations of several residues in the interface domain or by creating intermolecular disulfide cross-links between the dimer (Priel et al., 2006; Weston et al., 2006b; Zhang et al., 2006). These data suggest that desensitization process in AMPA and KA receptors has both conserved and divergent elements. In addition to S1 and S2 regions, a transduction linker coupling ligand-binding

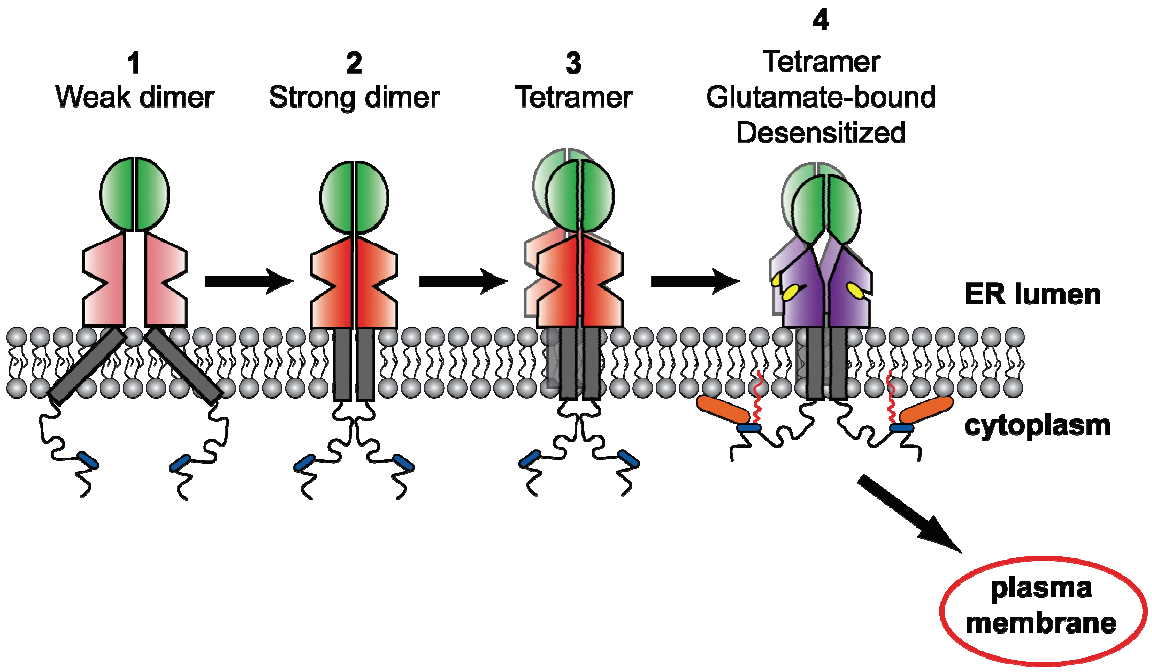

Figure 1.5: A model depicting AMPA and KA receptor maturation in the ER. (1) The N-terminal domains (green semicircles) mediate the formation of weak dimer during the translation process. (2) Inter-subunit interactions between the ligand binding domains along the dimer interface lead to the strong dimer conformation (pink to red transition). (3) Dimers of dimers assemble into tetramers. (4) Tetrameric receptors are desensitized (purple transition) after binding to glutamate (yellow ovals). This desensitized conformation of receptors is detected by the ER as the signal to export receptors out of the ER. The C-terminal domains of AMPA and KA receptors contain various trafficking motifs (blue rods), which interact with putative chaperone proteins (orange rods), and provides another level of receptor trafficking control. The model is modified from Greger et al., *Neuron*, 2006.

energy to channel permeation modulates AMPA and KA receptor desensitization to varying extents (Yelshansky et al., 2004). Mutations of inter-subunit and inter-domain residues also affect other aspects of receptor function and biosynthesis including ligand binding affinity and receptor assembly (Sun et al., 2002; Weston et al., 2006a). Our preliminary data showed that mutations at the M3-S2 transduction linker did not alter ligand binding affinity of GluR6a receptors. Thus, we aim to test the correlation between physiological phenomena and biosynthesis of KARs by measuring plasma membrane expression of receptor subunits with a range of desensitization behavior.

Mutation in domains associated with receptor function could reduce plasma membrane expression of iGluRs by interfering biosynthetic pathways. Protein folding, assembly, and ER-associated degradation (ERAD) by proteasomes regulate the intracellular retention of AMPA receptors. Disruptions of calcium permeation and glutamate binding block tetramerization of GluR2 AMPA receptors (Greger et al., 2003; Greger et al., 2006). The relatively low plasma membrane expression of GluR1 AMPA receptors is due to receptor degradation via the ERAD (Vandenberghe et al., 2005). In contrast, elimination of the glutamate binding site did not disrupt oligomerization of GluR6 KARs (Mah et al., 2005) or increase the degradation rate of KA2 KARs (Valluru et al., 2005). The early stages of KARs are largely uncharacterized. We will examine these processes to determine if mutations in the linker domain cause inappropriate folding, disrupting assembly process and/or increasing the degradation of receptors, which would contribute to the reduction of plasma membrane localization.

Proper folding, protein stability, oligomerization, and protein sorting are quality control processes controlled interactions with chaperone proteins in the ER lumen. Chaperone proteins recognize incompletely folded or incorrectly assembled proteins via the exposure of hydrophobic regions, unpaired cysteine residues, tendency to aggregate, or signal tags. For example, glucoses attached to glycoproteins associate with calnexin chaperone

proteins, mediating the retention of proteins in the ER. Ubiquitins attached to lysine side chains act as a degradation signal. Wildtype AMPA receptor subunits are reported to interact with BiP and calnexin proteins (Rubio and Wenthold, 1999), and ligand-binding deficient GluR6 mutants are shown to bind calnexin proteins to a greater degree than wildtype receptors (Fleck, 2006). Thus, chaperone proteins responsible for protein folding and degradation might play a role in the ER localization of KA mutants via interactions with the extracellular domain of receptors.

Biosynthesis and trafficking of KARs are tightly controlled processes. Several discrete trafficking motifs and critical checkpoints of KAR trafficking are identified; however, the mechanisms controlling these determinants in the early stages of receptor biosynthesis remains unresolved. It is known that KARs with different subunit compositions express to varying degrees at the plasma membrane and target to distinct synaptic and non-synaptic sites. The mechanisms underlying the assembly and trafficking of distinct KAR stoichiometries are largely unknown. Our characterization of KAR biosynthesis will yield insight to the cellular regulation of receptor trafficking and targeting, which will lead to a better understanding of the role of KARs in the CNS.

CHAPTER 2: INTRACELLULAR TRAFFICKING OF KA2 KAINATE RECEPTORS MEDIATED BY INTERACTIONS WITH COPI AND 14-3-3 CHAPERONE SYSTEMS

Assembly and trafficking of neurotransmitter receptors are processes contingent upon interactions between intracellular chaperone systems and discrete determinants in the receptor proteins. Kainate receptor subunits, which form ionotropic glutamate receptors with diverse roles in the central nervous system, contain a variety of trafficking determinants that promote either membrane expression or intracellular sequestration. In this report, we identify the coatomer protein complex I (COPI) vesicle coat as a critical mechanism for retention of the kainate receptor subunit KA2 in the endoplasmic reticulum. COPI subunits immunoprecipitated with KA2 subunits from both cerebellum and COS-7 cells, and β-COP protein interacted directly with immobilized KA2 peptides containing the arginine-rich retention/retrieval determinant. Association between COPI proteins and KA2 subunits was significantly reduced upon alanine substitution of this signal in the cytoplasmic tail of KA2. Temperature-sensitive degradation of COPI complex proteins was correlated with an increase in plasma membrane localization of the homologous KA2 receptor. Assembly of heteromeric GluR6a/KA2 receptors markedly reduced association of KA2 and COPI. Finally, the reduction in COPI binding was correlated with an increased association with 14-3-3 proteins, which mediate forward trafficking of other integral signaling proteins. These interactions therefore represent a critical early checkpoint for biosynthesis of functional kainate receptors.

Vivithanaporn et al. *J Biol Chem* **281**: 1068-1078, 2005.

2.1 INTRODUCTION

Kainate receptors (KARs) play a variety of roles in the mammalian central nervous system that include contributions to postsynaptic neurotransmission at a subset of excitatory synapses and presynaptic modulation of both excitatory and inhibitory transmission (Huettner, 2003; Lerma, 2003). These diverse physiological roles of KARs require selective assembly, subcellular trafficking, and targeting of these proteins to their functional sites. Elucidating the cellular mechanisms that control these processes is important for understanding the full spectrum of KAR-mediated signaling in the brain.

Oligomerization and intracellular trafficking of KARs are controlled in part through interactions with chaperone proteins that bind to discrete cytoplasmic domains on the receptor proteins themselves. For example, GluR6a KAR subunits contain a forward trafficking determinant in their cytoplasmic tail and therefore are highly expressed as homomeric receptors on the plasma membrane of heterologous cell lines (Yan et al., 2004), whereas the KA2 subunit has an endoplasmic reticulum (ER) retention/retrieval signal and consequently does not reach the plasma membrane in the absence of other KAR subunits (Ren et al., 2003a). The KA2 ER retention/retrieval signal consists primarily of an arginine-rich domain similar to that characterized on several other ionotropic glutamate receptor subunits, including NR1 (Scott et al., 2001) and GluR5-2c (Jaskolski et al., 2004), as well as other signaling proteins such as ATP-sensitive potassium channels (K_{ATP}) (Zerangue et al., 1999) and $GABA_B$ receptors (Margeta-Mitrovic et al., 2000). Although a number of trafficking motifs in KAR subunits have been identified (Jaskolski et al., 2005a), little is known about how these trafficking signals control localization of receptors and which chaperone proteins are responsible for the modulation of receptor trafficking.

Recently, arginine-based ER retention/ retrieval motifs similar to that in the KA2 subunit were shown to comprise non-canonical binding sites for the coatomer protein complex I (COPI) in nicotinic acetylcholine (nACh) receptor α subunits (Keller et al., 2001),

KCNK3 potassium channels (O'Kelly et al., 2002), and K_{ATP} Kir6.2 channels (Yuan et al., 2003). COPI complexes consist of 7 distinct subunits (α, β, β', γ, δ, ε, and ζ subunits) and play a central role in the retrograde trafficking from the Golgi to the ER of misfolded, unassembled proteins and ER-resident proteins (Lee et al., 2004). In KCNK3 and Kir6.2 channels, COPI-mediated ER retention was opposed by 14-3-3 proteins, a family of soluble proteins with diverse cellular functions (O'Kelly et al., 2002; Yuan et al., 2003). 14-3-3 proteins also promoted plasma membrane expression of other integral proteins such as nicotinic acetylcholine (nACh) receptors (Jeanclos et al., 2001) and TASK-1 and TASK-3 potassium channels (Rajan et al., 2002).

In this project, we tested the hypothesis that the polyarginine trafficking determinant in KA2 KAR subunits functions as a COPI interaction domain and thereby mediates sequestration of these subunits in the ER. We found that COPI did indeed associate with KA2 subunits, and this interaction was reduced upon mutation of the arginine-rich ER retention/retrieval domain. As well, mutations that reduced COPI association concomitantly increased association with endogenous and exogenous 14-3-3ζ proteins. The strong correlation between plasma membrane expression of KA2 receptors and interactions with COPI and 14-3-3ζ proteins support our hypothesis that these chaperone systems regulate the subcellular trafficking of KA2 subunits.

2.2 MATERIALS AND METHODS

2.2.1 Molecular biology

Myc-KA2, myc-KA2(R862-6A), myc-KA2(R862-6A,L908-9V), and GFP-GluR6/KA2 cDNAs were obtained from Dr. John Marshall (Brown University, Providence, RI). GFP-GluR6a cDNA was a gift from Dr. Stephen Heinemann (Salk Institute, La Jolla, CA). Myc-GluR6(Q), myc-GluR5-2b, and myc-GluR5-2c were received from Dr. Christophe Mulle (Université Bordeaux II, France). VSVG (vesicular stomatitis virus glycoprotein)-14-3-3ζ was a gift from Dr. Melanie Darstein. All cDNAs were in pcDNA3 vectors. Other cDNA mutants were generated using the QuikChange Site-Directed Mutagenesis protocol (Stratagene, La Jolla, CA). All mutants were subcloned back into the wild type vector using an *Eco*RI-*Xba*I site for myc-KA2 cDNAs. PCR-amplified sequences including the site mutations were verified by DNA sequencing.

2.2.2 Cerebellar lysate preparation

Cerebella were dissected from 129SvEv wildtype mice or $KA2^{-/-}$ mice at 21-25 days old, homogenized in 50 mM Tris HCl, 0.32 M sucrose, pH 7.4, and centrifuged at 800 X g for 5 min at 4°C. Supernatants were centrifuged again at 180,000 X g for 1 hr at 4°C. Pellets were resuspended in lysis buffer consisting of 50 mM Tris, 150 mM NaCl, 0.5% NP-40, 1 mM 4-(2-aminoethyl)-benzenesulfonylfluoride-HCl, 0.8 μM aprotinin, 20 μM leupeptin, 40 μM bestatin, 15 μM pepstatin A, and 14 μM L-trans-epoxysuccinyl-leucylamido(4-guanidino)butane.

2.2.3 Cell culture, transfection, and protein preparation

COS-7 cells were cultured in Dulbecco's modified Eagle's medium (DMEM) supplemented with 100 μg/ml penicillin, 100 μg/ml streptomycin, and 10% fetal bovine serum. COS-7 cells were plated in 100 mm dishes at 1 x 10^6 cells and transfected with total of 5 μg cDNA using FuGene6 reagent (Roche Applied Science, Indianapolis, IN)

following the manufacturer's recommended protocol. 48 hr after transfection, cells were washed twice with cold phosphate buffered saline (PBS) and lysed in 0.5 ml lysis buffer. Crude protein lysates were obtained after centrifugation at 13,000 X g at 4^{o}C for 20 min. Wildtype CHO (Chinese hamster ovary) and mutant CHO (ldlF) (clone 2) cells were a gift from Dr. Richard Anderson (University of Texas Southwestern Medical Center, Dallas, TX) and Dr. Monty Krieger (Massachusetts Institute of Technology, Cambridge, MA), and were maintained as described in Guo et al. (Guo et al., 1994). 48 hr after transfection, cells were transferred to 39.5^{o}C for 12 hr before biochemical analysis.

2.2.4 Immunoprecipitation and immunoblotting

Immunoprecipitations were performed by first incubating membrane preparations with 50 μl of either 50% protein A/G sepharose slurry (20422, Pierce, Rockford, IL), for COS-7 cell lysate, or TrueBlot anti-Rabbit Ig IP beads (00-8800, eBioscience, San Diego, CA), for cerebellar preparations, overnight at 4^{o}C to eliminate non-specific binding ("preclear" step). Preclear supernatants were incubated with 4 μg of anti-KA2 antibody (06-315, Upstate Biotechnology, Waltham, MA), anti-GluR6/7 (06-309, Upstate Biotechnology, Waltham, MA), anti-β-COP antibody (PA1-061, Affinity BioReagents, Golden, CO), anti-α-COP antibody (PA1-067, Affinity BioReagents, Golden, CO), anti-14-3-3β (K-19, sc-629, Santa Cruz Biotechnology, Santa Cruz, CA), anti-14-3-3γ (C-16, sc-731, Santa Cruz Biotechnology), anti-14-3-3ζ (C-16, sc-1019, Santa Cruz Biotechnology, Santa Cruz, CA), or anti-VSV glycoprotein antibody (clone P5D4, V5507, Sigma, Saint Louis, MO) at 4^{o}C for 2 hr, followed by the incubation with 50 μl of either 50% protein A/G sepharose beads or TrueBlot anti-Rabbit Ig IP beads at 4^{o}C overnight. After five washes in lysis buffer, bound proteins were eluted from beads by boiling in 2X Laemmli sample buffer (Bio-Rad, Hercules, CA) for 5 min and then separated by electrophoresis on 8% SDS-PAGE gels. 2 μg of COS-7 proteins and 10 μg of cerebellar proteins were loaded into lysate lane. Proteins were electro-transferred onto nitrocellulose membranes and probed with anti-β-COP antibody (1:2000), anti-KA2

antibody (1 μg/ml), anti-GluR6/7 antibody (1 μg/ml), anti-myc antibody (0.4 μg/ml, clone 9E10, Roche Applied Science, Indianapolis, IN), anti-GFP (1:500, 8371, JL-8, BD Biosciences, Palo Alto, CA), anti-14-3-3β (1:3000, H-8, Santa Cruz Biotechnology, Santa Cruz, CA), anti-14-3-3ζ (1:10000), or anti-VSVG antibody (1:200000). Immunoreactive bands were visualized using horseradish peroxidase (HRP)-conjugated sheep anti-mouse secondary antibody (1:5000, NA931V, Amersham Biosciences, UK), HRP-conjugated donkey anti-rabbit secondary antibody (1:5000, NA934V, Amersham Biosciences, UK) or HRP-conjugated anti-Rabbit IgG TrueBlot (1:2000, 88-1688, eBioscience, San Diego, CA). The density of bands was quantitated using an AlphaImager machine (Model 5500, AlphaInnotech, San Leandro, CA) and ChemiImager program (AlphaInnotech, San Leandro, CA). Quantitation of protein densities on Western blots was carried out by normalizing the immunoprecipitate band density to that of the lysate band (which was proportional to the expression levels of the protein). For each experiment, the density of the background preclear band was subtracted from the immunoprecipitate band density, and this value was divided by the density of the lysate band. The lysate lane in every Western blot was loaded with 2 μg, allowing us to compare density ratios between experiments. All experiments were performed at least three times. Statistical analyses were performed on the normalized values.

2.2.5 Immunolocalization and confocal microscopy

Transfected COS-7 cells were fixed with 4% paraformaldehyde for 20 min and then permeabilized with 0.2% Triton X-100 for 5 min. Cells were incubated with anti-myc (4 μg/ml in 10% goat serum) at room temperature for 2 hr. Cells were washed 3 times with PBS and subsequently incubated with anti-β-COP (1:500 in 10% goat serum), at room temperature for 2 hr. After 3 washes, cells were incubated with appropriate fluorescence-conjugated secondary antibodies: Alexa Fluor 488 or Alexa Fluor 594 (Molecular Probes, Eugene, OR) at room temperature for 1 hr. All images were taken from inverted LSM 510 Meta confocal microscope at the Optical Imaging Laboratory, University of Texas

medical branch using a Plan-Apochromat 63X/1.4 oil objective lens with excitation wavelength at 480 nm for Alexa Fluor 488 and at 543 nm for Alexa Fluor 594.

2.2.6 Peptide-binding assay

Two peptides containing the KA2 cytoplasmic arginine-rich trafficking determinant and the associated alanine mutant were synthesized with amide terminal groups (KA2-Rpep: CRKTSRSRRRRRP, KA2-Apep: CRKTSRSAAAAAP). These were linked to sepharose beads at the initial cysteine residue (21st Century Biochemicals, Malboro, MA). Peptide beads were incubated with COS-7 cell lysate overnight. After five washes in lysis buffer, bound proteins were eluted and separated as described in immunoblotting section. Band densities in Western blots were normalized to total β-COP expression in lysate. Experiments were performed four times.

2.2.7 Cell surface biotinylation assay

COS-7 cells were plated in 6-well plates and transfected with 1 μg of cDNA. CHO cells were plated into 100 mm dishes and transfected with 5 μg of cDNA. Transfected cells were washed twice with cold PBS and incubated with 0.5 mg/ml EZ-link sulfo-NHS-SS-biotin (21331, Pierce, Rockford, IL) in PBS pH 8.0 at 4^{o}C for 30 min with gentle agitation. Non-reacted biotin was quenched using quenching solution (50 mM glycine in PBS pH 8.0) for 3 times and then cells were washed 3 times with cold TBS (0.025M Tris and 0.15 M NaCl), pH 7.2. Cells were harvested in 0.5 ml lysis buffer containing protease inhibitors. Lysates were incubated with 50 μl of 50% streptavidin sepharose high performance beads (17-5113-01, Amersham, UK) at 4^{o}C for overnight. Beads were washed four times, and proteins were eluted and detected as co-immunoprecipitation experiments. In the experiments with CHO cells, the total lane was loaded with lysate equivalent to 1% of the protein loaded on the peptide-linked beads. Biotinylated proteins eluted from the beads (corresponding to subunits located in the plasma membrane) were normalized to total protein expression and reported in the term of percentage. All experiments were performed at least four times.

2.2.8 Enzyme-linked immunosorbent assay (ELISA)

COS-7 cells were inoculated at 4.5 x 10^4 cells and transfected with 0.6 μg cDNA using FuGene6 reagent in 12-well plates. After 48 hr, cells were washed once with cold PBS and incubated with anti-myc antibody (4 μg/ml in 10% goat serum) at 4^{o}C for 30 min to detect plasma membrane expression. Cells were then washed twice with cold PBS and fixed with 4% paraformaldehyde in PBS at room temperature for 20 min. For measuring total protein expression, cells were first fixed with paraformaldehyde, permeabilized with 0.2% Triton X-100 in PBS for 5 min, and incubated with anti-myc antibody at room temperature for 2 hr. Both groups were washed 3 times with PBS and incubated with HRP-conjugated sheep anti-mouse secondary antibody (1:1000 in 10% goat serum, NA931V, Amersham Biosciences, UK) at room temperature for 1 hr. After the third washing with PBS, the HRP substrate *o*-phenylenediamine dihydrochloride (P9187, Sigma, Saint Louis, MO) was added and the color reaction was developed for 1 hr. The optical density of 0.2 ml of supernatant was detected by spectrophotometer at 490 nm. All values were an average of four replicates in each experiment; the mean background absorbances of the negative controls (sham-transfected cells) were subtracted from surface and total absorbance values. Data is presented in form of a ratio of plasma membrane expression to total cellular expression. At least four experiments were performed with each cDNA.

2.2.9 Statistical analysis

Data were tested with a one-way analysis of variance (ANOVA) and the *post-hoc* Tukey-Kramer multiple comparison test, or a one-tailed paired Student's t-test.

2.3 RESULTS

2.3.1 Immunoprecipitation of KA2 and COPI proteins

The COPI chaperone complex was shown recently to be a critical mediator of ER retrieval mediated by polyarginine signals in a subset of integral membrane proteins (Jeanclos et al., 2001; O'Kelly et al., 2002; Yuan et al., 2003). The KA2 kainate receptor subunit is retained efficiently in the ER through a mechanism primarily mediated by a polyarginine signal in the cytoplasmic carboxy-terminal domain. To determine if COPI proteins subserve a retention/retrieval function for the KA2 kainate receptor subunit, we first tested for a biochemical interaction between KA2 subunits and members of the COPI complex in transfected COS-7 cells. N-terminal myc-tagged recombinant rat KA2, GluR5-2b, GluR5-2c or GluR6a cDNAs were transfected into COS-7 cells before immunoprecipitation of cell lysates with an anti-β-COP antibody; KA2 or other subunit protein was then detected in Western immunoblots using an anti-myc antibody. We found that homomeric myc-KA2 receptors co-precipitated with endogenous β-COP in either COS-7 cells (IP lane, Figure 2.1*A*) or in transfected HEK293 cells (data not shown). The PC lane in the Figure showed the nonspecific binding of protein to the beads used for immunoprecipitation. In contrast to KA2, myc-GluR5-2b, myc-GluR5-2c, and myc-GluR6a subunits did not co-immunoprecipitate with β-COP (Figure 2.1*A*), demonstrating that the interaction is relatively specific to KA2 subunits. We also tried the converse experiment, immunoprecipitation of myc-KA2 and immunoblotting for β-COP protein, and observed a very weak but detectable co-precipitation (Figure 2.1*B*). We postulate from these data that the majority of KA2 subunits are resident in the ER and that a relatively small proportion of the receptor subunit transiently associates with COPI during retrieval to the ER.

We next tested if the interaction between KA2 subunits and COPI complex proteins could be detected in the central nervous system. The KA2 subunit is highly expressed in

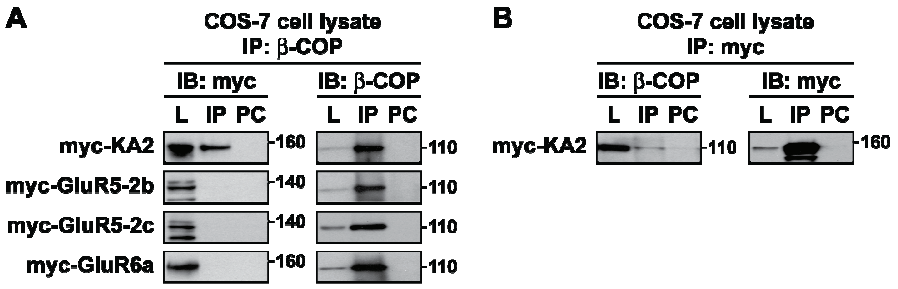

Figure 2.1: KA2 KAR subunits interact with β-COP vesicle coat proteins in COS-7 cells.

A, Homomeric myc-tagged kainate receptor subunits expressed in COS-7 cells were immunoprecipitated (IP) by an anti-β-COP antibody and detected in Western blots (IB, immunoblot) by an anti-myc antibody (*left panel*). Three lanes are shown for each Western blot: a lysate lane (L) containing 2 μg of membrane protein lysate, an immunoprecipitation lane (IP) loaded with 30 μl of the immunoprecipitate, and a preclear lane (PC) showing the background binding of proteins to beads lacking antibody. Anti-β-COP antibody immunoprecipitated KA2 subunits but not GluR5-2b, GluR5-2c or GluR6a subunits. Blots were stripped and re-probed with an anti-β-COP antibody (*right panel*) to verify precipitation of β-COP proteins. *B*, β-COP was weakly detected after immunoprecipitation with anti-myc antibody (*left panel*). Blots were stripped and re-probed with an anti-myc antibody (*right panel*) to demonstrate precipitation of myc-KA2 receptors.

cerebellar granule cells, where they likely form heteromeric receptors with GluR6 subunits and modulate excitatory synaptic transmission at parallel fiber synapses (Delaney and Jahr, 2002). Membrane protein lysates were prepared from homogenized cerebella from 129SvEv mice as well as $KA2^{-/-}$ gene-targeted mice (as a control for nonspecific interactions with the precipitating antibody). KA2 protein was immunoprecipitated from the lysates with an anti-KA2 antibody and β-COP was detected in Western blots (Figure 2.2*A*). As shown in the Figure, β-COP subunit co-immunoprecipitated with KA2 protein from wildtype but not $KA2^{-/-}$ cerebella (Figure 2.2*A*, left panels). Blots were stripped and re-probed with anti-KA2 antibody to verify that the immunoprecipitation of KA2 subunit protein was successful (Figure 2.2*A*, right

panel), and as expected immunoreactivity was not detected in the samples from KA2$^{-/-}$ mice. A reciprocal immunoprecipitation using an anti-β-COP antibody also supported a robust association between the KA2 subunit and β-COP (Figure 2.2*B*). Because cerebellar KA2 subunits likely assemble with GluR6 subunits as heteromeric receptors, we also tested to see if β-COP co-precipitated GluR6 either directly or in association with KA2. As shown in Figure 2.2*B*, GluR6/7 immunoreactivity did not precipitate with β-COP. In the reciprocal experiment, we immunoprecipitated GluR6/7 protein and Western blotted for β-COP. The vesicle protein was not detected in this assay (Figure 2.2*C*). These results support the interpretation that KA2 subunits exist in at least two distinct pools in cerebellum: those assembled with GluR6 as heteromeric KARs and those associated with the COPI retrograde trafficking pathway fated for retrieval to the ER.

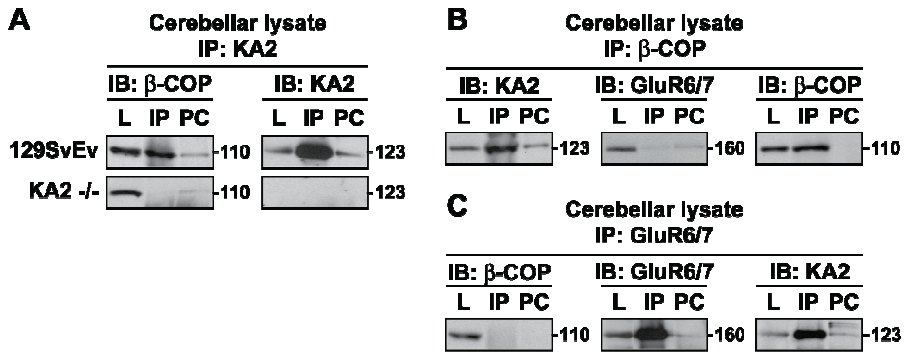

Figure 2.2: KA2 KAR subunits interact with β-COP vesicle coat proteins in cerebellum.

A, Cerebellar lysate prepared from 129SvEv or KA2$^{-/-}$ mice was used for immunoprecipitation with anti-KA2 antibody. β-COP protein co-precipitated with KA2 subunits in wildtype cerebellar lysate but not lysate from KA2$^{-/-}$ cerebella. The right panel demonstrates the presence of KA2 protein in the immunoprecipitate from wildtype mice. *B*, Immunoprecipitation of β-COP from cerebellar lysate from 129SvEv mice co-precipitated KA2 (*left blot*) but not GluR6/7 (*middle blot*) subunits. *C*, Immunoprecipitation of GluR6/7 subunits from cerebellar lysates did not co-precipitate β-COP protein (*left blot*), but did pull down GluR6/7 and KA2 protein (*middle and right blots*).

2.3.2 Subcellular co-localization of KA2 and β-COP proteins

Next, we determined if the subcellular localizations of KA2 subunits and COPI proteins were consistent with their interaction in our biochemical assays using confocal immunofluorescence staining of transfected COS-7 cells. Myc-KA2 subunits were detected with an anti-myc antibody (red in Figure 2.3) and β-COP was stained with an anti-β-COP antibody (green in Figure 2.3). In addition to COPI vesicle staining, anti-β-COP antibody strongly labels the Golgi apparatus, which is manifested as the intense green labeling in the image. The vast majority of KA2 receptor subunits are located in the ER and are unlikely to be actively associated with COPI, accounting for very weak β-COP bands when the KA2 subunit is the target of immunoprecipitation. As shown in the last row of images in Figure 2.1*F*, the discrete vesicle-like structures (punctate dots) positively stained for both KA2 and β-COP likely represent COPI vesicles containing KA2 as cargo protein.

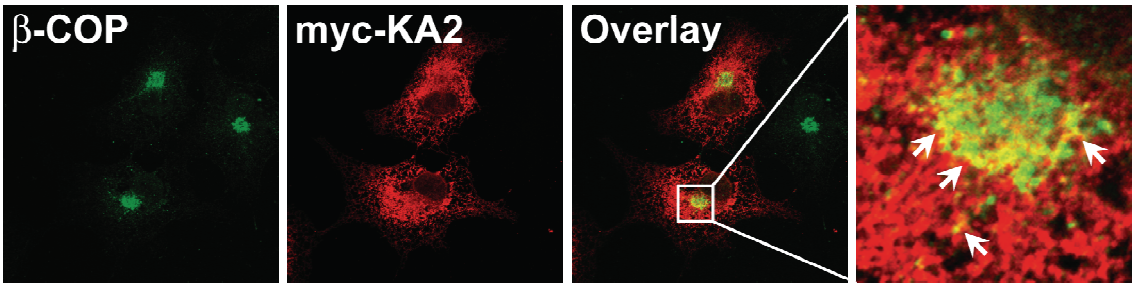

Figure 2.3: KA2 receptors partially colocalize with COPI proteins.

COPI staining (green) was most obviously localized to the Golgi apparatus and in small puncta likely representing transport vesicles. Homomeric myc-KA2 receptors staining (red) showed the characteristic reticular pattern of endoplasmic reticulum. An overlay of β-COP and KA2 immunofluorescence at higher magnification shows that KA2 subunits were partly co-localized with β-COP (arrows).

2.3.3 Elimination of COPI function promotes plasma membrane expression of KA2 receptors

If COPI association plays a central role in limiting forward trafficking of KA2 subunits beyond the *cis*-Golgi, homomeric KA2 receptors should exhibit higher plasma membrane expression when COPI functionality is disrupted. CHO(ldlF) cells contain a temperature-sensitive (ts) mutation in one subunit of the complex, ε-COP (Guo et al., 1994). At a nonpermissive temperature (39.5^{o}C), ε-COP is degraded and the cells lose the capability of forming COPI vesicle coats. We compared the plasma membrane expression of homomeric myc-KA2 receptors expressed in wildtype CHO cells and CHO(ldlF) cells using a cell surface biotinylation assay (Figure 2.4*A*). Cell surface proteins were labeled with biotin, purified on streptavidin columns, and eluted proteins were immunoblotted with anti-myc antibody. We included lanes with 1% of the input myc-KA2 protein, in order to determine the relative amount of KA2 expressed at the plasma membrane, and detected actin immunoreactivity to verify equivalent protein loading (Figure 2.4*A*). The relative plasma membrane to total protein expression of myc-KA2 receptors in CHO(ldlF) cells significant increased significantly by 3.6 fold ($n = 4$, $p < 0.05$) after a 12 hr incubation at 39.5ºC compared to CHO(ldlF) cells kept at 34ºC for the same period of time (Figure 2.4*B*). Transfected CHO cells kept at either 37ºC or 39.5ºC expressed the same relative level of myc-KA2 on the plasma membrane as CHO(ldlF) cells maintained at the permissive temperature. This data support the hypothesis that COPI-mediated retention/retrieval prevents plasma membrane expression KA2 receptors.

2.3.4 Dependence of COPI association on the KA2 trafficking determinant

We hypothesized that COPI proteins interacted with KA2 subunits at the arginine-rich domain in the intracellular carboxyl terminus. To determine if the critical amino acid residues responsible for COPI association site correlated with those required for ER sequestration, we examined COPI association with truncated and alanine-substituted KA2 subunits generated by site-directed mutagenesis of the receptor cDNA. The cytoplasmic

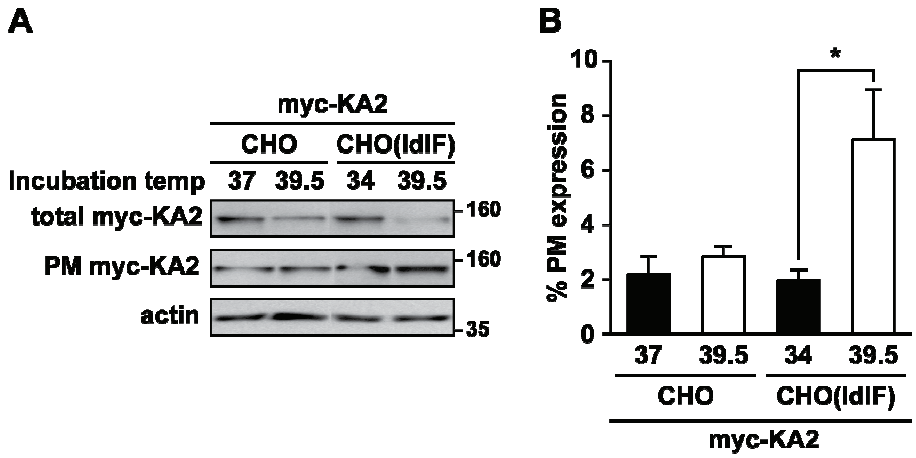

Figure 2.4: Plasma membrane expression of homomeric myc-KA2 receptors increases upon disruption of the COPI pathway.

A, Myc-KA2 was expressed in either CHO or CHO(ldlF) cells grown at 37ºC or 34ºC, respectively. Two days after transfection, one group from each type of transfected cell was shifted to 39.5ºC for 12 h, while the other groups were kept at the control temperatures. Cell surface proteins were then labeled with biotin. Biotin labeled plasma membrane proteins were purified on streptavidin columns and immunoblotted with anti-myc antibody (*middle panel*, "PM myc-KA2"). 1% of the total membrane protein loaded on the streptavidin beads was immunoblotted in order to normalize protein expression (*top panel*, "total myc-KA2"). The lower panel shows the actin loading controls of the total lysate. Incubation of CHO(ldlF) cells at the nonpermissive temperature (39.5ºC), resulting in the inactivation of COPI function, increased the relative level of plasma membrane KA2 subunits (while concurrently reducing total KA2 expression). *B*, Band density from Figure 2.4*A* was measured by densitometry. After 12 hr incubation at 39.5^{o}C, homomeric myc-KA2 receptors expressed in CHO(ldlF) cells had higher relative plasma membrane expression to total protein expression than cells incubated at 34 ^{o}C, representing a 3.6-fold increase. Data represent mean ± s.e.m. (n = 4, * $p < 0.05$).

tail of KA2 contains 155 amino acids; we generated a mutant subunit truncated at residue 827 (827-stop, with our numbering beginning at the initial methionine), which eliminated the bulk of the COOH terminus, and 856-stop, which terminated the cytoplasmic tail prior to the polyarginine domain (Figure 2.5*A*). Truncated myc-KA2(827-stop) and myc-

KA2(856-stop) subunits expressed in COS-7 cells exhibited significantly decreased association with β-COP in immunoprecipitation experiments (Figure 2.5*B*). Quantification of the optical density of the immunoprecipitated bands relative to that of their respective lysate bands revealed that the interaction between the truncated KA2 subunits and β-COP was reduced by 71 ± 9% and 78 ± 3% ($n = 3$, $p < 0.01$) for myc-KA2(827-stop) and myc-KA2(856-stop), respectively (Figure 2.5*C*).

These data indicated that the majority of β-COP association with KA2 subunits depended on domains downstream from the 856-stop site, consistent with the proposal that the polyarginine trafficking domain comprised a putative site for interaction. In addition to the polyarginine site, a pair of c-terminal leucine residues were shown to influence cell surface expression (Ren et al., 2003a) and therefore also were considered as a candidate interaction site. Alanine substitution of all five arginines, in the mutant construct myc-KA2(R862-6A), or both cytoplasmic trafficking determinants, in myc-KA2(R862-6A,L908-9V), markedly decreased the association of KA2 subunits with β-COP (by 59 ± 11% and 67 ± 6%, $n = 6$ and 3, respectively, $p < 0.01$) to a level similar to that observed for the truncated KA2 subunits (Figure 2.5*B* and 2.5*C*). In order to further define the COPI binding site, we tested the interaction of β-COPI with two KA2 mutants in which the polyarginine determinant was substituted with two sets of three alanines: myc-KA2(R862-4A) and myc-KA2(R864-6A). Association of β-COP protein with either of these mutants was not reduced from that of wildtype KA2 subunits (Figure 2.5*B* and 2.5*C*), suggesting that all five arginine residues (or a different subset of residues) in KA2 are necessary for interaction with the chaperone system. All blots were stripped and re-probed with an anti-β-COP antibody to verify the efficiency of COPI immunoprecipitation (Figure 2.5*B*).

β-COP is one of seven proteins that comprise the COPI chaperone system; to further validate the association between KA2 subunits and the COPI complex we tested for association between the receptor subunit and α-COP, another component of COPI vesicle

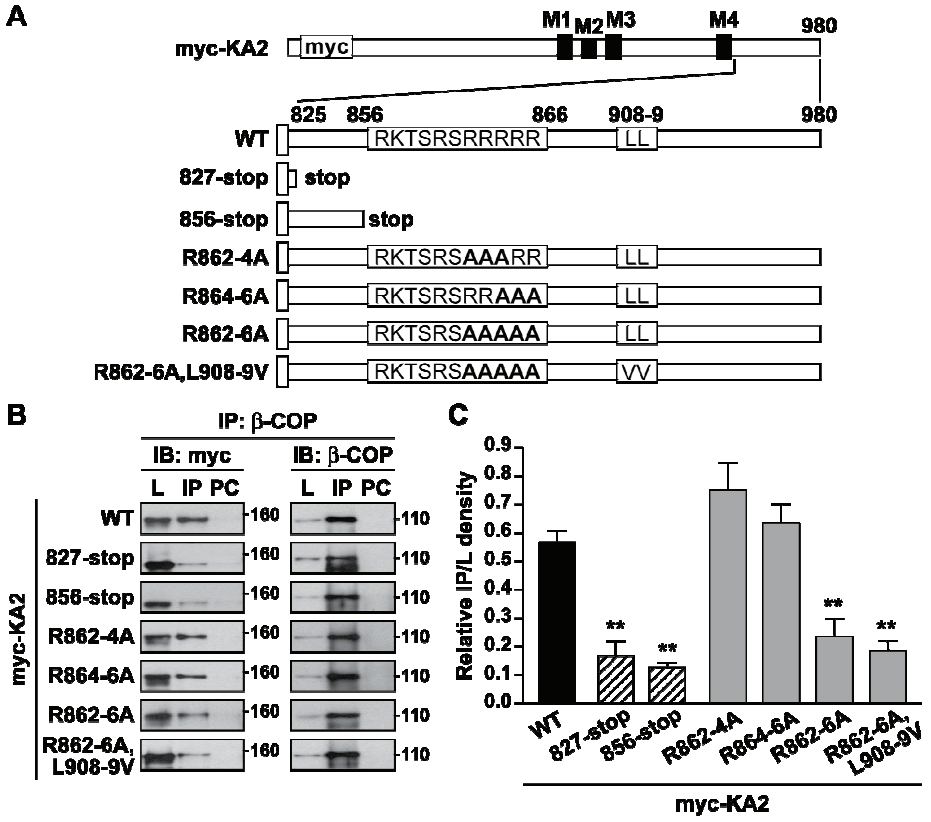

Figure 2.5: The polyarginine trafficking determinant in carboxy-terminus of the KA2 subunit is a COPI association site.

A, The diagram illustrates the truncation and substitution mutants made in the KA2 carboxy-terminus. KA2 mutants were generated with truncations at residues 827 and 856, and the polyarginine domain from residues 856 to 866 and the dileucine signal at residues 908-9 were substituted with alanines and valines, respectively. *B*, Immunoprecipitation of β-COP co-precipitated significantly less myc-KA2(827-stop), myc-KA2(856-stop), myc-KA2(R862-6A) and myc-KA2(R862-6A,L908-9V) protein compared to unmodified myc-KA2 (*left panel*). Immunoprecipitation controls are shown from re-probed blots in the *right panel*. Abbreviations: L, lysate; IP, immunoprecipitate; PC, preclear background. *C*, Quantitation of the IP band densities normalized to their corresponding lysate band density. Co-precipitation of the indicated receptor subunits was significantly reduced by 2.4- to 4.5-fold compared to unmodified receptors. (n = 3-6, ** $p < 0.01$). Data represent mean ± s.e.m.

coats. Immunoprecipitation of KA2-transfected cells with α-COPI antibody resulted in co-precipitation of KA2 protein (Figure 2.6*A*). As with β-COP, the truncation of receptor (myc-KA2(856-stop)) and mutation of the polyarginine motif (myc-KA2(R862-6A)) markedly reduced association with α-COP (by 88 ± 4 % and 66 ± 15%, n = 3, respectively, p <0.01) (Figure 2.6*A* and 2.6*B*). These results further support our hypothesis that the arginine-rich domain plays a role in COPI association.

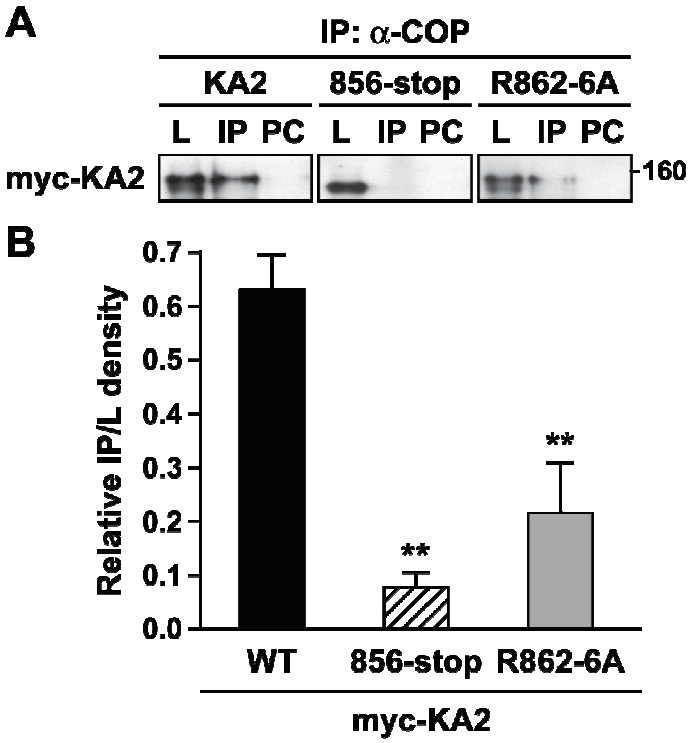

Figure 2.6: KA2 KAR subunits interact with α-COP vesicle coat proteins.

A, Immunoprecipitation with an anti-α-COP antibody co-precipitated myc-KA2 protein, and this was reduced upon truncation or alanine substitution of the receptor subunit (L, lysate; IP, immunoprecipitate; PC, preclear background). *B*, Quantitation of the IP band densities normalized to their corresponding lysate band density. Co-precipitation of myc-KA2(856-stop) and myc-KA2(R862-6A) protein was significantly reduced compared to unmodified receptors by 8.2- and 2.9-fold, respectively. (n = 3, ** p <0.01). Data represent mean ± s.e.m.

2.3.5 Interactions between β-COP and peptide containing the KA2 trafficking determinant

We next tested if the association inferred from our immunoprecipitations likely resulted from a direct interaction between COPI proteins and the polyarginine domain in the KA2 subunit. This was tested comparing by binding of β-COP protein in COS-7 cell lysates to two short peptides, KA2-Rpep and KA2-Apep, which were conjugated to a Sepharose beads (Figure 2.7*A*). KA2-Rpep contained the KA2 cytoplasmic arginine-rich trafficking determinant whereas KA2-Apep had the five alanine substitution used in previous immunoprecipitation experiments. The "Lysate" lane in the Figure shows expression of

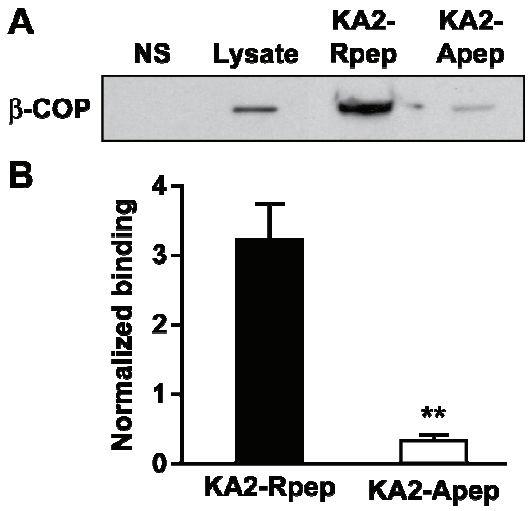

Figure 2.7: β-COP bound to peptide containing the KA2 polyarginine trafficking motif.

A, COS-7 membrane lysates were applied to beads containing KA2-Rpep or KA2-Apep peptides (see text for sequence details), and the eluates were immunoblotted for β-COP protein. Lysate lanes contain 1% of the protein loaded on the peptide-conjugated beads. The nonspecific (NS) lane was loaded with membrane protein applied to beads lacking peptide. *B*, Quantitation of the IP band densities normalized to their corresponding lysate band density. Elimination of the polyarginine site by alanine substitution nearly completely eliminates affinity for β-COP. Data represent mean ± s.e.m. (n = 4, ** $p < 0.01$ compared to KA2-Rpep).

the β-COP protein in the COS-7 lysate, and the "NS" lane shows the non-specific interaction between lysate and sepharose beads. We found that β-COP was readily detected in Western blots after elution from KA2-Rpep beads. In contrast, the protein was only weakly detected after elution from the KA2-Apep peptide (Figure 2.7*A*). To quantitate this result, we normalized the band densities of β-COP staining in the peptide lanes to the density of the lysate lane (each experiment was run with all four groups in parallel). We found that alanine substitution in the peptide reduced the interaction with β-COP by 90 ±_3% (n = 4, p <0.01) (Figure 2.7*B*). This result strongly supports the hypothesis that COPI proteins directly interact with the KA2 receptor at the arginine-rich sequence in the c-terminus.

2.3.6 COPI association is reduced in heteromeric GluR6a/KA2 receptors

Co-assembly of GluR6a with KA2 subunits leads to efficient plasma membrane expression of heteromeric GluR6a/KA2 receptors, suggesting that the interaction between COPI and KA2 subunits and consequent ER retention is occluded in the presence of GluR6a subunits. To test this hypothesis, COS-7 cells were co-transfected with myc-KA2 and GFP-GluR6a cDNAs, and cell lysate was immunoprecipitated with an anti-β-COP antibody. As predicted, we found a reduction in co-precipitated myc-KA2 (by 64 ± 6%, n = 5, p <0.01, Figure 2.8*A* and 2.8*B*). GFP-GluR6a was not detectable in the immunoprecipitated complex of β-COP and myc-KA2 (Figure 2.8*A*), suggesting that heteromeric GFP-GluR6a/myc-KA2 receptors did not interact with COPI to a significant degree. It therefore is likely that myc-KA2 detected after immunoprecipitation in these experiments represented a pool of unassembled or homomeric subunits that were not associated with GFP-GluR6a subunits.

Inhibition of COPI association with KA2 by GluR6a subunits could occur through masking of the polyarginine retention motif similar to the mechanism proposed for K^+ channels (Zerangue et al., 1999) and $GABA_B$ receptors (Margeta-Mitrovic et al., 2000),

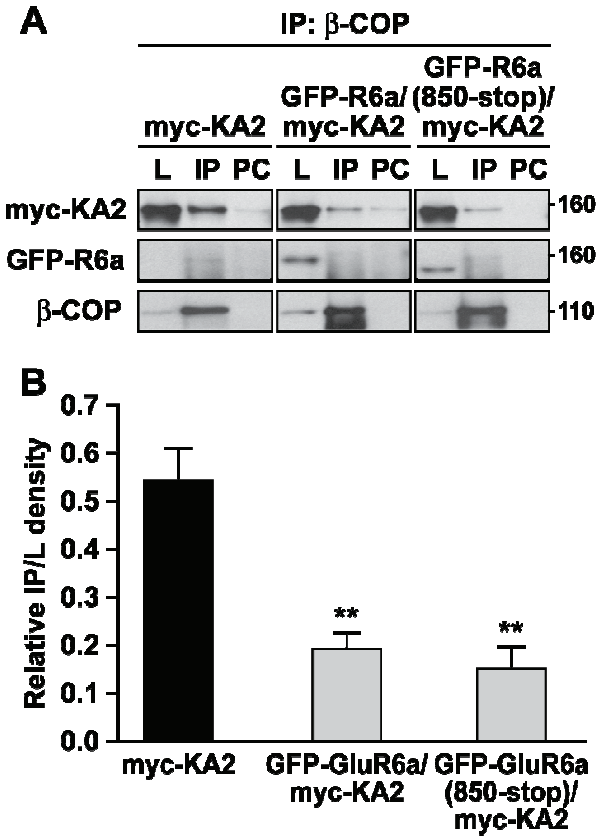

Figure 2.8: Heteromeric assembly to GluR6a subunits reduced COPI binding to KA2 subunits.

A, GFP-GluR6a wildtype or truncated GFP-GluR6a(850-stop) cDNAs were co-transfected with myc-KA2 cDNA in COS-7 cells, and lysate was immunoprecipitated by anti-β-COP antibody. *Top panel* showed Western blots with anti-myc antibody to detect KA2 subunits. Heteromeric GluR6a/KA2 receptors showed a great reduction of immunoprecipitated band of KA2 subunits. Blots were stripped and re-probed with anti-GFP antibody to detect GluR6a subunits (*middle panel*). GFP-GluR6a subunits were not detectable in immunoprecipitate complex. Blots were re-probed with anti-β-COP antibody to determine the efficiency of immunoprecipitation (*bottom panel*). Abbreviations: L, lysate; IP, immunoprecipitate; PC, preclear background. *B*, KA2-COPI association was reduced by 2.8-fold and 3.6-fold in heteromeric GluR6a/KA2 and GluR6(850-stop)/KA2 compared to homomeric KA2 receptors. Data represent mean ± s.e.m. (n = 5, ** $p < 0.01$ compared to homomeric KA2 receptors).

although our previous data suggested that this was not the case for ER retention of KA2 subunits (Yan et al., 2004). To test if COPI association with KA2 was masked by the GluR6a c-terminal tail, we co-transfected myc-KA2 with GFP-GluR6a(850-stop) cDNA, a truncated mutant that lacks most of GluR6a cytoplasmic tail. Previously, we showed that heteromeric GFP-GluR6a(850-stop)/myc-KA2 receptors were expressed at the plasma membrane (Yan et al., 2004), suggesting that retention signals in KA2 were suppressed despite the absence of the forward trafficking motif in GluR6a. We found that heteromeric assembly of myc-KA2 with GFP-GluR6a(850-stop) subunits decreased myc-KA2-βCOP interaction by 72 ± 9% ($n = 5$, $p < 0.01$) (Figure 2.8*A* and 2.8*B*). These data support our earlier hypothesis that the retention signal in KA2 subunits were not masked by the GluR6a cytoplasmic tail, but rather became unavailable for COPI association as a result of conformational changes in the KA2 subunit induced by heteromeric assembly.

2.3.7 Association of 14-3-3 proteins with kainate receptors subunits

One of the many cellular functions of members of the protein 14-3-3 gene family is modulation of plasma membrane expression of several integral proteins by competing directly or indirectly with the COPI complex for binding to cargo (O'Kelly et al., 2002; Yuan et al., 2003). We tested for interactions between KA2 subunits and three endogenous isoforms of 14-3-3 - 14-3-3β, 14-3-3γ and 14-3-3ζ - in myc-KA2-transfected COS-7 cells. Using anti-14-3-3 antibodies specific to the β, γ and ζ isoforms for immunoprecipitation, we found that homomeric myc-KA2 receptors associated with all three 14-3-3 proteins. The association with 14-3-3ζ protein increased (by 3.5-fold, $n = 4$, $p < 0.001$) when the ER retention/retrieval trafficking determinants (Arg residues 862-6 and Leu residues 908-9) were mutated to alanines and valines respectively (Figure 2.9*A* and 2.9*B*); in contrast, there were no significant differences in association of 14-3-3β or 14-3-3γ with myc-KA2 and myc-KA2(R862-6A,L908-9V) receptors (Figure 2.9*A* and 2.9B). Western blots were re-probed with anti-14-3-3β, anti-14-3-3γ or anti-14-3-3ζ to verify immunoprecipitation of 14-3-3 proteins (Figure 2.9*A*), which were successful

despite the relatively low abundance of 14-3-3γ and 14-3-3ζ (both were undetectable in the lysate lanes).

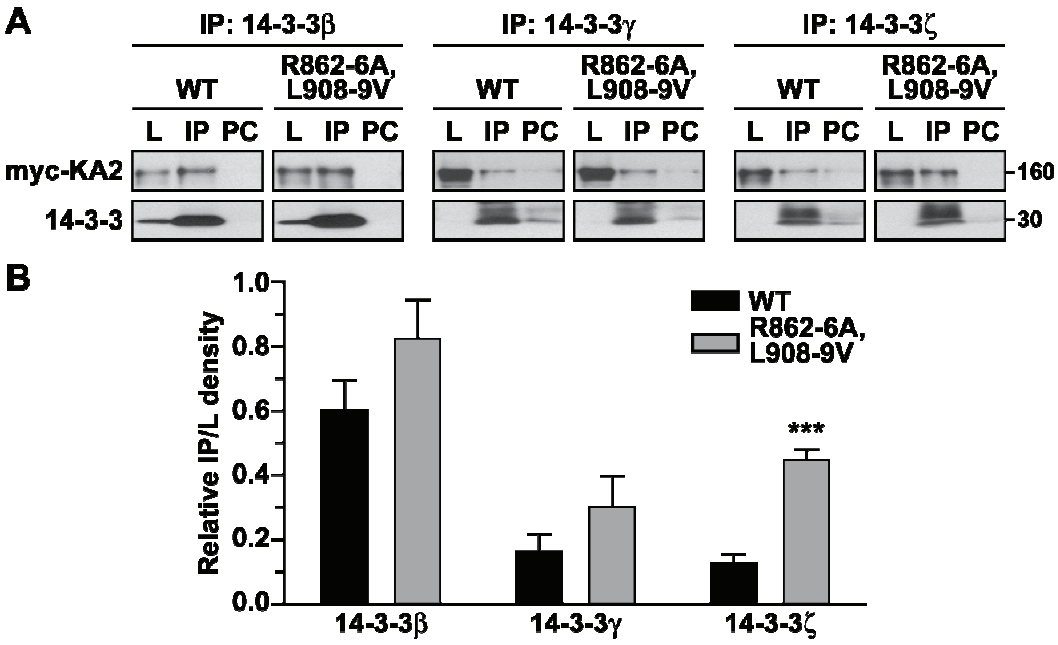

Figure 2.9: Elimination of the COPI binding site increased associations between KA2 receptors and endogenous 14-3-3 proteins.

A, Myc-KA2 transfected lysate was immunoprecipitated by anti-14-3-3β, anti-14-3-3γ, or anti-14-3-3ζ antibody and myc-KA2 receptors were detected via anti-myc antibody in Western blots (*top panel*). Myc-KA2(R862-6A,L908-9V) receptors co-precipitated with 14-3-3β, 14-3-3γ, and 14-3-3ζ to a higher degree than wildtype receptors. The 14-3-3 immunoprecipitation was verified by immunoblotting with anti-14-3-3 antibodies specific for different isoforms (*bottom panel*). 14-3-3γ and 14-3-3ζ isoforms were not detected from lysate but could be detected in immunoprecipitated lane. Abbreviations: L, lysate; IP, immunoprecipitate; PC, preclear background. *B*, Quantitation of the IP band densities normalized to their corresponding lysate band density showed that myc-KA2(R862-6A,L908-9V) co-precipitated to a similar degree as wildtype myc-KA2 with 14-3-3β and 14-3-3γ, but precipitation of the mutant was significantly higher with 14-3-3ζ proteins (3.5-fold increase, n = 4, *** $p < 0.001$). Data represent mean ± s.e.m.

To further explore the interaction between KA2 and 14-3-3ζ proteins, we co-transfected myc-KA2 and VSVG-tagged 14-3-3ζ cDNAs and immunoprecipitated the complexes with anti-VSVG antibody. Homomeric KA2 receptors bound to exogenous 14-3-3ζ proteins and this interaction was clearly increased in all the alanine-substituted mutants

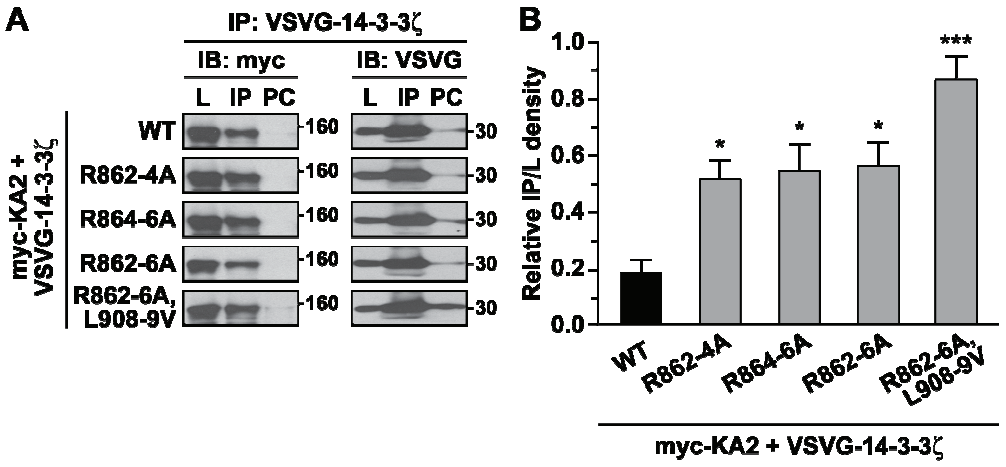

Figure 2.10: Elimination of the COPI binding site increased associations between KA2 receptors and exogenous 14-3-3ζ proteins.

A, Myc-KA2 receptors and exogenous VSVG-14-3-3ζ proteins co-expressed in COS-7 cells were immunoprecipitated with an anti-VSVG antibody, and myc-KA2 receptors were detected by an anti-myc antibody in Western blots. All alanine substitutions at the polyarginine ER retention/retrieval motif increased co-precipitation of myc-KA2 receptors with VSVG-14-3-3ζ proteins (*left panel*). The immunoprecipitation was verified by detecting 14-3-3ζ proteins with an anti-VSVG antibody (*right panel*). *B*, Relative band densities of normalized immunoprecipitated band over lysate band from Figure 2.10*C* indicated a greater association between KA2 receptors and exogenous 14-3-3ζ proteins when arginines in the polyarginine domain were mutated to alanines. 14-3-3ζ binding of myc-KA2(R862-4A), myc-KA2(R864-6A), and myc-KA2(R862-6A) receptors was 3-4-fold higher than wildtype receptors. The additional mutation at the putative di-leucine endocytic signal (myc-KA2(R862-6A,L908-9V)) further increased association to 14-3-3ζ ~5 times higher than wildtype receptors. Data represent mean $\pm$ s.e.m. (n = 3-4, * $p < 0.05$, *** $p < 0.001$).

we tested, including myc-KA2(R862-4A) and myc-KA2(R864-6A) (2.9- and 3.1-fold, respectively, n = 4, p <0.05), the three alanine mutants that did not show altered interactions with COPI. The highest level of association with VSVG-14-3-3ζ interaction was observed with myc-KA2(R862-6A,L908-9V) (4.8-fold, n = 4, p <0.001) (Figure 2.10*A* and 2.10*B*). Immunoprecipitation of 14-3-3ζ was confirmed in Western blots with the anti-VSVG antibody (Figure 2.10*A*). These data demonstrate that residues critical to COPI interaction also influence receptor association with 14-3-3 proteins.

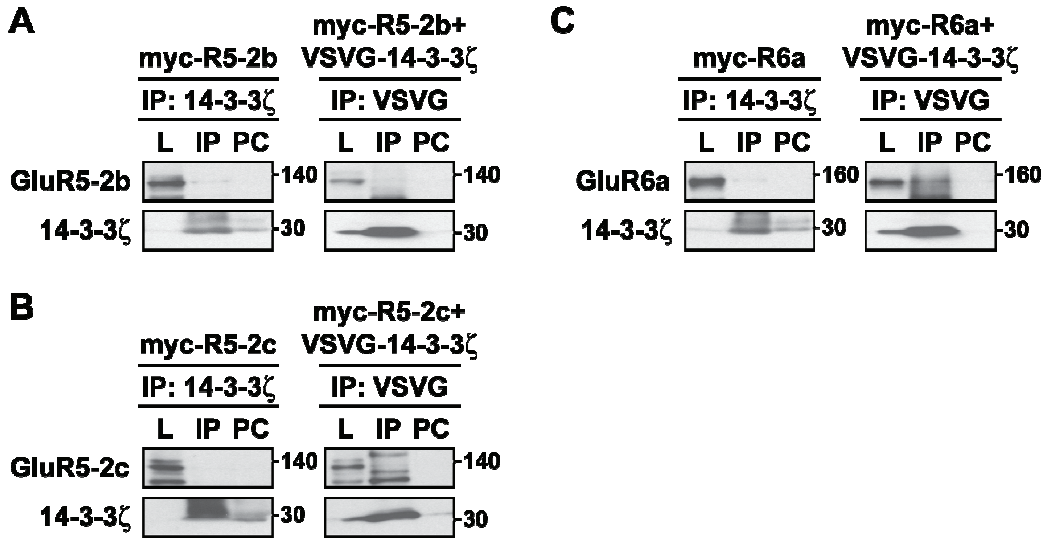

Figure 2.11: GluR5 and GluR6 KAR subunits weakly interacted with 14-3-3ζ proteins.

A, Interactions of endogenous 14-3-3ζ and exogenous VSVG-14-3-3ζ with GluR5-2b receptors were tested utilizing anti-14-3-3ζ and anti-VSVG antibodies, respectively. Western blotting with an anti-myc antibody showed that myc-GluR5-2b receptors weakly co-precipitated with endogenous 14-3-3 and exogenous VSVG-14-3-3ζ. *Top blots* were stripped and re-probed with anti-14-3-3ζ and anti-VSVG antibodies for endogenous 14-3-3ζ and exogenous 14-3-3ζ, respectively. Abbreviations: L, lysate; IP, immunoprecipitate; PC, preclear background. *B*, GluR5-2c receptors did not show detectable association with endogenous 14-3-3 or exogenous VSVG-14-3-3ζ. *C*, Similar to GluR5-2b receptor experiments, GluR6a receptors showed weak association with exogenous VSVG-14-3-3ζ.

The interaction with 14-3-3ζ proteins was much weaker, but still detectable, with the GluR5-2b, and GluR6a but not with GluR5-2c subunits. Homomeric myc-GluR5-2b and myc-GluR6a receptors were weakly co-precipitated with endogenous 14-3-3ζ, and GluR6a was more strongly associated with exogenous VSVG-14-3-3ζ (Figure 2.11*A* and 2.11*C*). In contrast, myc-GluR5-2c subunits did not exhibit detectable levels of immunoprecipitation with either endogenous or exogenous 14-3-3ζ (Figure 2.11*B*). The association of each of these receptor subunits with endogenous 14-3-3ζ was significantly lower than that observed with myc-KA2 subunits (Figure 2.9).

2.3.8 Plasma membrane expression of KA2 and mutant subunits

To correlate the competitive interaction of COPI and 14-3-3 proteins with localization of KA2 protein on the plasma membrane, we measured the surface expression of KA2 relative to total pools of the protein in cell ELISA assays. As is shown in Figure 2.12*A*, only ~1% of myc-KA2 protein is transported to the plasma membrane, consistent with the efficient retention mechanism mediated by the cytoplasmic polyarginine signal. Truncation of the c-terminal tail at either residue 827 or 856 increased the cell surface expression by 2.7- and 3.7-fold, respectively ($n = 4$, $p < 0.05$). Relative plasma membrane expression was enhanced further by partial alanine substitution of the polyarginine domain [myc-KA2(R862-4A), 3.9 ± 0.4%, $n = 4$, $p < 0.05$ and myc-KA2(864-6A), 5.3 ± 1.4%, $n = 4$, $p < 0.001$], and complete substitution of polyarginine domain [myc-KA2(R862-6A), 5.4 ± 0.6%, $n = 8$, $p < 0.001$]. Finally, substitution of both the polyarginine domain and the di-leucine motif in the myc-KA2(R862-6A,L908-9V) mutant increased plasma membrane expression to 8.5 ± 1.6% ($n = 4$, $p < 0.001$).

To support these results, we also compared the relative plasma membrane expression of myc-KA2 receptor and mutants after labeling surface proteins with biotin. KA2 protein purified on streptavidin columns was immunoblotted in parallel with lysate lanes loaded with 1% of the input protein and actin loading controls (Figure 2.12*B*). Truncation of the

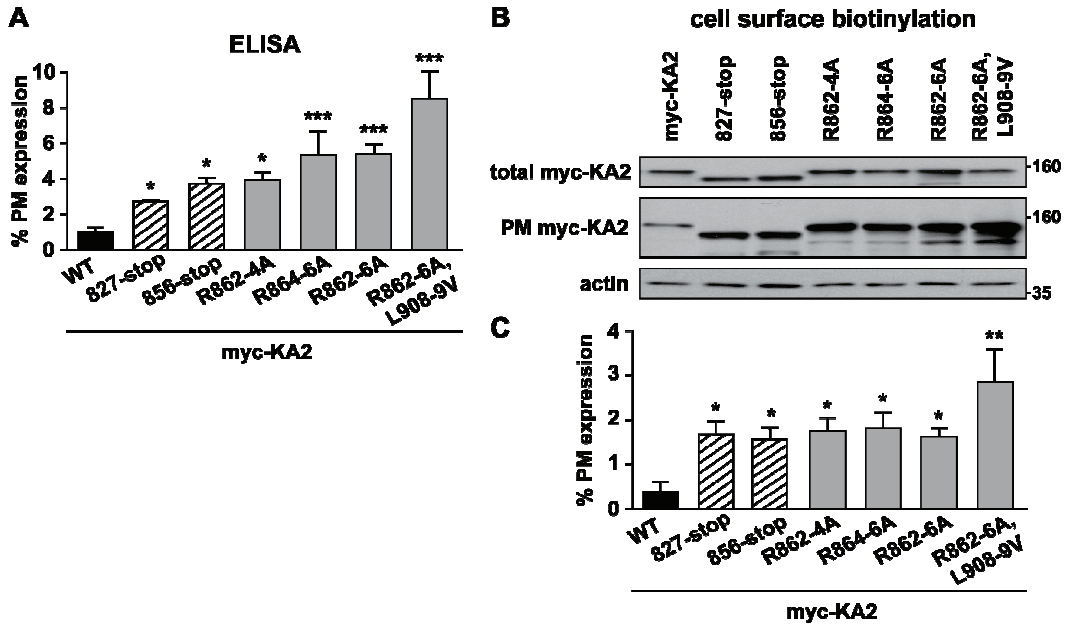

Figure 2.12: Truncation and alanine substitution at the KA2 polyarginine signal increases plasma membrane expression of homomeric myc-KA2 receptors.

A, Cell ELISAs were used to determine the relative level of plasma membrane expression. Anti-myc antibody was used to label plasma membrane receptors (in live cells) or all the KA2 subunits (in permeabilized cells) in parallel sets of transfected COS-7 cells. The relative plasma membrane expression of KA2 subunits increased with truncation and alanine substitution from a basal level of 1.0 ± 0.3% (myc-KA2(827-stop), 2.7 ± 0.1%; myc-KA2(856-stop), 3.7 ± 0.4%; myc-KA2(R862-4A), 3.9 ± 0.4%; myc-KA2(R864-6A), 5.3 ± 1.4%, and myc-KA2(R862-6A), 5.4 ± 0.6%). Myc-KA2(R862-6A,L908-9V) receptors showed the highest plasma membrane expression at 8.5 ± 1.6%. Data represent mean ± s.e.m. (n = 4-8, * $p < 0.05$, and *** $p < 0.001$). *B*, Equivalent experiments in which surface proteins were labeled with biotin and purified on streptavidin columns before immunoblotting. Total myc-KA2 expression was measured by loading 1% of the membrane protein loaded on the streptavidin column. Actin was detected as an additional loading control. *C*, Densitometric quantitation showed the truncated and alanine-substituted mutants were expressed at higher levels on the plasma membrane compared to wildtype receptors (myc-KA2, 0.4 ± 0.2%; myc-KA2(827-stop, 1.5 ± 0.3%), myc-KA2(856-stop, 1.5 ± 0.2; myc-KA2(R862-4A), 1.7 ± 0.3%; myc-KA2(R864-6A), 1.7 ± 0.3%, myc-KA2(R862-6A), 1.5 ± 0.2%; and myc-KA2(R862-6A,L908-9V), 2.7 ± 0.6%)). Data represent mean ± s.e.m. (n = 5, * $p < 0.05$ and ** $p < 0.01$)

c-terminus at either residue 827 or 856 and alanine substitution at residue 862-6 promoted the plasma membrane expression of myc-KA2 receptors as shown in the "PM myc-KA2" lane (Figure 2.12*B*). The relative plasma membrane to total protein expression of myc-KA2 receptors showed a significant increase by 3.6- to 4.1-fold ($n = 5$, $p < 0.05$) in myc-KA2(827-stop), myc-KA2(856-stop), myc-KA2(R862-4A), myc-KA2(R864-6A), and myc-KA2(R862-6A) receptors. Similar to the cell ELISA assay, the myc-KA2(R862-6A,L908-9V) mutant had the highest plasma membrane expression with a 6.7-fold increase ($n = 5$, $p < 0.01$) compared to the wildtype receptors (Figure 2.12*C*). These data are consistent our earlier results that measured plasma membrane expression of a chimeric Tac receptor containing the KA2 c-terminal tail (Ren et al., 2003a).

2.4 DISCUSSION

The intracellular chaperone systems that control assembly and entry of kainate receptors into the secretory pathway are largely unknown. In this study, we elucidated the cellular mechanism for retention of homomeric KA2 kainate receptors in the ER. These receptors do not form functional glutamate receptors when expressed on the plasma membrane, and therefore retention of these subunits contributes to the assembly of appropriately functional heteromeric channels when other KAR subunits are expressed. Endogenous KA2 subunits in the cerebellum, where they are expressed at high levels in granule cells, and exogenous KA2 in transfected cells both associated with COPI proteins in immunoprecipitation assays. The association was dependent upon the arginine-rich determinant in the cytoplasmic tail of KA2 and results in efficient sequestration of KA2 subunits in the ER. We also found that KA2 subunits immunoprecipitated with a variety of endogenous 14-3-3 proteins. As well, association with the 14-3-3ζ isoform was increased by mutations of the arginine-rich COPI interaction site, suggesting that 14-3-3 proteins might play a role in the KA2 biosynthetic pathway. These changes in COPI and 14-3-3 association were correlated with altered plasma membrane expression of KA2 receptors, In summary, our results identify the first set of proteins associated with critical trafficking determinants in kainate receptor subunits.

2.4.1 Regulation of ER localization of homomeric kainate receptor subunits by COPI

The major function of COPI in the intracellular trafficking of proteins is thought to be retrieval of ER-resident proteins from the Golgi back to the ER (Lee et al., 2004). Membrane proteins containing arginine-based trafficking motifs, such as K_{ATP} channels and $GABA_B$ receptors, exhibit an association with COPI inversely correlated with their level of plasma membrane expression (Yuan et al., 2003; Brock et al., 2005). We also found that either the disruption of COPI functionality, in the CHO(ldlF) cells, or a

reduction in KA2-COPI association by mutagenesis was similarly correlated with increased cell surface expression (by 3-8-fold). We note that, despite this significant increase, the large majority of KA2 protein remained in intracellular compartments (predominantly the ER). This suggests other mechanisms exist that limit the forward progress of homomeric KA2 receptors through the biosynthetic pathway. Amongst the possibilities are inefficient folding or oligomerization processes. Indeed, our antibody-based detection assays would not differentiate between KA2 proteins in monomeric, dimeric or tetrameric assemblies, and therefore much of the total KA2 protein we detect in these assays could be in immature forms. Finally, GluR5-2b and GluR5-2c receptors, both of which are largely retained in the ER via arginine-based determinants (Ren et al., 2003b; Jaskolski et al., 2004), did not associate with COPI at a detectable level, suggesting that other retention/retrieval pathways exist for these receptors.

2.4.2 The arginine-rich motif as a COPI interaction domain in homomeric KA2 receptors

The classically defined COPI binding motif consists of a cytoplasmic di-lysine motif K(X)KXX (McMahon and Mills, 2004), but more recent research has demonstrated that the protein complex also mediates arginine-based retention/retrieval mechanisms in a variety of proteins that include Iip35, KCNK3 channels and K_{ATP} channels (Nufer and Hauri, 2003; Michelsen et al., 2005). Importantly, Yuan and colleagues demonstrated that this interaction occurred through a direct binding of the RKR sequence of K_{ATP} channels by COPI proteins, rather than an association through intermediary proteins (Yuan et al., 2003). We found that the string of arginines comprising residues 862-866 in the cytoplasmic tail of KA2 are critical for intracellular retention and immunoprecipitation with COPI vesicle coat proteins. As well, this determinant controlled interaction between β-COP protein and immobilized KA2-Rpep peptide. Thus, the robust interaction between COPI and immobilized peptide and myc-KA2 receptors was significantly reduced upon alanine substitution of all five of the constituent arginines in the trafficking determinants

(by 90 ± 3% and 59 ± 11%, respectively). In contrast, alteration of either the first or last three arginines did not decrease COPI association with myc-KA2 mutants compared to wildtype KA2 subunit. COPI association also was unaffected by added mutation of a di-leucine motif known to play a role in plasma membrane expression of KA2 receptors (Ren et al., 2003a). Interestingly, the residual COPI association remaining after c-terminal truncation or mutation of the arginine trafficking determinant, and the nearly complete absence of binding to the KA2-Apep peptide, suggest that additional COPI association domains exist within the KA2 subunit. These could be located within the c-terminal juxtamembrane domain or in the short intracellular loops between membrane domains. Indeed, the first intracellular loop in the KA2 subunits contains a putative arginine-based retention/retrieval signal -RAR- that could represent the site of residual COPI association. It will be of interest to determine if these residues also promote intracellular retention of KA2 subunits. We thus conclude that COPI vesicle coat proteins are important mediators of the efficient intracellular sequestration of homomeric KA2 proteins via an interaction with the polyarginine determinant, given the similar reduction in the COPI α and β subunit association upon mutation of KA2 at R862-866, the direct interaction of β-COP protein with the KA2-Rpep peptide, the correlation with plasma membrane expression, and the co-localization of KA2 subunits and β-COP in vesicular structures.

2.4.3 Inactivation of COPI binding to KA2 by heteromeric assembly of KARs

In neurons, KA2 subunits are assembled with other KAR subunits to form defined sets of heteromeric receptors that likely are differentially targeted to various membrane domains. We predicted that co-assembly of KA2 with other subunits would relieve COPI-mediated retention, because heteromeric KARs are trafficked to plasma membrane (in heterologous cell lines) and pre- and postsynaptic sites of action (in neurons). This was indeed the case; co-expression of KA2 with GluR6a subunits reduced association of β-COP with KA2 subunits by 64 ± 6%, consistent with the robust plasma membrane expression of heteromeric GluR6a/KA2 receptors. It is likely that the residual interaction between

COPI and KA2 occurred with subunits that had not formed heteromeric assemblies with GluR6a, because the latter subunit was not detectable in the immunoprecipitates isolated with the anti-β-COP antibody. Thus, the arginine-based retention/ retrieval in KA2 becomes occluded upon heteromeric assembly of receptors.

The mechanism of occlusion of the KA2 trafficking determinant upon assembly with GluR6a subunits is obscure. Similar motifs in K_{ATP} channels, the major histocompatibility protein MHC II, NMDA receptors and $GABA_B$ receptors are thought to be sterically masked by heterotypic cytoplasmic domains in other subunits or associated proteins (Michelsen et al., 2005). More recently, Gassmann and colleagues proposed that inactivation of the $GABA_{B1}$ subunit RSRR retention signal upon heteromeric assembly with $GABA_{B2}$ subunits occurred because the determinant was removed from an "active zone" rather than by being masked through coiled-coiled domain interactions (Gassmann et al., 2005). Similarly, we previously reasoned that steric masking of the KA2 signal by cytoplasmic domains of co-assembled kainate receptor subunits (e.g., GluR6a) did not underlie inactivation of the KA2 arginine determinant because GluR6a subunits with truncated c-terminal domains assembled with KA2 subunits and promoted forward trafficking to the plasma membrane (Yan et al., 2004). Our current results further support this interpretation. Heteromeric assembly of KA2 with truncated GluR6a(850-stop) subunits, which contains only 9 amino acids in the c-terminus, markedly decreased COPI binding by 72 ± 9%, demonstrating that the occlusion of COPI binding and resulting release of the heteromeric KAR into the secretory pathway likely did not occur through direct masking by the c-terminus of GluR6a subunits. These observations are most consistent with our hypothesis that structural alterations within the KA2 subunit itself upon assembly with appropriate partner subunits into hetero-oligomers are responsible for occlusion of COPI binding and inactivation of the retention/retrieval signal.

2.4.4 Suppression of arginine-based ER retention/retrieval motif via other chaperone proteins

Inactivation of COPI-dependent arginine-based ER retention/retrieval signals in a number of integral membrane proteins results from competitive binding to cytoplasmic domains by other chaperone proteins, which permits egress from the ER into the secretory pathway. In particular, interactions with 14-3-3 protein family were shown to counteract the COPI associations through both phosphorylation-dependent and phosphorylation-independent mechanisms (Nufer and Hauri, 2003; Michelsen et al., 2005). Several novel binding sites of 14-3-3 proteins overlap with arginine-based ER retention/retrieval motif (O'Kelly et al., 2002; Yuan et al., 2003; Brock et al., 2005). It has been proposed that the association to 14-3-3 proteins competes and prevents COPI binding, leading to the release of proteins from the ER retrieval pathway (O'Kelly et al., 2002; Yuan et al., 2003), although this hypothesis was challenged recently (Brock et al., 2005). 14-3-3 proteins are a widely expressed family of chaperone proteins that subserve a variety of cellular functions including cell cycle and growth control, signal transduction, and apoptosis (van Hemert et al., 2001). Their participation in subcellular trafficking pathways and modulation of the signaling function of ion channels has only recently begun to be elucidated.

Our interest in the potential relevance of 14-3-3 proteins to KA2 subunit trafficking was initiated by low-stringency analysis of protein-protein interactions domains in the KA2 cytoplasmic tail, which identified a putative 14-3-3 binding site overlapping the arginine-based trafficking determinant (Obenauer et al., 2003). Consistent with this prediction, we found that KA2 subunits interacted with multiple 14-3-3 isoforms including those endogenous to the COS-7 heterologous cell line. However, mutagenesis of the polyarginine domain unexpectedly increased 14-3-3ζ binding, effectively eliminating the possibility that a putative association with the KA2 subunit occurs in a directly competitive fashion with COPI (at least at this particular site). The domain in KA2 that mediates association with 14-3-3 proteins has yet to be elucidated. We found that all

mutations to the KA2 C-terminus that increased 14-3-3ζ binding correlated with a higher relative expression on the plasma membrane, even if the mutations did not significantly effect COPI interactions. For example, mutation of the di-leucine motif (Leu residues 908-909), which increases surface expression and 14-3-3ζ association, does not significantly effect COPI binding; this site is a putative endocytic signal and therefore it is possible that reduction in the rate of endocytosis increases pool of KA2 subunits available for interaction with 14-3-3ζ proteins. Because the interaction between KA2, 14-3-3ζ and COPI is correlative in our study, it also is possible that 14-3-3 association with the KA2(R862-6A) and other mutant receptors increased because of greater availability in subcellular compartments not readily accessed in the presence of COPI-mediated retention/retrieval. Thus, the precise role of the association with 14-3-3 proteins in KA2 subunit trafficking remains unclear.

Interestingly, proteomic analysis of proteins associated with GluR6a subunits from mouse brain identified the 14-3-3γ isoform as an interacting chaperone protein, suggesting that this interaction is relevant to kainate receptor trafficking in the central nervous system (Coussen et al., 2005). We did not observe robust interactions between 14-3-3ζ and GluR6a (or GluR5-2b and GluR5-2c), in contrast to KA2 subunit, and therefore postulate that different 14-3-3 isoforms could be involved in heteromeric kainate receptor biosynthesis through interactions with distinct subunits.

In conclusion, COPI vesicle coat association with the arginine-rich trafficking determinant in the KA2 C-terminus leads to the ER localization of these receptors. This ER retention process is inactivated by conformational changes following heteromeric assembly with GluR6 subunits and is inversely correlated with interactions between KA2 and 14-3-3 chaperone proteins. The COPI pathway therefore constitutes an important early pathway for cellular control of KAR subunits and their availability for assembly into functional receptors.

CHAPTER 3: CRITICAL ROLES FOR A TRANSDUCTION LINKER DOMAIN AT MULTIPLE STAGES OF KAINATE RECEPTORS BIOSYNTHESIS

Kainate receptors (KARs) are neuronal proteins that exhibit a highly polarized distribution in the mammalian central nervous system. Biosynthesis, intracellular trafficking, and synaptic targeting of KARs and other ionotropic glutamate receptors are processes controlled, in part, by various determinants within the constituent subunit proteins themselves. Recently, domains traditionally associated with receptor function, such as the ligand-binding and gating domains, were implicated in early steps in KAR biosynthesis. These observations led to a novel hypothesis that postulated the existence of an early checkpoint for egress of either AMPA or KA receptors from the endoplasmic reticulum; this functional checkpoint consists of a glutamate-bound, nonconducting channel conformation analogous to the desensitized state in physiological studies. One implication of this hypothesis is that a direct correlation might exist between desensitization behavior and receptor trafficking. As well, the precise stage of biosynthesis that is disrupted in desensitization mutants is unclear. Here we tested the correlation between GluR6a KAR desensitization properties and plasma membrane trafficking using a series of mutants at two charged residues within the extracellular linker between the third membrane domain (M3) and the S2 region of the ligand-binding domain; mutation of these two sites had opposing effects on desensitization rates of glutamate-evoked currents. We found that intracellular retention of GluR6a receptor mutants did not correlate strongly with their rates or degrees of desensitization, and the reduction in plasma expression in part resulted from significantly attenuated oligomerization and increased degradation rates. Finally, charge swapping of the two adjacent residues normalized the receptor physiological behavior and reversed the deficits in assembly and degradation, but only partially restored plasma membrane expression of the receptors, demonstrating that the linker domain plays a role at both the assembly and

post-assembly stages of biosynthesis. These results are consistent with the existence of a conformationally-specific quality control checkpoint for KAR biosynthesis, but that this process is likely multifactorial and not solely associated with a block of egress of otherwise functional receptors from the ER. This data contributes to understanding the cellular controls of receptor assembly and trafficking that will be important for relating receptor stoichiometry to their neuronal targeting and function.

3.1 INTRODUCTION

The appropriate function of ionotropic glutamate receptors (iGluRs) in excitatory neurotransmission and other fundamental brain processes relies in part on tight cellular control of the earliest stages of receptor biosynthesis. N-methyl-D-aspartate (NMDA), α-amino-3-hydroxy-5-methyl-4-isoxazolepropionic acid (AMPA), and kainate receptor (KAR) subunit proteins contain within their primary amino acid sequences many determinants that influence the rates of assembly, subcellular trafficking, and ultimately the polarized receptor distribution within neurons (Perez-Otano and Ehlers, 2005; Pinheiro and Mulle, 2006; Greger and Esteban, 2007). As well, subunit-dependent interactions with activity-dependent cellular trafficking and signaling systems comprise a major mechanism for control of synaptic plasticity at excitatory synapses (Kennedy and Ehlers, 2006; Derkach et al., 2007). Elucidating the nature of these determinants, and how they are engaged during the lifespan of distinct populations of iGluRs, is necessary for understanding the spectrum of roles played by glutamate receptors in the brain.

Many of the intracellular trafficking determinants in AMPA and KAR subunits are found in the cytoplasmic carboxy-terminal domain (Pinheiro and Mulle, 2006), but recently other elements of the proteins more typically associated with receptor function, such as the pore-forming and ligand-binding domains, were implicated in receptor trafficking behavior. Elimination of glutamate binding caused ER retention of *C. elegans* GLR-1 AMPA (Grunwald and Kaplan, 2003), KA2 kainate (Valluru et al., 2005), and GluR6 kainate receptors (Mah et al., 2005). As well, RNA editing of the Q/R site in the M2 domain of the GluR2 subunit alters trafficking and assembly, as does S2 domain editing and splicing of the flip/flop site in AMPA receptors (Coleman et al., 2006; Greger et al., 2006). These unexpected observations led to the hypothesis that glutamate binding, and associated conformational changes, comprise an early checkpoint that probed the functional state of nascent receptors in the ER. This checkpoint was explicitly proposed to consist of a glutamate-bound, non-conducting conformation analogous to the

physiologically and structurally defined desensitized state of the receptors (Priel et al., 2006). Glutamate binding to the S1-S2 ligand binding domain triggers channel gating and a rapid conformational change to the desensitized state; the associated structural model suggests that desensitization of iGluRs results from the rearrangement of inter-subunit interactions that relieve tension on linker domains, thereby closing the channel pore (Sun et al., 2002). In support of this hypothesis, mutant AMPA and KARs with significantly attenuated desensitization properties traffic poorly to the plasma membrane (Fleck et al., 2003; Greger et al., 2006; Priel et al., 2006; Zhang et al., 2006).

In addition to receptor trafficking, domains that impact receptor function also can have integral roles in other aspects of receptor biosynthesis, including the oligomerization process. Both the membrane domains and the carboxy-terminal portion of the S2 domain are involved in AMPA and kainate receptor assembly, in addition to the N-terminal region of the subunit protein (Ayalon and Stern-Bach, 2001). As well, the amino acid found at the GluR2 Q/R editing site in the M2 P-loop domain, which profoundly influences calcium permeability and single-channel conductance (Huettner, 2003), determines the efficiency of ER export, receptor stability in the ER, and the transition from dimeric to tetrameric quaternary structure of this AMPA receptor (Greger et al., 2002; Greger et al., 2003). Greger and colleagues found more recently that the R/G editing site and neighboring flip/flop slice domain in GluR2 also had a central role in AMPA receptor biosynthesis (Greger et al., 2006). It remains unknown whether analogous domains in KARs play a similar role in controlling the availability of particular subunit isoforms.

We initiated this study to test further the association between the physiological characteristics of iGluR desensitization and early receptor biosynthetic and trafficking events. To achieve this, we examined a series of mutants in the M3-S2 linker domain of the GluR6a KAR subunit. This domain is typically modeled as a critical linker that tranduces ligand binding energy into channel opening, because the relative distance

between the putative position of this domain in resolved dimer structures is correlated with agonist efficacy (Jin and Gouaux, 2003). The actual tertiary structure of the M3-S2 domain is unknown, however, because it is not present in the resolved structures. It was shown previously that mutation of a conserved pair of charged residues (the glutamate-arginine, or ER, site) in this domain in AMPA and KAR subunits increased or decreased the rate of desensitization to varying degrees (Yelshansky et al., 2004), but the resultant consequences for receptor trafficking was not explored. In this study, we examined receptor "ER" mutants to determine how closely changes in desensitization and trafficking behavior are correlated. Our initial results demonstrated only a weak correlation, and for that reason we examined more rigorously the possible underlying mechanisms for the observed reductions in plasma membrane expression of a subset of GluR6a receptor mutants. Surprisingly, we found that alteration of R663 had a significant impact on KAR assembly, degradation rates and receptor trafficking. These and other observation lead us to conclude that the M3-S2 domain, and specifically the arginine at position 663, is engaged at two points in receptor biosynthesis: in the formation of tetramers from dimers, and in a later post-assembly trafficking stage. Thus, this gating domain plays essential roles in multiple stages of KAR biosynthesis.

3.2 MATERIALS AND METHODS

3.2.1 Molecular biology

The myc-GluR6a cDNA was obtained from Dr. Christophe Mulle (Université Bordeaux II, France). Point mutations were generated using QuikChange site-directed mutagenesis protocol (Stratagene, La Jolla, CA). All mutations were submitted to DNA sequencing for verification.

3.2.2 Cell culture and transfection

Hippocampal neuronal cultures were prepared from 18-day embryonic Sprague–Dawley rats as previously described (Banker and Cowan, 1977). Neurons were plated at 120,000 cells/well on poly-L-lysine (1 mg/ml, P1524, Sigma, St. Louis, MO) coated coverslips in 24-well plate. Cultures were maintained in Neurobasal medium plus B27 supplements (Invitrogen, Carlsbad, CA) at 37^{o}C with 5% CO_2. COS-7 cells were cultured in DMEM supplemented with 100 μg/ml penicillin, 100 μg/ml streptomycin, and 10% heat-inactivated fetal bovine serum. Neurons were transfected at day in vitro (DIV) 12-14 using Lipofectamine 2000 (11668, Invitrogen). 2 μg of cDNA was mixed with 4 μl of Lipofectamine 2000 in 100 μl Dulbecco's modified Eagle's medium (DMEM). Coverslips were transferred to new wells and neurons were incubated with this mixture for 4 hours at 37^{o}C. Following the transfection incubation, coverslips were transferred back to their original wells. COS-7 cells were transfected with myc-GluR6a cDNAs using FuGene6 reagent (Roche Applied Science, Indianapolis, IN) following the manufacturer's recommended protocol.

3.2.3 Electrophysiology

Whole-cell patch-clamp recordings were carried out as previously described (Schiffer et al., 1997). Extracellular solution contained 150 mM NaCl, 2.8 mM KCl, 1.8 mM $CaCl_2$, 1.0 mM $MgCl_2$, and 10 mM 4-(2-hydroxyethyl)-1-piperazineethanesulfonic acid

(HEPES) (adjusted to pH 7.3). Intracellular solution contained 110 mM CsF, 30 mM CsCl. 4 mM NaCl, 0.5 mM $CaCl_2$, 10 mM HEPES, and 5 mM ethyleneglycol bis(2-aminoethyl ether)-N,N,N'N'-tetraacetic acid (EGTA) (adjusted to pH 7.3). HEK 293-T/17 cells were transfected with wildtype or mutated myc-GluR6a and enhanced green fluorescent protein (eGFP) cDNAs. Patch electrodes from thick-walled borosilicate glass (Warner Instruments, Hamden, CT) were pulled and fire polished to a resistance of 3-4 mΩ. Transfected cells were lifted from the coverslip into a laminar stream of extracellular solution for fast application of saturation concentrations of glutamate (10-90% rise-time of ~1 ms). Analysis was performed off-line using Clampfit 10 software (Axon Instruments).

3.2.4 Enzyme-linked immunosorbent assay (ELISA)

COS-7 cells were inoculated at 4.7 x 10^4 cells and transfected with 0.6 μg cDNA in 12-well plates. Forty-eight hours post-transfection, cells were washed twice with cold phosphate-buffered saline (PBS) and fixed with 4% paraformaldehyde in PBS at room temperature for 20 min. After fixation, cells were washed 3 times and incubated with anti-myc antibody (1.6 μg/ml, clone 9E10, Roche Applied Science) in 10% goat serum at room temperature for 1 hour to detect plasma membrane expression. For measuring total protein expression, a parallel set of cells were first fixed with paraformaldehyde, permeabilized with 0.2% Triton X-100 in PBS for 5 min, and incubated with primary antibody at room temperature for 1 hour. Both groups were washed 3 times with PBS and incubated with horseradish peroxidase (HRP)-conjugated anti-mouse secondary antibody (1:1000 in 10% goat serum, NA931V, Amersham Biosciences, UK) at room temperature for 1 hour. After the third washing with PBS, the HRP substrate *o*-phenylenediamine dihydrochloride (P9187, Sigma) was added and the color reaction was developed for 1 hour. The optical density of 0.2 ml of supernatant was detected by spectrophotometer at 490 nm. All values were an average of three replicates in each experiment; the mean background absorbances of the negative controls (sham-transfected cells) were subtracted from surface and total absorbance values. Data is presented as a ratio of plasma

membrane expression to total cellular expression. At least three separate experiments were performed with each cDNA.

3.2.5 Immunolocalization of receptors and confocal microscopy

Transfected hippocampal neurons (DIV 14-16) were washed twice with cold PBS and fixed with 4% paraformaldehyde for 20 min. Cells were incubated with a mouse monoclonal anti-myc antibody (4 μg/ml in 2% goat serum) for 1 hour to stain receptors at the plasma membrane. Neurons were then permeabilized with 0.1% Triton X-100 in PBS containing 2% goat serum for 30 min, and incubated with a rabbit polyclonal anti-myc antibody (5 μg/ml, 06-549, Upstate Biotechnology, Waltham, MA) for 1 hour to label total expression of receptors. Cells were incubated with anti-mouse rhodamine (31650, Pierce Biotechnology, Rockford, IL) and anti-rabbit fluorescein (Vector laboratories, Burlingame, CA) for 1 hour. All steps were performed at room temperature and separated by 3 washes with PBS. Coverslips were mounted with ProLong® Gold antifade reagent (P36934, Molecular Probes, Eugene, OR). For colocalization of receptors with organelle markers, transfected COS-7 cells were fixed with 4% paraformaldehyde for 20 min and then permeabilized with 0.2% Triton X-100 for 5 min. Cells were incubated with anti-myc antibody (4 μg/ml in 10% goat serum) for 1 hour, and subsequently incubated with anti-giantin (1:500, Covance, Richmond, CA) for 1 hour. After 3 washes, cells were incubated with appropriate fluorescence-conjugated secondary antibodies: Alexa Fluor 488 or Alexa Fluor 594 (Molecular Probes, Eugene, OR) for 1 hour. All images were taken from an inverted LSM 510 Meta confocal microscope at the Cell Imaging Facility at Northwestern University using a Plan-Apochromat 63X/1.4 oil objective lens with excitation wavelength at 480 and 543 nm. The fluorescence intensity of images was analyzed using Metamorph software (Molecular Devices). A fluorescence intensity threshold was applied to extract the signal above background and regions of interest were created to measure integrated intensity. The plasma membrane expression intensity was divided by the total expression intensity, and the ratio values of each mutant were normalized to the value of wildtype receptors.

3.2.6 Saturation analysis with radioligand binding assays

Crude protein lysates were obtained from transiently transfected COS-7 cells by homogenizing cells in buffer (50 mM Tris HCl and 0.32 M sucrose, pH 7.4) and centrifuging at 800 X g at 4^{o}C for 10 min. The pellet was again resuspended in homogenizing buffer, and the process was repeated twice. The supernatant was re-centrifuged at 20,000 X g at 4^{o}C for 20 min to obtain the crude membrane protein pellet, which was resuspended in 50 mM Tris HCl, pH 7.4. Membrane proteins (25 μg) were incubated with various concentrations of [^{3}H]kainate (NET-875, specific activity 47.0 Ci/mmol, PerkinElmer Life and Analytical Sciences, Boston, MA) at 4^{o}C for 1 hour. Non-specific binding was measured in the presence of 1 mM glutamate. Proteins were harvested by rapid filtration through Whatman GF/C membranes by a Brandel Cell Harvester (Biomedical Research and Development Laboratories, Gaithersburg, MD) followed by three washes with cold 0.9% saline solution. After addition of scintillation fluid, membranes were incubated at room temperature for 1 hour before quantitation on a Beckman LS6000 scintillation counter (Beckman Instruments, Inc., Fullerton, CA). The percentage of bound proteins (% Bmax) was in a range from 34 to 280 cpm/μg. Data was graphed and fitted with a one-site binding (hyperbola) using Prism 4 (GraphPad Software, Inc.).

3.2.7 Endoglycosidase digestion assay

Forty-eight hours after transfection, COS-7 cells were incubated in DMEM medium containing additional 20 mM HEPES at 15^{o}C for 2 hours to block the secretory pathway of proteins as described previously (Kuismanen and Saraste, 1989). Cells were washed twice with PBS and subsequently lysed in 100 μl lysis buffer containing protease inhibitors (50 mM Tris, 150 mM NaCl, 0.5% NP-40, 1 mM 4-(2-aminoethyl)-benzenesulfonylfluoride-HCl, 0.8 μM aprotinin, 20 μM leupeptin, 40 μM bestatin, 15 μM pepstatin A, and 14 μM L-trans-epoxysuccinyl-leucylamido(4-guanidino)butane). Crude protein lysates were centrifuged at 20000 x g for 20 min and supernatants containing membrane proteins were collected. Proteins were denatured and digested with

endoglycosidase H (Endo H, P0702S, New England Biolab, Ipswich, MA) and peptide N-glycosidase F (PNGase F, P0704S, New England Biolab) as described in the manufacturer's recommended protocol.

3.2.8 Immunoblotting and Western analysis

COS-7 cells were plated at 4.7 x 10^4 cells and transfected with 0.4 μg cDNA in 12-well plates. For analysis of denatured proteins, forty-eight hours after transfections proteins were harvested as described in the previous paragraph. 10 μg of cell lysate proteins were denatured by boiling in 2X Laemmli sample buffer (Bio-Rad, Hercules, CA) for 5 min and separated by sodium dodecyl sulfate-polyacrylamide gel electrophoresis (SDS-PAGE). Proteins were electro-transferred onto nitrocellulose membranes using a semi-dry process and were probed with a mouse anti-myc antibody (0.06 μg/ml) and an anti-actin antibody (1:60000, A4700, Sigma). Immunoreactive bands were visualized using HRP-conjugated anti-mouse secondary antibody (1:5000) and quantitated using the ImageJ program (National Institute of Health). Myc-GluR6 protein expression was normalized to actin expression. All experiments were performed at least three times. To examine oligomerization, blue-native PAGE was carried out as described (Schagger et al., 1994) with the following modifications. 10 μg of cell lysate proteins were separated on 3%-12% precast Bis-Tris gels (BN1001Box, Invitrogen), which lack aminocaproic acid. Coomassie blue-G250 was added to the sample (0.25%) and cathode buffer (0.004%) to induce a charge shift on the membrane proteins. NativeMark™ unstained protein marker (LC0725, Invitrogen) was used to calculate relative sizes of GluR6 subunit complexes. Proteins were electro-transferred onto polyvinylidene difluoride (PVDF) membranes. To remove excess Coomassie blue, membranes were briefly washed in methanol and subsequently stained with Ponceau S dye to visualize the molecular weight of markers before immunoblotting.

3.2.9 Pulse-chase assay

COS-7 cells were plated in 60 mm dishes at 5 x 10^5 cells and transfected with 2 μg cDNA using FuGene6 reagent. Thirty-six hours after transfection, COS-7 cells were incubated in cysteine- and methionine-free DMEM starvation media (21013-024, Invitrogen) for 30 min. Starvation media was removed and replaced with DMEM labeling media containing EXPRE^{35}S^{35}S protein labeling mix (100 μCi/dish, NEG072007MC, PerkinElmer Life Sciences) and brefeldin A (10 μg/ml, Sigma). After 30 min, cells were rinsed twice with PBS and returned to normal growth media including brefeldin A (10 μg/ml) for the duration of the chase times. At each specified time point, cells were washed twice with ice-cold PBS and incubated on ice for 10 min in the lysis buffer with protease inhibitors. Proteins from the cell lysate were immunoprecipitated with a mouse anti-myc antibody (1.2 μg/ml) and 40 μl of 50% protein A/G sepharose slurry (20422, Pierce Biotechnology). Proteins were subsequently separated by SDS-PAGE gel. The radiolabel bands were quantified on a Personal Molecular Imager (Bio-Rad). The measured densities at each time point were normalized to the image density at time point zero. Data was graphed and fitted with a one-phase exponential decay using Prism 4 program.

3.2.10 Statistical analysis

All data were tested by one-way analysis of variance (ANOVA) and the Tukey-Kramer multiple comparison test as a post hoc or two-tail paired T-test.

3.3 RESULTS

3.3.1 Mutations in the M3-S2 transduction linker affect receptor desensitization and plasma membrane expression of GluR6a kainate receptors

In order to test the relationship between desensitization behavior and kainate receptor trafficking, we first mutated two charged residues, E662 and R663, in the M3-S2 transduction linker of the GluR6a kainate receptor (Figure 3.1). We chose to examine these conserved residues because their mutation in an AMPA receptor subunit in a previous study produced receptors with a variety of desensitization rates (Yelshansky et al., 2004). Conservative and non-conservative mutations were made to E662 and R663 (to A, C, Q, S at both sites, D and R at E662, and E and K at R663, Figure 3.1), before characterizing functional properties using patch-clamp recordings of glutamate-induced

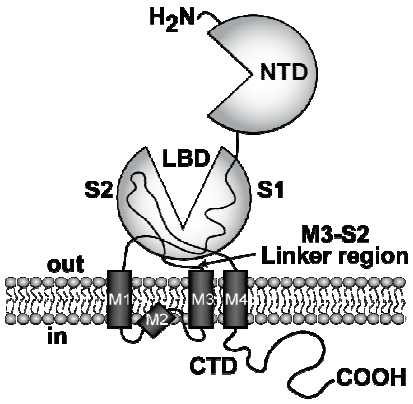

		M3	M3-S2 linker	S2
GluR1	611	SYTANLAA	FLTVERMVS	PIESAE
GluR2	615	SYTANLAA	FLTVERMVS	PIESAE
GluR5	650	SYTANLAA	FLTVERMES	PIDSAD
GluR6	650	SYTANLAA	FLTVERMES	PIDSAD
GluR7	652	SYTANLAA	FLTVERMES	PIDSAD
KA1	635	SYTANLAA	FLTVQRMEV	PIESVD
KA2	634	SYTANLAA	FLTVQRMES	PVESAD

Figure 3.1: The M3-S2 linker in ionotropic glutamate receptors.

Illustration of the domain structure of kainate receptors and other ionotropic glutamate receptors; the arrow indicates the region that contains the residues studied in this report. Abbreviations: NTD, amino-terminal domain; LBD, ligand-binding domain; M, membrane domains; CTD, carboxy-terminal domain. An alignment of M3-S2 linker sequences in selected AMPA and kainate receptor subunits is also shown, with our mutation sites in the black background.

currents from transfected HEK 293-T/17 cells. Rapid application of saturating concentrations of glutamate (10 mM, 100 ms) to wildtype and mutant GluR6a receptors elicited inward currents of varying amplitudes that subsequently desensitized. Similar to previous reports, the current decay in wildtype GluR6a receptors was well-fitted with a single exponential function that yielded a mean τ value of 4.2 ± 0.2 ms (n = 10), and the currents desensitized by 99.2 ± 0.3% (Swanson et al., 1997; Yelshansky et al., 2004).

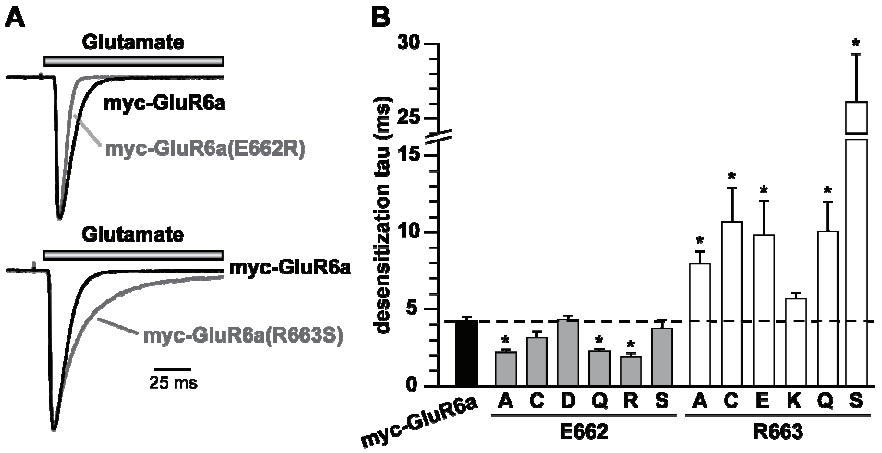

Figure 3.2: Mutation of E662 and R663 in the myc-GluR6a subunit had opposite effects on kinetics of desensitization.

A, Examples glutamate-evoked currents from myc-GluR6a and myc-GluR6a(E662R) (top) or GluR6a(R663S) (bottom) receptors. Receptors were expressed in HEK 293-T/17 cells and patch-clamp recordings were carried out at a holding potential of -70 mV. Glutamate (10 mM) was rapidly applied for 100 ms. Sample traces from the mutant receptors were scaled to the peak amplitude of myc-GluR6a currents to illustrate the difference in desensitization rates. *B*, Desensitization τ values derived from single-exponential fits to the current decay in the presence of glutamate for all the receptors in this study. Myc-GluR6a(R663S) was best-fit with two exponential compounds; the value shown is a mean tau weighted for the contribution of both exponential decay components. Wildtype myc-GluR6a receptors desensitized with a τ_{des} of 4.2 ± 0.2 ms. The τ values of E662- and R663-substituted mutants were 2.1-4.3 ms and 5.6-26.1 ms, respectively (n = 3-7, *, $p < 0.05$). Application of glutamate to myc-GluR6a(R663E) receptors failed to elicit a current in 26 of 29 transfected cells. Data represent mean ± s.e.m.; individual values are given in Table 3.1.

Receptor	τ_{des} (ms)	%des	%PM expression COS-7	neurons
myc-GluR6a	4.2 ± 0.2	99.7 ± 0.1	85.6 ± 2.7	100.0 ± 5.0
E662A	***2.2 ± 0.2***	99.8 ± 0.1	84.2 ± 4.8	ND
E662C	3.1 ± 0.4	99.2 ± 0.3	80.9 ± 6.8	ND
E662D	***4.3 ± 0.3***	99.7 ± 0.1	63.4 ± 5.3	96.3 ± 15.8
E662Q	***2.3 ± 0.1***	99.2 ± 0.6	87.1 ± 3.3	ND
E662R	***2.0 ± 0.2***	99.5 ± 0.2	91.8 ± 5.6	101.8 ± 10.9
E662S	3.5 ± 0.4	100.0 ± 0.1	94.0 ± 11.8	ND
R663A	***9.1 ± 2.4***	***78.8 ± 5.3***	***13.3 ± 1.0***	***12.2 ± 6.7***
R663C	***10.6 ± 2.3***	***89.3 ± 2.7***	***13.5 ± 1.3***	***19.7 ± 9.7***
R663E	***9.8 ± 2.1***	***81.8 ± 9.5***	***3.6 ± 1.2***	***3.9 ± 2.7***
R663K	5.6 ± 0.5	98.8 ± 0.2	80.4 ± 5.9	121.4 ± 5.2
R663Q	***10.1 ± 2.9***	99.1 ± 0.2	***37.8 ± 2.0***	***58.6 ± 8.3***
R663S	***26.1 ± 3.3***	92.1 ± 2.2	***21.2 ± 2.0***	***25.2 ± 6.3***
E662R,R663E	4.3 ± 0.1	99.4 ± 0.1	***30.4 ± 0.8***	***35.2 ± 6.0***

Table 3.1: Desensitization properties and plasma membrane expression of GluR6a(E662) and GluR6a(R663) mutants.

The desensitization rate and the degree of desensitization of glutamate-evoked currents were measured in patch-clamp recordings as detailed in the Methods (n = 3-10). Relative plasma membrane localization of receptors in COS-7 cells and cultured hippocampal neurons were analyzed using cell ELISAs (n = 3 with the exception of myc-GluR6a, n = 6) and immunofluoresecence (n = 4-8), respectively. Data represent mean ± s.e.m. Values that are statistically different ($p < 0.05$) from myc-GluR6a are shown in bold italics. Abbreviations: PM, plasma membrane; ND, not determined.

The majority of GluR6a E622 mutants desensitized more rapidly than wildtype receptors, whereas the converse was true for R663 mutant receptors (Figure 3.*2A* and 3.2*B*). Sample traces from three recordings, myc-GluR6a, myc-GluR6a(E662R), and myc-GluR6a(R663S), are shown in Figure 3.2*A*; mutant receptor currents have been scaled up in order to compare the relative time courses of desensitization. Substitution of E662 with either neutral amino acids (A, C, Q) or with a positively charged residue (R) significantly increased the rate of entry into the desensitized state, with τ_{des} values ranging from 2.0 to

3.1 ms (n = 3-7); only the conserved E662D and polar E662S substitution mutants had desensitization rates similar to that of wildtype receptors. All myc-GluR6a E662 receptor mutants desensitized nearly completely (by >99.0%, n = 3-7, see Table 3.1 for desensitization rates and percentages of desensitization). In contrast, substitutions at R663 slowed down the desensitization rate to various extents, with the exception of the conservative R663K mutation. Myc-GluR6a(R663S) receptors exhibited the slowest rate of desensitization (26.1 ± 3.3 ms, n = 4; Figure 3.*2A* and 3.2*B*) and did not completely desensitize (92.1 ± 2.2%). In addition to their slower desensitization rates, several of the 663 mutants (R663A, R663C, and R663E in particular) gated currents that desensitized to a significantly lesser degree (78.8 - 89.3%, n = 3-5) and were of considerably lower amplitude than GluR6a receptors, suggesting that a functional, trafficking or biosynthetic deficit existed for these mutants.

The relative level of plasma membrane expression of these receptors was determined next in cell ELISA assays. We found that 86.1 ± 5.0% of the total GluR6a protein was localized to the plasma membrane of transfected COS-7 cells (n = 6), consistent with the presence of an effective forward trafficking motif in the carboxy terminal domain (Yan et al., 2004). Mutation of myc-GluR6a at E662 had little or no effect on this distribution, with only the E662D mutant exhibiting a modest reduction in surface expression (Figure 3.3 and see Table 3.1 for percentages of plasma membrane localization). In contrast, all R663 mutants, again with the exception of the lysine substitution, greatly diminished the plasma membrane expression of myc-GluR6a receptors. GluR6a(R663E), in particular, was reduced by 24-fold so that only 3.6 ± 1.2% of the receptor was localized to the plasma membrane (n = 3, $p < 0.001$). Substitution of R663 with alanine, cysteine or serine also significantly reduced myc-GluR6a receptor plasma membrane expression 4-6-fold (n = 3, $p < 0.001$). Myc-GluR6a(R663Q) receptors were expressed at 37.8 ± 2.0% on the cell surface, a reduction of ~2-fold (n = 3, $p < 0.001$). Thus, all the receptors with slowed desensitization rates had reduced surface expression, whereas trafficking was largely unaffected for those receptors with increased rates of desensitization.

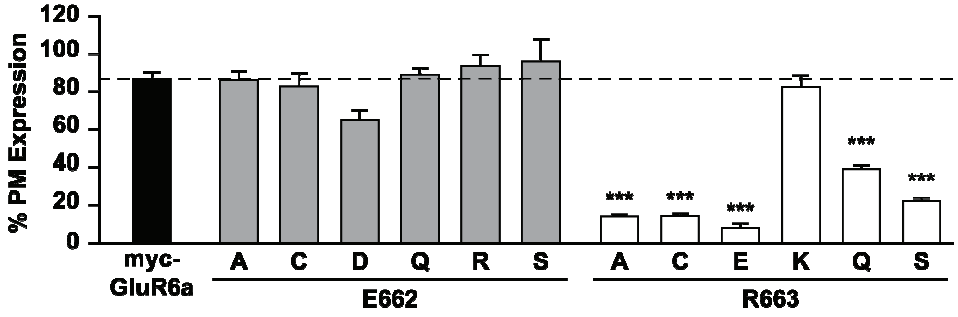

Figure 3.3: Elimination of positive charge at residue 663 in the M3-S2 linker reduced plasma membrane localization of myc-GluR6a receptors.

Plasma membrane expression of myc-GluR6a, E662, and R663 mutants were quantitated by cell ELISA assays in transfected COS-7 cells. Wildtype myc-GluR6a receptors showed 85.6 ± 2.7% (n = 6) plasma membrane localization relative to total protein expression. Myc-GluR6a(E662) mutants were localized to the plasma membrane at near-wildtype levels, from 63.4 to 94.0% (n = 3-4), whereas all myc-GluR6a(R663) mutants, with the exception of R663K, showed significantly lower cell surface expression (3.6 to 37.8%, n = 3 for all mutants, ***, $p < 0.001$ compared to wildtype receptors; individual values given in Table 3.1). Data represent mean ± s.e.m.

These patterns of plasma membrane expression were reproduced in transfected hippocampal neurons as measured using relative immunofluorescence (Figure 3.4 and Table 3.1). In these experiments, plasma membrane-localized receptors were labeled with primary antibody before permeabilization of the neurons to detect total receptor protein; distinct flourophore-conjugated secondary antibodies facilitated visualization of total (green) and plasma membrane (red) myc-tagged receptors. We found myc-GluR6a(E662D), myc-GluR6a(E662R) and myc-GluR6a(R663K) receptors highly expressed in neuronal plasma membranes. Substitution of R663 with alanine, cysteine, glutamate, and serine greatly decreased cell surface expression of mutant receptors compared to wildtype receptors, by 4- to 26-fold (measured as the relative intensity of red to green fluorescence, n = 4-8, $p < 0.001$). Similar to the ELISA results, R663Q mutants had only modestly decreased plasma membrane expression by ~2-fold (n = 7, $p < 0.01$) (Figure 3.4).

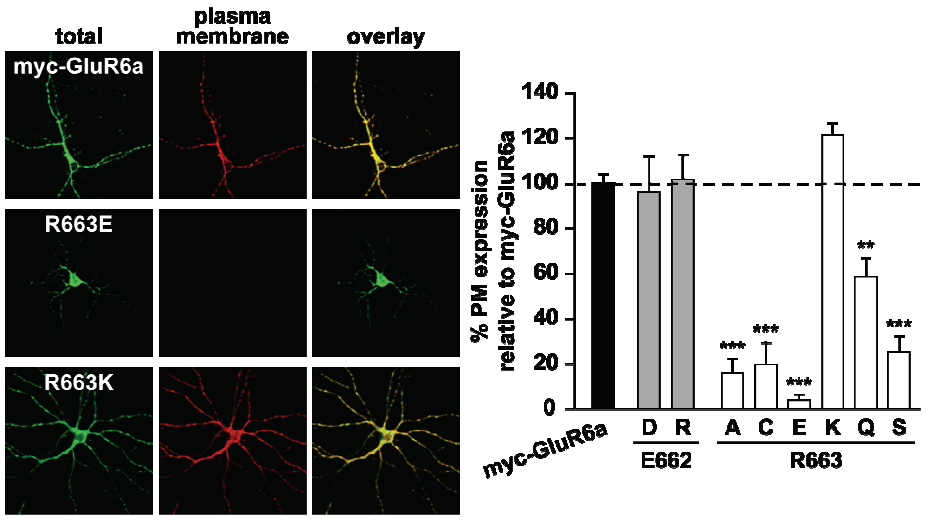

Figure 3.4: Elimination of the positive charge at residue 663 in the M3-S2 linker reduced plasma membrane localization of neuronal myc-GluR6a receptors.

Confocal images of myc-GluR6a, R663E and R663K receptors in transfected hippocampal neurons. Total expression of myc-GluR6a receptors was detected after permeabilization (left column, green). Plasma membrane localized receptors were detected under non-permeabilized conditions (middle column, red). GluR6a(R663E) was largely absent from the plasma membrane. These results and data from other receptor mutants were quantitated by calculating the ratio of red to green fluorescence intensity; E662D, E662R, and R663K mutants exhibited the same level of plasma membrane expression as myc-GluR6a receptors (0.96-1.21, n = 3-4). In contrast, other R663 substitutions caused profound reductions in neuronal membrane receptors (0.04-0.59, n = 3-8, **, $p < 0.01$, ***, $p < 0.001$ compared to wildtype receptors; individual values given in Table 3.1. Data represent mean ± s.e.m.

To determine if the physiological desensitization properties played a role in the intracellular trafficking of kainate receptors, we correlated the rate (Figure 3.5A) and degree (Figure 3.5B) of desensitization with the plasma membrane expression of the wildtype GluR6a and linker mutants. We found that plasma membrane expression of GluR6a kainate receptors was weakly correlated with their rate of desensitization and

percentage of desensitization (r^2 = 0.46 and 0.52, respectively, Figure 3.5), suggesting that the desensitization properties of the receptors plays a small but not exclusive role in controlling the level of plasma membrane expression.

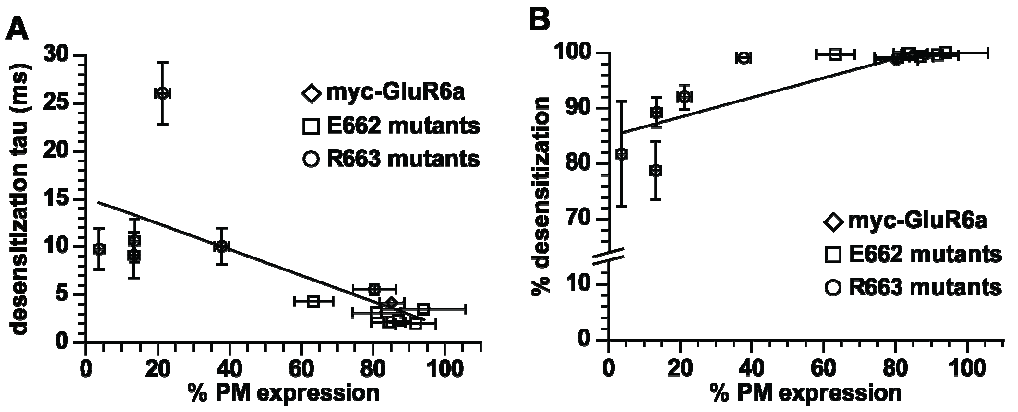

Figure 3.5: Correlation of desensitization properties and plasma membrane expression of GluR6a receptor mutants.

A, Each point represents the wildtype or mutant receptors and values are as given in Table 3.1. Plasma membrane expression plotted against desensitization rates. The line shows the linear correlation, which had an r^2 value of 0.46. *B*, Plasma membrane expression plotted against the degree of desensitization (percent reduction in peak current amplitude). The line shows the linear correlation, which had an r^2 value of 0.52.

3.3.2 Effects of mutation of E662 and R663 on other aspects of GluR6a receptor biosynthesis

We inferred from the weak correlation that additional factors in the biosynthesis of the KARs contributed to the reduction in plasma membrane expression of R663 mutants. To begin to explore possible mechanisms, we first examined the relative levels of equilibrium GluR6a receptor protein expression in transfected COS-7 cells using SDS-PAGE and Western blots (Figure 3.6*A*). To quantitate the Western blots, the band densities of myc-GluR6a proteins were normalized to the density of actin protein with the

same cells. Three mutants, myc-GluR6a(R663A), R663C, and R663E, exhibited a significantly reduction in equilibrium expression, by 40-50%, compared to wildtype receptors (n = 7, $p < 0.05$). This observation could also be explained simply by reduced transfection efficiency for these cDNAs, but it is noteworthy that these three receptor mutants correspond to those with the most significantly impacted plasma membrane expression, whereas the receptor mutant with the greatest change in desensitization properties, R663S, is expressed at equilibrium levels similar to that of wildtype GluR6a.

It is possible that alteration of the M3-S2 linker domain, and the resultant effect on desensitization properties, might also have had secondary effects on the affinity of the receptors for glutamate, because it is known that the ligand affinity is influenced by inter-domain and inter-subunits interactions in iGluRs (Stern-Bach et al., 1998; Weston et al., 2006a). We measured binding affinity of these mutants for [^{3}H]kainate. Membrane proteins were isolated from COS-7 cells expressing recombinant myc-GluR6a, R663A, R663E, or R663Q receptors. The dissociation constant (K_D) of [^{3}H]kainate in myc-GluR6a receptors was 25.2 ± 6.8 nM (Figure 3.6*B*), consistent with previous reports (Tygesen et al., 1994; Mah et al., 2005). Saturation binding isotherms and the K_D showed that myc-GluR6a(R663A), R663E and R663Q had similar [^{3}H]kainate affinities to that of wildtype receptors, with K_D values measured at 45.4 ± 10.4, 24.0 ± 5.4 and 36.8 ± 5.8 nM, respectively (n = 3). Thus, the reduced plasma membrane expression of these mutants was not caused by altered agonist-binding affinity.

We next determined if the reduced plasma membrane expression of GluR6a(R633E) occurred through sequestration in a pre-Golgi compartment by examining the subcellular distribution in co-localization assays in transfected COS-7 cells. Myc-GluR6a receptors were detected with an anti-myc antibody (green color) and giantin, a Golgi-resident protein, was stained with an anti-giantin antibody (red color). As shown in the last row of images in Figure 3.7*A*, wildtype receptors were highly colocalized with the Golgi marker (yellow color). In contrast, myc-GluR6a(R663E) receptors were predominantly

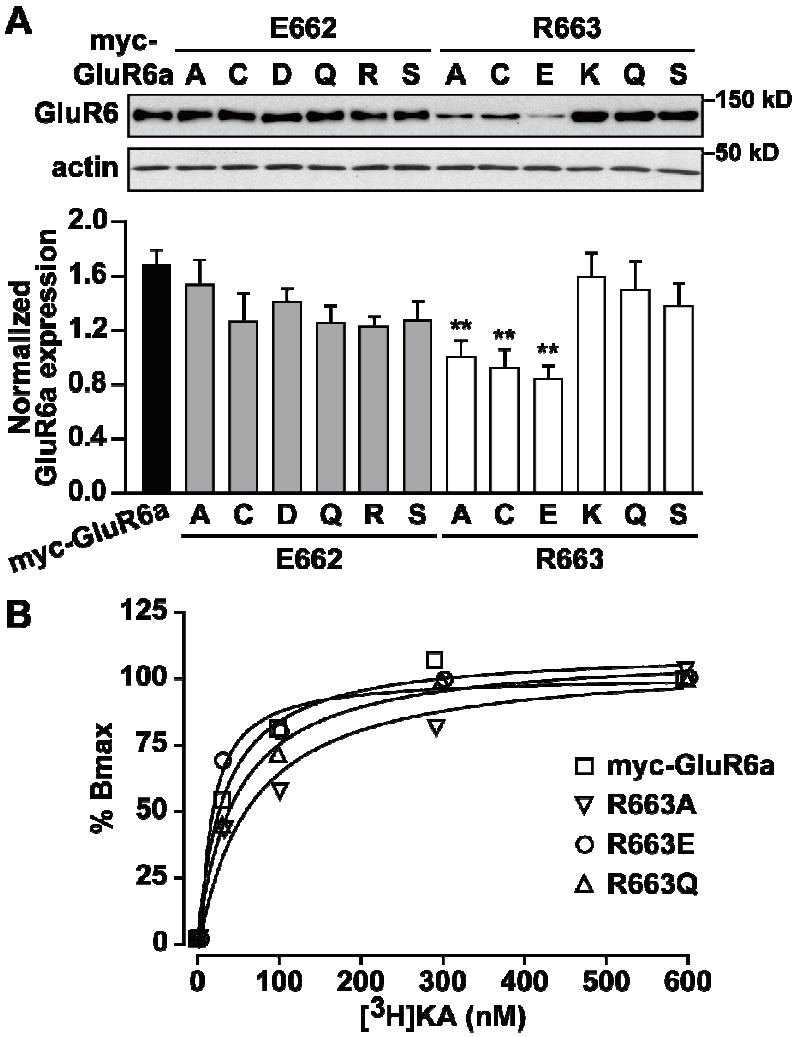

Figure 3.6: Total protein expression of GluR6a linker domain mutants and analysis of agonist-binding affinity.

A, Total protein levels were significantly lower for only three receptor mutants - R663A, R663C, and R663E - in Western blots with an anti-myc antibody (n = 3-8, ** $p < 0.01$). Actin immunoreactivities were detected as loading controls and quantitation normalized the receptor band densities to that of the corresponding actin control. *B*, Saturation binding experiments of myc-GluR6a subunits demonstrates that ligand-binding affinity was not altered by mutagenesis of the linker domain (K_D 45.4 ± 10.4, 24.0 ± 5.4 and 36.8 ± 5.8 for R663A, R663E, and R663Q, respectively, n = 3). Data were fitted with one-site binding curves.

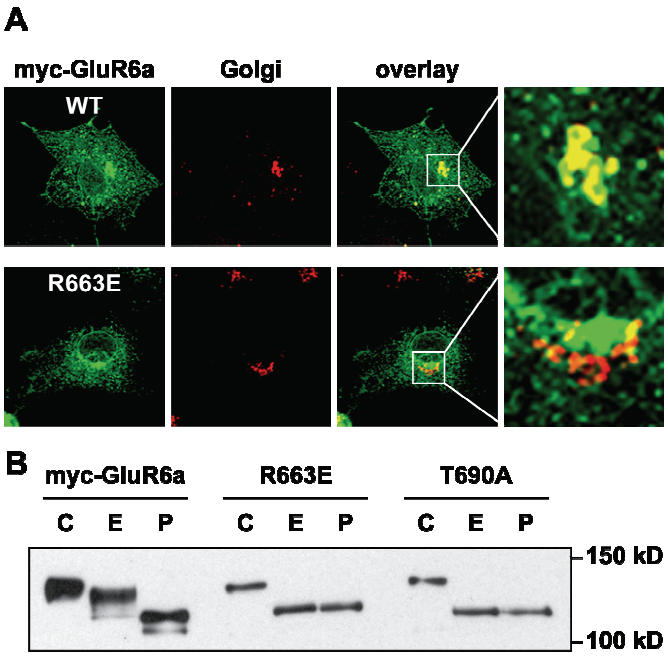

Figure 3.7: GluR6a(R663E) linker mutants are retained in the ER.

A, Myc-GluR6a receptors, but not R663E mutants, co-localized with a Golgi maker in immunofluorescence labeling of transfected COS-7 cells (myc immunoreactivity, green; giantin, red; overlay, yellow). *B*, Myc-GluR6a receptors, but not R663E or T690A mutants, exhibit an Endo H-resistant band following digestion with the glycosidase. This is evident in the myc-GluR6a lanes because the Endo H-digested protein (E) is a higher molecular weight than the PNGase F digested protein (P), which represents the completely de-glycosylated form of the receptor subunit. In contrast, the molecular weight of myc-GluR6a(R663E) and T690A subunits were identical in the Endo H and PNGase F lanes, indicating that neither mutant was processed in the Golgi complex. Abbrevations: C, control undigested proteins; E, Endo H digested; P, PNGase F digested.

not colocalized with the marker, suggesting that this mutant did not traffic to the Golgi. As expected the mutant receptor was co-localized to a high degree with the ER marker protein disulphide isomerase (data not shown). These qualitative results were substantiated in assays that compared the glycosylation state of wildtype, R633E, and the ligand binding mutant GluR6a(T690A), which was previously shown to be sequestered in the ER (Mah et al., 2005). Resistance to endoglycosidase H (Endo H) is commonly used

as a diagnostic assay for transit of glycoproteins through the medial Golgi, In contrast, peptide N-glycosidase F (PNGase F) enzyme completely cleaves all the oligosaccharides. For these experiments we enhanced the degree of glycosylation by trapping receptors in pre-*trans*-Golgi network compartments with a low temperature incubation (15^{o}C) prior to isolating membrane protein for treatment with glycosidase. A comparison of control (undigested, "C"), Endo H digested ("E") and PNGase F digested ("P") myc-GluR6a receptor demonstrated that the wildtype protein was substantially resistant to Endo H digest, whereas digest with Endo H and PNGase F produced indistinguishable lower-molecular weight bands with R633E and T690A (Figure 3.7*B*), consistent with interpretation that biosynthesis of these receptor mutants was arrested at a compartment upstream of the medial Golgi complex. The observation that both mutants were modified with immature, Endo H-sensitive mannose residues demonstrates that the mutations did not generally occlude *N*-glycosylation.

3.3.3 Mutation of R663 disrupts subunit assembly of GluR6a receptors

To test if inefficient assembly of GluR6a KARs contributed to the reduction in plasma membrane expression of linker domain mutants, we compared the oligomerization state of wildtype GluR6a and R663 mutants two days after transfection using blue-native PAGE and Western blotting. Under non-denaturing conditions, myc-GluR6a receptors (detected with anti-myc antibody) appeared as four distinct bands in Western blots and densitometric line scans (Figures 3.8*A* and 3.8*B*). The most prominent band had a molecular weight approximately that of a tetrameric assembly of GluR6a subunits when calibrated with a standard curve of native molecular weight markers fitted with a one-phase exponential decay (Figure 3.8*C*). Other bands present on the BN-PAGE correlated well with predicted molecular weights of monomers, dimers, and trimers. The presence of a small but reproducible population of trimers was reported previously for GluR6a kainate receptors (Mah et al., 2005) but was not observed with GluR2 AMPA receptors

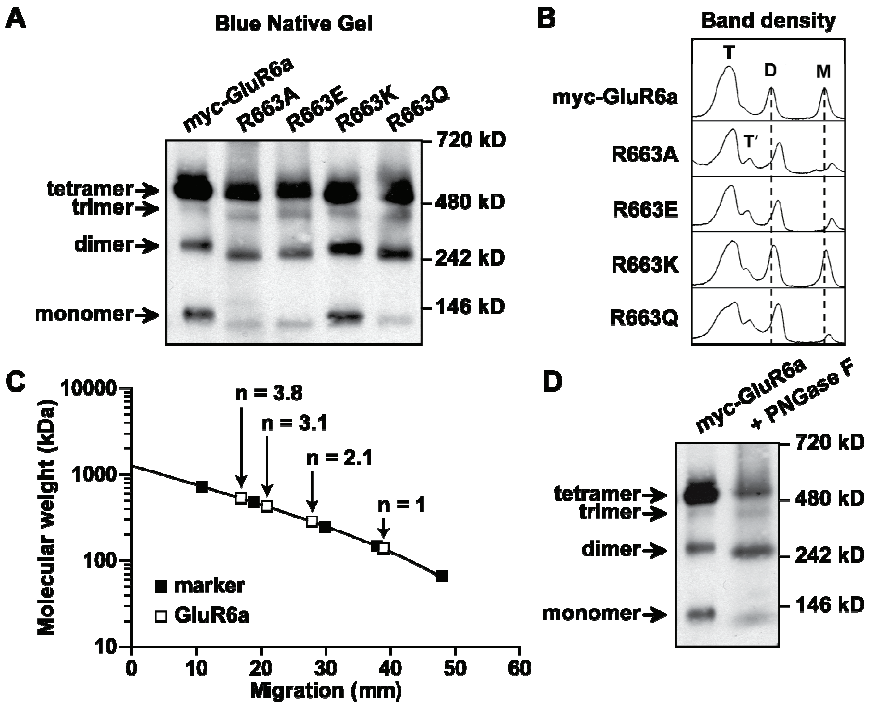

Figure 3.8: Mutation of residue R663 did not alter tetramerization of GluR6a receptors at equilibrium.

A, Oligomeric states of myc-GluR6a and myc-GluR6a(R663) mutants was analyzed following separation of non-denatured receptor protein on a 3-12% Bis-Tris gradient gel. Proteins were detected with anti-myc antibody in Western blots. Proteins were harvested from COS-7 cells at 48 hours post-transfection. The receptor proteins were separated into four primary bands with molecular weights predicted to correspond to monomers, dimers, trimers, and tetramers. *B*, Densitometric line scans of bands in panel 3.8*A* reveal the density profiles used to measure the migration of the predominant protein bands. Abbreviations: T, tetramer; T′, trimer; D, dimer; M, monomer. *C*, Native molecular weight markers (dark squares) electrophoresed on the same gel as the receptor proteins were used to generate a standard curve consisting of a one-phase exponential decay fitted to the data. Migration distances of the predominant bands of the myc-GluR6a receptors were then used to estimate the molecular weights based on the standard curve (empty squares). From the molecular weight of the monomeric subunit, the larger bands were composed of 2.1 subunits (dimer), 3.1 subunits (trimer) and 3.8 subunits (tetramer), confirming our tentative assignment of quaternary structure in panel 3.8*A*. *D*, Deglycosylation of myc-GluR6a receptors with PNGase F caused a shift in molecular weights of monomer and dimer bands to molecular weights similar to those observed in myc-GluR6a(R663A), R663E, and R663Q receptors.

(Greger et al., 2003), suggesting that the dimer-of-dimer assembly paradigm is less stringent for KARs than for AMPA receptors. The assembly patterns of myc-GluR6a(R663A), R663E and R663Q mutants were quite similar to the wildtype receptors with the exception that the dimers and monomers of these mutants, which had lower cell surface expression, showed notably lower molecular weights (Figures 3.8*A* and 3.8*B*). In contrast, the monomer and dimer bands for R633K were identical to that of GluR6a, demonstrating that a correlation existed between the shifted molecular weights and trafficking behavior in cell ELISAs. The difference between monomeric and dimeric molecular weights could be ascribed to reduced glycosylation of the R633 mutants because treatment of wildtype receptors with PNGase F before BN-PAGE reproduced the difference in molecular weights between GluR6a and R633 mutants (Figures 3.8*D*).

We hypothesized that the R663 mutation could affect the rate of tetramerization of GluR6a receptors, which might not have been apparent in the preceding set of experiments because receptor expression, assembly, and degradation had likely reached an equilibrium state two days after transfection. To test this possibility, we examined the rate of receptor assembly by carrying out similar BN-PAGE analysis at earlier time points after transfection (12, 18 and 24 hours). We also tested for myc-GluR6a subunit expression at 6 hours post-transfection but did not detect myc-tagged receptors in Western blots (data not shown). For these experiments, we again included as a control the ligand-binding mutant T690A, which previously was shown to assemble as tetramers (Mah et al., 2005). Twelve hours after transfection, only tetramers of wildtype myc-GluR6a receptors were detected (Figures 3.9*A* and 3.9*B*); no expression of R633E was detectable and the T690A mutant exhibited very weak expression of all four stoichiometric assemblies as well as larger molecular weight aggregates. The pattern of assembly diverged significantly at 18 and 24 hours post-transfection. Myc-GluR6a receptors were predominantly assembled as tetramers, consistent with the high proportion of functional, plasma membrane-localized receptors. In contrast, dimers were the most prominent quaternary structure of R633E subunits, and formation of tetramers proceeded

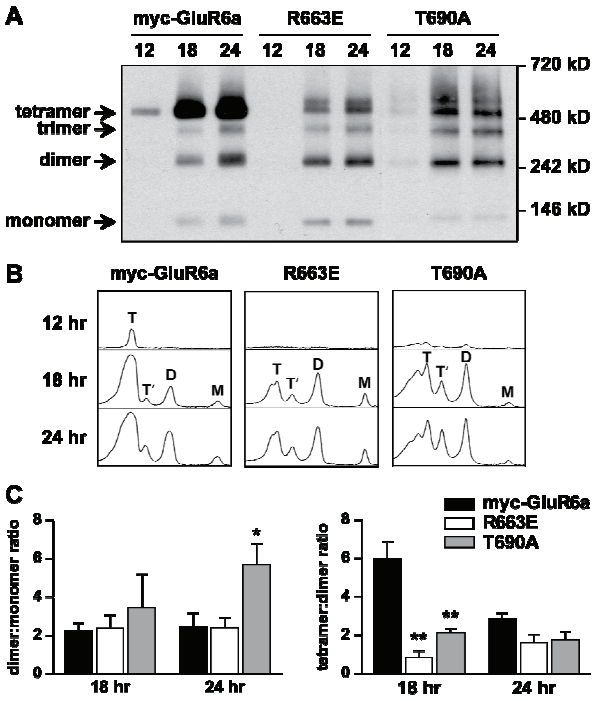

Figure 3.9: Reduced efficiency of tetrameric assembly of GluR6a receptor subunits mutated at both the M3-S2 linker and the ligand-binding domain.

A, Non-denaturing PAGE and Western blots for anti-myc immunoreactivity were used to assess the assembly states of myc-GluR6a, GluR6a(R663E) (linker mutant) and GluR6a(T690A) (ligand-binding mutant) receptors at relatively early time points (12, 18 and 24 hours) following transfection of COS-7 cells. Wildtype myc-GluR6a receptors were predominantly observed as tetramers at all time points after transfection. In contrast, the dimeric form was predominant for R663 at 18 hours post-transfection. T690A also showed significantly lower proportional representation of the tetrameric structure at the 18 hour time point. *B*, Densitometric line scans of band densities shown in Figure 3.9*A*. The areas under each peak were integrated to determine the percentage of monomers, dimers, trimers, and tetramers. *C*, *Left,* Dimer:monomer ratios of integrated areas from densitometric scans were not significantly different at 18 hours post-transfection, but at 24 hours the T690A mutant showed a larger proportion of dimers (5.7 ± 1.1 versus 2.5 ± 0.7 for myc-GluR6a, n = 3, *, $p < 0.05$). *Right*, Tetramer:dimer ratios of integrated areas from densitometric scans for myc-GluR6a(R663E) and T690A (0.8 ± 0.4 and 2.1 ± 0.2, n = 3, respectively) were greatly reduced compared to wildtype receptors at 18 hours after transfection (6.0 ± 1.0; **, $p < 0.01$). No difference in this ratio was apparent at 24 hours post-transfection. Data represent mean ± s.e.m.

only modestly even at 24 hours post-transfection. Densitometric line scans showed that the ratio of dimer to monomer forms of the myc-GluR6a(R663E) receptors was equivalent to that of myc-GluR6a at both 18 and 24 hours post-transfection, suggesting that mutation of 663 did not impose a barrier to formation of the dimeric structure. In contrast, the tetramer to dimer ratio was significantly lower, by 86.7%, for the mutant receptor compared to wildtype receptors at 18 hours post-transfection (n = 3, $p < 0.05$) (Figure 3.9*C*). Dimeric forms of the myc-GluR6a receptor accumulated at the later time point (24 hours), possibly as a result of saturation of biosynthetic pathways, leading to equivalent relative levels of tetramers and dimers as that seen with the R663E mutant. Assembly of T690A was distinct from either GluR6a or R633E, in that an increased dimer:monomer ratio was observed at 24 hours post-transfection, whereas the transition to tetramers was impeded to a similar degree (65%) as GluR6a(R633E) at the 18 hours time point (n = 3, $p < 0.01$). GluR6a(T690A) receptors also exhibited a substantial proportion of larger molecular weight complexes and smearing of the protein bands at the later time points, suggesting that this ligand binding mutant was subject to aggregation or protein misfolding (Figure 3.9*C*). These data demonstrate that the both the M3-S2 linker domain and the ligand binding site are important determinants of the rate of GluR6a KAR oligomerization, and that trapping of subunits in pre-tetrameric complexes partially underlies the reduction in plasma membrane expression of the receptors.

3.3.4 Mutations in the transduction linker increase the degradation rate of GluR6a receptors

The existence of assembly intermediates and, in the T690A mutant most apparently, misfolded and aggregated protein complexes, suggested that the ER-associated degradation system (ERAD) might be engaged to clear assembly-compromised KARs. To measure the degradation rate of GluR6a and receptor mutants, we performed pulse-chase assays followed by immunoprecipitation, SDS-PAGE, and phosphorimager analysis of labeled proteins. Receptor-expressing COS-7 cells were labeled with

[S^{35}]methionine and [S^{35}]cysteine before chasing with media containing unlabeled methionine and cysteine for 0–24 hours as indicated in Figure 3.10*A*. Brefeldin A, which disrupts the Golgi complex, was added to both labeling and chasing media to block protein transport from the ER to the Golgi (and thereby compare the stability of ER-localized subunits). The degradation of myc-GluR6a subunit protein was fitted with a one-phase exponential decay with a half life of 9.1 ± 1.3 hours (n = 3). Myc-GluR6a(R663E) and T690A proteins were degraded at a significantly faster rate than wildtype receptors (4.9 ± 0.3 and 4.0 ± 0.4 hours, respectively, n =3, $p < 0.05$) (Figure 3.10*A*). The relatively rapid rate of degradation of these mutants likely underlies, at least in part, the delayed appearance of the mutant receptor proteins in the oligomerization analysis in Figure 5. We further tested the role of proteasomal degradation in myc-GluR6a(R663E) receptors by treating transfected cells with 10 μM MG-132 in DMSO, a proteasome inhibitor, for 8 hours. Plasma membrane expression of MG-132 treated cells was normalized to a DMSO-treated group. We found that the inhibition of proteasome-mediated degradation significantly promoted plasma membrane expression of myc-GluR6a(R663E), by 1.9-fold, but did not increase surface wildtype receptors, (n = 3, $p < 0.01$) (Figure 3.10*B*). These data indicate that the ERAD system is engaged to increase degradation of R633E linker mutants, and this induction likely contributes to the reduction in both plasma membrane and overall expression of myc-GluR6a(R663E) receptors.

To determine if the deficits in assembly and increased degradation of the M3-S2 linker and the ligand binding site mutants result from defective protein folding, we measured the association of wildtype and mutated GluR6a receptors with calnexin chaperone proteins, which associate with misfolded proteins during biosynthesis in the ER. We used anti-calnexin antibody to immunoprecipitate proteins from KAR-expressing cells and assessed the presence of myc-tagged GluR6a receptors and mutants in Western blots. We found that myc-GluR6a and GluR6a(R663E) receptors co-precipitated with endogenous calnexin proteins to an equivalent degree (IP lane, Figure 3.11). In contrast,

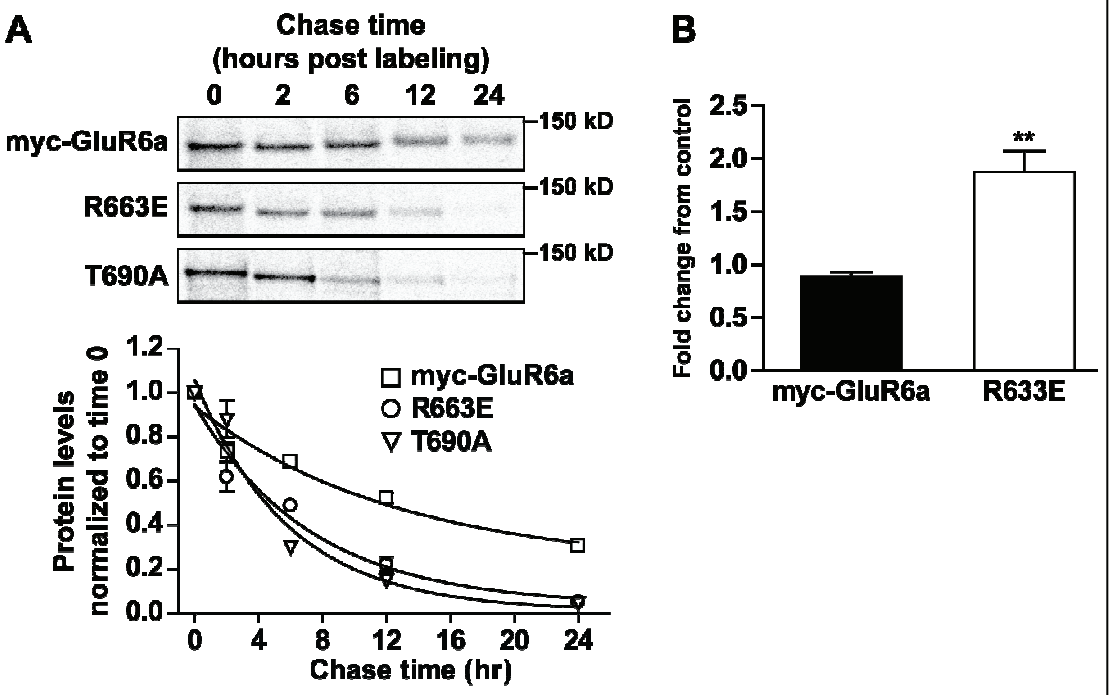

Figure 3.10: Increased degradation rates of GluR6a mutants.

A, A pulse-chase analysis demonstrates that the R663 and T690A mutants are degraded faster than wildtype GluR6a receptors. For the analysis, phosphorimager quantitations at several chase times were normalized to the band values at time zero (when no degradation had yet occurred). Graphs were fitted with a one-phase exponential decay. The half life values (τ_{decay}) of myc-GluR6a, R663E and T690Awere 9.1 ± 1.3, 4.9 ± 0.3 and 4.0 ± 0.4 hours, respectively (n =3, $p < 0.05$ for each mutant versus GluR6a receptors). Data represent mean ± s.e.m. *B*, Plasma membrane expression of myc-GluR6a and myc-GluR6a(R663E) receptors measured in cell ELISAs after transfected COS-7 cells were incubated with 0.05% dimethyl sulfoxide (DMSO) or the proteasome inhibitor MG-132 (10 μM) in 0.05% DMSO for 8 hours. The graph is plotted as the fold change relative to the relative plasma membrane localization in the DMSO control. Plasma membrane receptors of myc-GluR6a receptors were slightly decreased after MG-132 treatment (DMSO: 74.5 ± 4.7% and MG-132: 65.4 ± 2.1%, n = 3), whereas plasma membrane localization of myc-GluR6a(R663E) receptors were increased significantly after MG-132 treatment (DMSO: 10.4 ± 1.4% and MG-132: 18.9 ± 1.0%, n = 3, **, $p < 0.01$). Data represent mean ± s.e.m.

association of the T690A receptor with calnexin was >4-fold higher than that observed with myc-GluR6a receptors (n = 3, $p < 0.01$), as has been reported previously (Fleck, 2006). A similar result was obtained when the receptor proteins were immunoprecipitated and calnexin detected in Western blots (data not shown). Thus, increased associations with the ER chaperone calnexin occur upon mutation of the ligand-binding domain but not R633 in the M3-S2 gating linker.

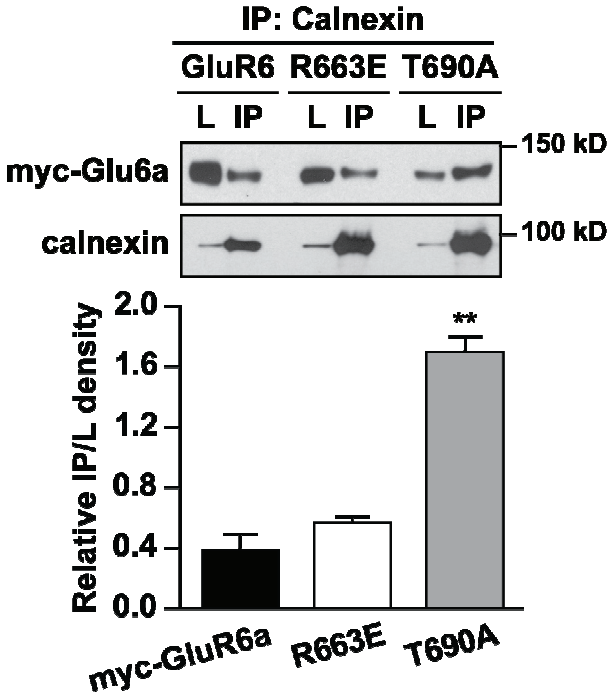

Figure 3.11: Myc-GluR6a(R663E) receptors interacted with calnexin similar to wildtype receptors.

Myc-GluR6a proteins were immunoprecipitated (IP) with an anti-calnexin antibody and detected in Western blots using an anti-myc antibody. The lysate lane (L) was loaded with 2 μg of membrane protein lysate and the immunoprecipitation lane (IP) with 30 μl of the immunoprecipitant. We quantified the IP band densities normalized to their corresponding lysate band densities. Myc-GluR6a(R663E) receptors co-precipitated with calnexin proteins at a similar degree as wildtype receptors, whereas association of myc-GluR6a(T690A) with calnexin was increased by 4.3-fold. Data represent mean ± s.e.m. (n = 3, ** $p < 0.01$).

3.3.5 Normalization of the receptor desensitization rate partially reverses biosynthetic deficits of linker domain mutants

We hypothesized that if plasma membrane expression of kainate receptors is partially or wholly determined by their desensitization properties, normalization of the GluR6a desensitization rates should restore some or all of the deficits we observed with the R633E mutant. Previously, normalization of receptor kinetics was achieved through charge-swapping of the analogous residues in GluR2 AMPA receptors (Yelshansky et al., 2004). Similarly, we found that the desensitization of myc-GluR6a(E662R,R663E) receptors was identical to wildtype receptors (τ_{des} 4.3 ± 0.1 ms and 99.4 ± 0.1% desensitization, n = 4) (Figure 3.12*A*). Despite the restoration of apparently normal function, the plasma membrane expression of myc-GluR6a(E662R,R663E) receptors remained significantly reduced relative to myc-GluR6a receptors in cell ELISA assays in transfected COS-7 cells, by 3-fold (30.4 ± 0.8%, n = 3, $p < 0.001$) (Figure 3.12*B*), and in immunofluorescent analysis of transfected hippocampal neurons (measured as the relative intensity of red to green fluorescence, n = 8, $p < 0.001$). While reduced compared to wildtype GluR6a receptors, the plasma membrane expression of the double mutant was significantly higher than the single mutant myc-GluR6a(R663E) (Figures 3.12*C* and 3.12*D*). As well, myc-GluR6a(E662R,R663E) receptors exhibited a small but detectable Endo H resistant band (data not shown), consistent with the increased plasma membrane of this mutant. These data indicate that normalization of the receptor desensitization rate partially restored the plasma membrane localization of GluR6a receptors.

In contrast to the partial recovery of membrane localization, oligomerization and degradation processes were completely restored to wildtype rates. In assembly assays with BN-PAGE, myc-GluR6a(E662R,R663E) receptors efficiently formed tetramers at early times after transfection (Figure 3.13*A*), similar to myc-GluR6a subunits. The proportional representation of tetramers, dimers and monomers were indistinguishable from wildtype receptors, despite the observation that the dimers and monomers were again of lower molecular weight than their GluR6a counterparts. Total protein expression

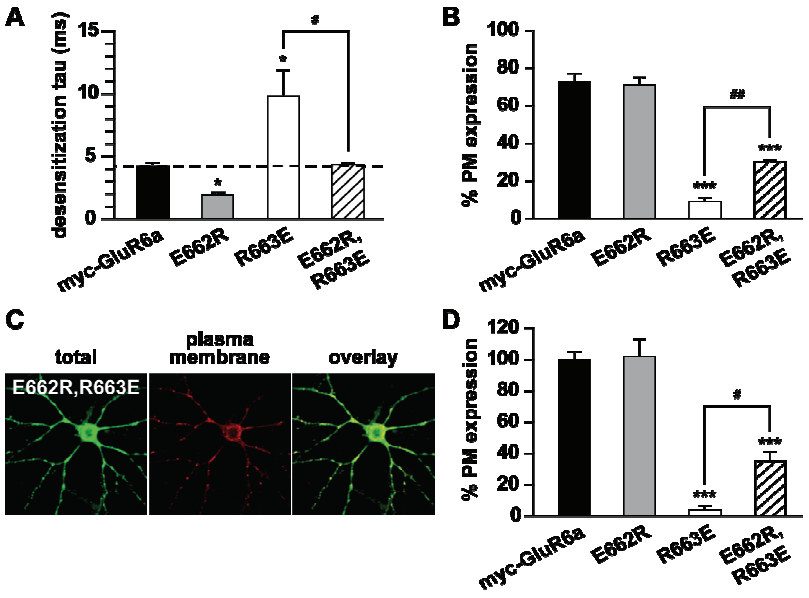

Figure 3.12: Normalization of desensitization properties by charge swapping of E662 and R663 only partially reverses the deficit in plasma membrane localization.

A, The desensitization rate (τ_{des}) of myc-GluR6a(E662R,R663E) receptors measured in patch-clamp recordings from transfected HEK 293-T/17 cells was 4.3 ± 0.1 ms (n = 4), which was markedly reduced from myc-GluR6a(R663E) receptors (9.8 ± 2.1 ms, n = 3, #, $p < 0.05$) to the same rate as wildtype GluR6a receptors (dashed line). *B*, Plasma membrane expression of myc-GluR6a(E662R,R663E) receptors measured using cell ELISA was 30.4 ± 0.01% (n = 3, ***, $p < 0.001$ compared to wildtype receptors, ##, $p < 0.01$ compared to R663E mutants). *C* and *D*, Plasma membrane expression of myc-GluR6a(E662R,R663) receptors in cultured hippocampal neurons also was partially restored but remained lower than myc-GluR6a membrane expression (35.2 ± 6.0%, n = 8, ***, $p < 0.001$). Data represent mean ± s.e.m.

of myc-GluR6a(E662R,R663E) protein was similar to myc-GluR6a subunits in SDS-PAGE and Western blots (data not shown). Finally, we found that the degradation rate of ER-localized myc-GluR6a(E662R,R663E) proteins was similar to wildtype receptors using pulse-chase assays with [S^{35}]methionine and [S^{35}]cysteine (half-life 10.5 ± 3.2 hours, n =3, Figure 3.13*B*). These results demonstrate that charge reversal and

normalization of desensitization properties in GluR6a(E662R,R663E) receptor mutants restores oligomerization efficiency and stabilizes the protein in the ER, but these changes are not accompanied by a return to wildtype levels of Golgi processing and plasma membrane expression. Thus, R633 is engaged at two distinct stages of KAR biosynthesis and trafficking.

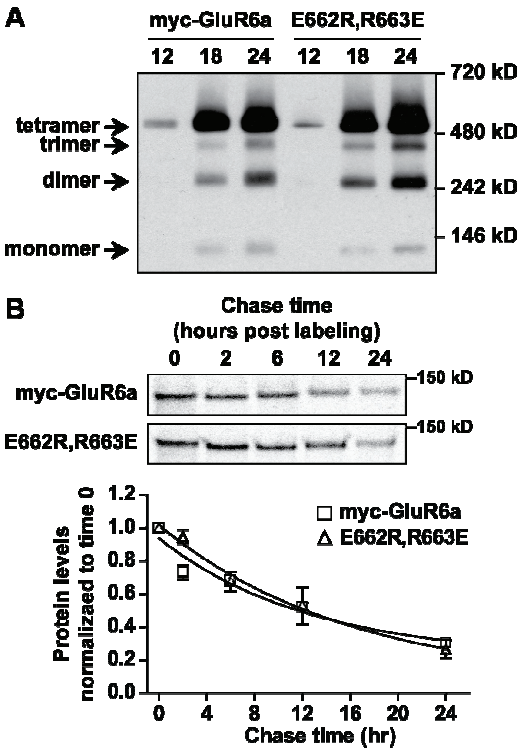

Figure 3.13: Normalization of desensitization rates correlates with restoration of efficient oligomerization and increased receptor stability in the ER.

A, myc-GluR6a(E662R,R663E) receptors efficiently formed tetramers at 12 hours post-transfection, similar to GluR6a receptors. Despite the restoration of normal oligomerization, the molecular weights of monomers and dimers were lower than those for GluR6a. *B*, GluR6a(E662R,R663E) receptors were degraded at the same rate as wildtype receptors in pulse-chase assays. Protein levels were normalized to phosphorimager densities at time zero. Graphs were fitted with a one-phase exponential decay. The τ_{decay} of myc-GluR6a(E662R,R663E) was 10.5 ± 3.2 (n =3).

3.4 DISCUSSION

Elucidation of the early events in glutamate receptor biosynthesis is important for understanding how receptors of diverse subunit composition are assembled, trafficked and targeted to their sites of action in the brain. A number of recent studies focused on defining how different segments of AMPA and kainate receptor subunit proteins participate in these events, and from these efforts a picture has emerged of a complex, tightly controlled biosynthetic process that engages multiple receptor domains (Greger and Esteban, 2007). In the current study we identified a residue in the M3-S2 linker of the GluR6a KAR subunit, R633, which is involved during both assembly and post-assembly trafficking stages. Mutation of this residue alters the functional properties of GluR6a receptors without affecting their glutamate binding affinity, and these functional changes are accompanied by significant intracellular effects on tetrameric assembly, degradation rates, and plasma membrane expression in heterologous cell lines and in neurons. Normalization of receptor desensitization rates through reversal of a putative dipole formed with a neighboring residue, E662, restored most of the assembly-related defects but only partially reversed the reduction in plasma membrane expression. Our study provides further support for the existence of a functional checkpoint within the ER consisting of the glutamate-bound, non-conducting conformational state of tetrameric receptor. It also makes evident, however, that the profound reductions in plasma membrane expression observed upon mutation of functional domains such as the ligand-binding domain (Mah et al., 2005; Valluru et al., 2005), inter-subunit interfaces (Greger et al., 2006; Priel et al., 2006), and transduction linkers (our study) likely do not result solely from disruption of a single post-assembly conformational state, but rather result from decreased efficiency of progression through a number of transitional stages of receptor biosynthesis.

3.4.1 Probing the relationship between KAR desensitization and ER export

The hypothesis that AMPA and kainate receptors necessarily bind glutamate in the ER as a requisite step in forward trafficking to the plasma membrane is relatively new. This idea was originally formulated on several studies that observed a marked reduction in plasma membrane expression of glutamate-binding receptors mutants, of the GLR-1 *C. elegans* AMPA receptor (Grunwald and Kaplan, 2003) and the GluR6a and KA2 kainate receptors (Mah et al., 2005; Valluru et al., 2005) in particular. Subsequent studies with weakly desensitizing AMPA and KA receptor mutants, in which alteration of inter-subunit and inter-domain residues resulted in intracellular retention of receptors, further elucidated several important aspects of the functional checkpoint for ER egress (Greger et al., 2006; Priel et al., 2006). Ion flux was shown not be relevant to the trafficking checkpoint of the GluR6a KAR (Priel et al., 2006), confirming an earlier proposal based on the behavior of non-functional homomeric KA2 subunits (Valluru et al., 2005). A rigorous examination of mechanisms of GluR2 AMPA receptor assembly supported the existence of a post-tetrameric assembly checkpoint in which receptors were sampled for ER export competence (Greger et al., 2006). In addition to these mutagenesis-based studies, competition for glutamate binding to nascent receptors in the ER using high concentrations of competitive antagonists reduced plasma membrane expression of GluR6a receptors (Fleck, 2006), supporting an essential trafficking role for conformational changes subsequent to glutamate binding in the ER lumen.

This trafficking checkpoint has been associated explicitly with AMPA and KAR desensitization properties (Greger et al., 2006; Priel et al., 2006). The first goal of our current study was to test this proposal and determine if altered desensitization properties (and, by inference, different structural states) exclusively underlay changes in ER export of KARs. The residues we examined, in the M3-S2 linker domain, are thought to be involved in transduction of binding energy into channel gating. Because they reside outside of resolved S1-S2 structures, it is not clear how they interact with other domains or subunits. Similar to AMPA receptors mutated at the same position, alteration of E662

predominantly accelerated desensitization, whereas R633 mutants generally desensitized slower than wildtype GluR6a receptors. Unlike ligand-binding domain or inter-subunit mutations such as the L507Y in GluR3 AMPA receptors (Stern-Bach et al., 1998), alteration of E662 and R663 did not alter apparent affinity of the GluR6a receptors. Slowing of desensitization rates and reduction in the degree of desensitization of R633 mutants was accompanied by reduction in plasma membrane expression of some, but not all mutant receptors, and thus the functional properties and plasma membrane were not highly correlated (Figure 3.5). In particular, myc-GluR6a(R663S) receptors had the slowest desensitization rates but their expression at the plasma membrane was higher than other slowly-desensitizing mutant receptors (e.g., R633E). Conversely, mutations at E662 increased the desensitization rate but did not elevate receptor expression at the plasma membrane, unlike a mutant of the GluR2 AMPA receptor with a similar physiological phenotype (Greger et al., 2006). Myc-GluR6a KARs express at very high levels - >85% - on the plasma membrane in our assays, however, and it is possible that this represents a constraint in assessing putative increases with the E662 mutants. The fact that a correlation exists, even if relatively weak, suggests that occluded entry into the desensitized conformation partially contributes to the trafficking phenotype of the R633 and other mutants, including ligand-binding mutants such as GluR6a(T690A). Our subsequent results made clear that other mechanisms, such as subunit assembly and degradation, play a critical role in the regulation of the expression of these KARs at the plasma membrane.

3.4.2 Multiple roles for the M3-S2 linker in KAR biosynthesis

In addition to the roles in receptor gating, our results demonstrate that R663 in the M3-S2 linker is critical for efficient receptor biosynthesis and trafficking. Mutagenesis or natural variation of other domains typically associated with receptor function - including the membrane domains, part of the S2 domain (including the flip/flop domain) and glutamate-binding residues in AMPA receptors - impair protein folding and

tetramerization of AMPA receptors (Ayalon and Stern-Bach, 2001; Greger et al., 2003; Coleman et al., 2006; Greger et al., 2006). The full spectrum of biosynthetic changes associated with mutagenesis of functional domains in KARs has been less clear. Elimination of the glutamate binding site did not disrupt oligomerization of GluR6 receptors in an earlier study (Mah et al., 2005) nor did it increase the degradation of homomeric KA2 receptors (Valluru et al., 2005). We observed quite substantial effects on the rate of oligomerization of GluR6a receptors mutated at either the linker domain, R663, or the ligand binding site, T690A. These results can be reconciled with those from Mah et al., as well our own data shown in Figure 3.9, by postulating that the tetrameric receptor is substantially more stable than other quaternary structures and thus accumulates disproportionately when the analysis is performed after an equilibrium is established in the expressing cells. This increased stability could occur because tetrameric receptors are intrinsically more stable in the ER, or because a small but significant proportion of the tetrameric receptors are exported from the ER and are thereby subject to slower degradation processes. We also noted that the R663E and T690A receptor mutant exhibited two separated peaks close to the tetrameric molecular weight, and, in the case of the latter protein particularly, a smear of high molecular weight proteins suggestive of aggregated folding intermediates (see Figure 3.9). This observation is consistent with the increased rate of degradation of the R663E and T690A GluR6a mutants and with the increased association of the latter mutant with the folding chaperone calnexin, as was reported previously (Fleck, 2006).

Mutation of the R663 residue appeared to alter glycosylation of monomers and dimers of the receptor subunits. A lower molecular weight of monomers also was found previously with the ligand-binding mutant T690A (Mah et al., 2005). In fact, all mutated GluR6a receptors with deficits in plasma membrane expression, including GluR6a(E662R,R663E) receptors (which assembled normally), exhibited lower molecular weight dimers and monomers (and possible tetramers), suggesting that this altered glycosylation did not affect protein folding and assembly but rather was

associated specifically with deficits in KAR trafficking. Glycosylation of the receptor could have an important role in post-assembly trafficking by serving as a recognition signal for lectin proteins in the secretory pathway, such as ERGIC-53 (Appenzeller-Herzog and Hauri, 2006). Taken together, our results suggest that inefficient subunit assembly and activation of the ER degradation system are shared mechanisms engaged upon disruption of diverse functional domains in the GluR6a KAR subunit.

The unusual "normalization" of GluR6a KAR desensitization behavior following reversal of the charged residues at positions 662 and 663 (ER→RE) is analogous to the effects of equivalent mutations in GluR2 AMPA receptors, with the exception that GluR2(ER→RE) mutants exhibited larger steady-state currents than wildtype GluR2 receptors (Yelshansky et al., 2004). These results suggest that the orientation of the putative dipole formed by the charge pair impacts the stability of the desensitized conformation in AMPA receptors but not KARs. This electrostatic interaction between the two residues in the gating linker appears to have further importance in KAR biosynthesis. While elimination of the positive charge at residue 663 slowed desensitization, impacted receptor assembly and promoted degradation of GluR6a receptors, charge swapping in the double mutant to restore the ionic interaction reversed the deficits in assembly and degradation. Thus, the presence of this electrostatic interaction, rather than an absolute requirement for a positively charged residue at 663, is critical for most KAR assembly and desensitization properties - independent of the orientation of the putative dipole. In contrast to the functional properties and biosynthetic deficits, plasma membrane expression of myc-GluR6a(E662R,R663E) receptors was only partly restored to wildtype levels, suggesting that the basic charge on R663 is required for efficient post-assembly trafficking. This could occur indirectly, for example by promoting appropriate glycosylation at a distinct site on the receptor subunit, as was mentioned previously. Alternatively, R663 could function as a chaperone recognition site that becomes exposed when tetrameric receptors bind glutamate in the ER and subsequently shift into the desensitized conformation. Although the secondary structure

of the M3-S2 transduction linker is unknown, the analogous residue to R663 in GluR2 AMPA receptors was more sensitive to modification by methanethiosulfonate when exposed in the desensitized state compared to the active and unliganded conditions, consistent with a conformation-dependent shift in accessibility that would be operative while the receptors are resident in the ER (Yelshansky et al., 2004).

In conclusion, we identified a specific amino acid in the M3-S2 transduction linker that not only plays a role in receptor gating but also in regulated biosynthesis and trafficking of kainate receptors. Our results suggest that non-cytoplasmic domains in KAR subunits are important both for ensuring that fully assembled receptors assume an export-competent conformation upon binding of glutamate in the ER as well as in earlier stages of receptor oligomerization. These ER quality control mechanisms and functional checkpoints will likely control the rate of assembly of different stoichiometries of receptors and thereby in part determine the neuronal fate of the receptors. Systematic approaches to elucidating these mechanisms will lead to a clearer model for KAR biosynthesis and targeting in the mammalian brain.

CHAPTER 4: CONCLUSIONS AND FUTURE EXPERIMENTS

Synaptic strength and plasticity are in part determined by the polarized distribution of iGluRs. The trafficking and targeting of iGluRs are tightly controlled by selective assembly, trafficking determinants and chaperone proteins that interact with these sites. Although several trafficking determinants of KARs have been identified, cellular mechanisms regulating these determinants are poorly understood and it is our major interest to characterize these mechanisms. These studies will yield understanding of how cells determine the subunit composition and synaptic expression of KARs, which lead to knowledge of how polarized distribution of KARs regulates the excitatory neurotransmission. In this dissertation, we characterized chaperone proteins that regulated the intracellular trafficking and elucidated the cellular mechanisms underlying the regulated trafficking of non-cytoplasmic determinants of KARs.

Our first aim focused on two chaperone proteins, COPI and 14-3-3 proteins, which competitively regulate the intracellular trafficking of other membrane proteins containing arginine-based ER retention/retrieval determinants. We found that COPI proteins modulated the retention of homomeric KA2 receptors in the ER by binding with the arginine-rich domain in the carboxy terminus. Elimination of the COPI binding site or the COPI complex resulted in increased plasma membrane localization of KA2 receptors. Association of COPI with KA2 subunits in heteromeric GluR6a/KA2 receptors was masked by conformational changes from heteromeric assembly rather than steric masking from GluR6a carboxy termini. Furthermore, COPI association was specific to KA2 receptors; COPI proteins did not associate with GluR5-2b, GluR5-2c and GluR6a receptor subunits. Our results suggest that COPI proteins play a role in segregating the intracellular trafficking of homomeric KA2 receptors from heteromeric receptors containing KA2 subunits, ensuring a residual pool of KA2 subunits are available for heteromeric assembly. Although these studies were conducted in cell lines, we hypothesized that COPI proteins play a similar role in the trafficking and targeting of

neuronal KARs. We are interested in testing whether the disruption of COPI binding using a peptide containing the arginine-rich motif will change the expression of KARs and synaptic activity in neuronal cultures. These studies will contribute to the understanding of retention mechanisms for KAR biosynthesis.

In the second part of the first aim, we focused our attention to study the role of 14-3-3 proteins in the trafficking of KARs. We found that several isoforms of 14-3-3 proteins associate with KAR subunits. 14-3-3 proteins were reported to promote forward trafficking of potassium channels by competing with COPI-mediated ER localization (O'Kelly et al., 2002; Yuan et al., 2003). Our results showed that association of 14-3-3ζ isoforms with KA2 receptors correlated with decreased COPI association and increased plasma membrane expression, suggesting that 14-3-3ζ proteins play a role in forward trafficking of KA2-containing KARs. Mutation of the putative endocytic di-leucine motif in KA2 subunits increased the association of KA2 and 14-3-3ζ proteins. It is possible that the increase in KA2-14-3-3ζ association could be a result of more available KA2 subunits when the COPI-mediated ER localization signal is absent. Although homomeric KA2 receptors do not express at the plasma membrane, KA2 subunits play a variety of physiological roles by heteromeric assembly with other KAR subunits and thus interaction of KA2 and 14-3-3ζ proteins might be more relevant to trafficking of heteromeric KARs. This result led us to investigate the role of 14-3-3 proteins in the trafficking of other KAR subunits. In our study of KA2 and 14-3-3ζ, we did not identify the binding site of 14-3-3 proteins in the cytoplasmic tail of KA2 subunits or the intracellular compartment(s) in which KA2 receptors interact with 14-3-3 proteins. We aim to characterize the binding site on each KAR subunits, the role of phosphorylation in the 14-3-3 binding, and the intracellular compartments in which this association occurs. These future studies will lead to the understanding of how 14-3-3 proteins regulate KAR biosynthesis and trafficking and potentially modulate synaptic transmission.

As part of our studies in the associations of KA2 and 14-3-3 proteins, we also found that 14-3-3β isoforms strongly interacted with GluR5-2b receptors. We first hypothesized that 14-3-3β isoforms control forward trafficking of GluR5-2b receptors similar to KA2 receptors. Surprisingly, our preliminary data showed that association of GluR5-2b and 14-3-3 proteins was reduced when the polybasic ER retention/retrieval site in the GluR5-2b cytoplasmic tail was mutated (Figure 4.1), a mutation which was previously shown to increase the plasma membrane expression of GluR5-2b receptors (Ren et al., 2003b).

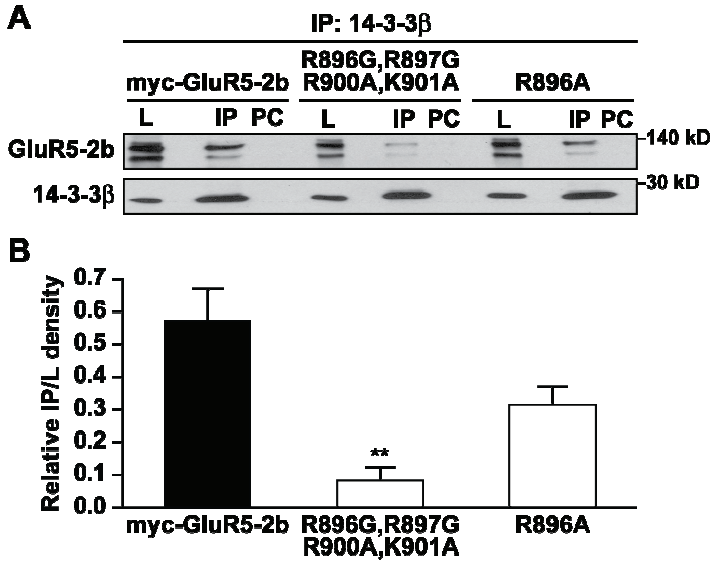

Figure 4.1: Elimination of the retention/retrieval motif reduced GluR5-2b association with 14-3-3β proteins.

A, myc-GluR5-2b transfected lysate was immunoprecipitated by an anti-14-3-3β antibody and myc-GluR5-2b receptors were detected via anti-myc antibody in Western blots (top panel). Myc-GluR5-2b receptors with mutations of basic residues in C-termini co-precipitated with 14-3-3β less than wildtype receptors. Blots were probed with anti-14-3-3β to determine the efficiency of immunoprecipitations (bottom panel). Abbreviations: L, lysate; IP, immunoprecipitated; PC, preclear background. *B*, Densitometric quantitation of the IP band densities normalized to their corresponding lysate band density showed that association of GluR5-2b and 14-3-3β was significantly decreased in myc-GluR5-2b(R896G,R897G,R900A,K901A) receptors by 84% (n = 3-4, ** p <0.01). Data represent mean ± s.e.m.

This result suggests that 14-3-3β proteins might play a role in the ER localization of GluR5-2b receptors. We therefore modified our hypothesis to postulate that the arginine-based motifs in GluR5-2b receptors might act as a binding site for 14-3-3β proteins similar to 14-3-3 associations with K_{ATP} channels (Yuan et al., 2003). Proteomic analysis supported an association between 14-3-3γ isoforms and the C-terminus of GluR6a receptors (Coussen et al., 2005). To test the role of 14-3-3 proteins in trafficking of KA2, GluR5-2b, and GluR6a subunits, we will examine the plasma membrane expression of KARs when 14-3-3 proteins are over-expressed or interactions of 14-3-3 and KARs are disrupted. A number of methods exist to interfere with protein interactions in cell lines and neuronal culture, e.g. RNA interference of 14-3-3 expression or a peptide competitor. The short peptide R18, PHCVPRDLSWLDLEANMCLP, can be expressed from the pSCM138 plasmid and as an antagonist of 14-3-3 function by competitively binding to the ligand-binding site of 14-3-3 proteins. A scrambled peptide will be expressed from the pSCM174 as a control (Masters and Fu, 2001). Plasma membrane expression of KARs will be measured by cell ELISA and cell surface biotinylation assays. We hypothesize that if 14-3-3β regulates the ER localization of GluR5-2b receptors, over-expression of 14-3-3β by transfection with 14-3-3β cDNAs should reduce plasma membrane expression of receptors; in contrast, inhibition of association between 14-3-3β and GluR5-2b subunits by RNA interference or competitive peptide will promote the plasma membrane expression. Our studies demonstrate the diversity in 14-3-3 associations with KAR subunits and their possibly different roles in trafficking, which might explain how different synapses express distinct KARs.

We are interested in identifying the binding site of 14-3-3 proteins on KAR subunits and the intracellular association site of KAR and 14-3-3 proteins. We will use a series of truncated and alanine-substituted mutations similar to the method that we used successfully to identify the forward trafficking motif of GluR6a subunits (Yan et al., 2004). If the association sites of 14-3-3 proteins contain either serine or threonine residue, we will determine if this association is regulated by phosphorylation and which

protein kinase plays a role in it using mutagenesis and pharmacological approaches. The intracellular association site of KARs and 14-3-3 proteins will be detected using confocal immunofluorescence techniques with specific markers for intracellular compartments such as ER exit sites, ER-Golgi intermediate compartment (ERGIC), *cis*-Golgi, medial-Golgi, and *trans*-Golgi. These future studies will yield insight on how chaperone proteins interact with the intracellular carboxy-terminus and regulate the early trafficking of KARs and how to manipulate these interactions in order to control KAR expression and synaptic plasticity.

The role of synaptic activity in modulation of the exocytic pathway of KARs is largely unknown. Activation and inhibition of synaptic activities controls the expression and subunit compositions of AMPA and NMDA receptors. Synaptic activation increases the insertion of GluR1-containing AMPA receptors at the post-synaptic membrane under the control of interactions between GluR1 subunits and PDZ-binding proteins (Shi et al., 2001) and alters mRNA splicing of NR1 NMDA subunits, resulting in increased interactions with COPII proteins and egress of receptors from the ER (Mu et al., 2003). We hypothesize that synaptic activity modulates the association level of chaperone proteins with KARs. We are interested in testing how synaptic activation or inhibition modulates the COPI or 14-3-3 association with KARs and if the change in the association is correlated with the alteration of ER export. ER export will be measured by colocalization and co-immunoprecipitation of KARs with the ER export marker such as COPII proteins. Furthermore, we are interested in determining whether synaptic activation affects receptor assembly, induces the change in the subunit composition of KARs at the synapse or alters splicing of GluR5-7 mRNAs. For example, we speculate that synaptic activity might change mRNA splicing of the GluR6 C-terminus to create GluR6a subunits instead GluR6b subunits, resulting in higher expression of GluR6-containing KARs at the synapse. These future studies will contribute to the understanding of how synaptic activity modulates the expression and selective targeting of neuronal KARs to synapses.

In Specific Aim 2, we explored the importance of an extracellular linker region that couples ligand binding energy to channel permeation in biosynthesis of GluR6a receptors. We found that this transduction linker was engaged in desensitization processes as well as multiple stages of GluR6a biosynthesis. The prevailing hypothesis prior to our study was that the egress of AMPA and KARs from the ER depended on the efficiency of transition to the desensitized state, because mutations in the ligand-binding domains ultimately affect receptor desensitization. We found that elimination of a conserved positively charged residue at the transduction linker domain led to ER localization of GluR6a receptors by disrupting desensitization, subunit assembly, protein degradation and unknown post-assembly stages, underscoring the importance of electrostatic charges in KAR function and biosynthesis. Normalization of the desensitization rate of GluR6a receptors by charge swapping of two adjacent residues in the transduction linker reversed the deficits in oligomerization and degradation; however, the expression of receptors at the plasma membrane did not return to levels similar to wildtype receptors. This result suggests that the predicted dipole orientation in the transduction linker is critical for KAR biosynthesis. It also indicates that plasma membrane expression of KARs is not solely determined by receptor desensitization.

Mechanisms and steps in receptor biogenesis in which each domain plays a role in the exocytic pathways remain elusive although several trafficking determinants have been identified in KARs. Our results, together with other studies on AMPA and KA receptor biosynthesis, indicate that at least five domains regulate plasma membrane expression of receptors: the cytoplasmic, ligand-binding, pore-forming, inter-subunit, and transduction linker domains. Previous studies on kainate receptor biosynthesis primarily focused on identifying trafficking determinants that modulated plasma membrane expression. In this dissertation, we established methods to analyze folding, assembly, degradation and chaperone protein interactions. Thus it will be of interest to characterize how each domain regulates these biogenesis steps of KARs in heterologous cell lines and cultured neurons using similar methods to this dissertation. Additionally, the precise localization

of trapped receptors is largely unknown. We are interested in identifying the retention site of trafficking compromised KARs by colocalization assays with a similar method as that used for characterizing the intracellular compartments in which KARs associate with 14-3-3 proteins. These future experiments will lead to determination of how and where each domain becomes critical for plasma membrane localization of KARs and will create a more comprehensive model of KAR biosynthesis.

Lectin chaperone proteins play a major role in the control of protein folding and assembly in the ER; however, knowledge of lectin functions in KAR trafficking and biosynthesis is limited. We found that monomers and dimers of trafficking-compromised receptors in the extracellular domain such as the GluR6a(R663E) mutant were lower than wildtype receptors and these reductions were probably caused by the difference in glycosylation. Lectins interact with glycosaccharides on the extracellular domain of glycoproteins. We hypothesize that mutations in the transduction linker possibly affect protein folding and subsequently association with lectin chaperone proteins. Calnexin, which interacts with incorrectly folded proteins to allow proteins to refold, and BiP, which targets misfolded proteins to the ERAD, have previously been reported to modulate AMPA and KAR biosynthesis (Rubio and Wenthold, 1999; Fleck, 2006). We found that mutations in the transduction linker did not alter association of KARs with calnexin. However, there are other lectin chaperone proteins that modulate protein folding in the ER such as calreticulin and ERp57 and trafficking between the ER and the Golgi such as COPII and ERGIC-53. It will be our interest to identify chaperone proteins that regulate deficit in trafficking of non-cytoplasmic trafficking mutants. We will measure the correlation of protein interactions with KARs and the level of KAR expression at the plasma membrane similar to Specific Aim 1. These experiments will help us identify lectin chaperone proteins that control the intracellular trafficking of KARs.

We are also interested in studying how chaperone proteins control the trafficking of KARs with a mutation at the non-cytoplasmic domain. To test whether chaperone

proteins directly interact with non-cytoplasmic determinants, we will test if mutations of these residues disrupt the secretion of a soluble form of the ligand-binding domain. The ligand-binding core of iGluRs can be expressed separately as soluble S1-S2 proteins, which are secreted into culture medium and detected by Western blots. We obtained a GluR6 S1-S2 construct from Dr. Mark Mayer (NIH) and generated a myc-tagged GluR6 S1-S2 construct containing the transduction linker between S1 and S2 domains. Critical ligand-binding residues and the conserved arginine in the transduction linker will be mutated. We hypothesize that if these non-cytoplasmic determinants act as a binding site for chaperone proteins, secretion of mutated soluble proteins will be reduced to a similar degree as the reduction in plasma membrane expression of myc-GluR6a(R663E) and myc-GluR6(T690A) receptors. These experiments will lead to an understanding of how chaperone proteins associate with non-cytoplasmic determinants and play a role in ER retention of KARs.

How subunit stoichiometry controls the folding and assembly of KARs remains an outstanding question. Homomeric KA2 receptors without retention/retrieval signals express on the plasma membrane very weakly (~8%) whereas heteromeric GluR6a/KA2 receptors express around 40-50% on the plasma membrane. These results suggest that other mechanisms exist to limit forward trafficking of homomeric KA2 receptors. We hypothesize that homomeric KA2 receptors do not fold properly and do not form tetramers efficiently. Heteromeric assembly of KA2 subunits with GluR5-7 subunits form functional receptors that express at synapses. We propose that heteromeric assembly overcome defects in folding and assembly of homomeric KA2 receptors. Our preliminary data using native gel electrophoresis assays showed that KA2 receptors did not assemble to form tetramers but rather aggregated into larger complexes (Figure 4.2). The smearing of proteins also indicates that KA2 receptors do not fold properly. These results support our hypothesis that the intracellular retention of KA2 receptors is largely caused by deficits in protein folding and assembly. We will test whether the heteromeric assembly of KA2 subunits with GluR5-7 subunits changes the efficiency of tetramer formation, and

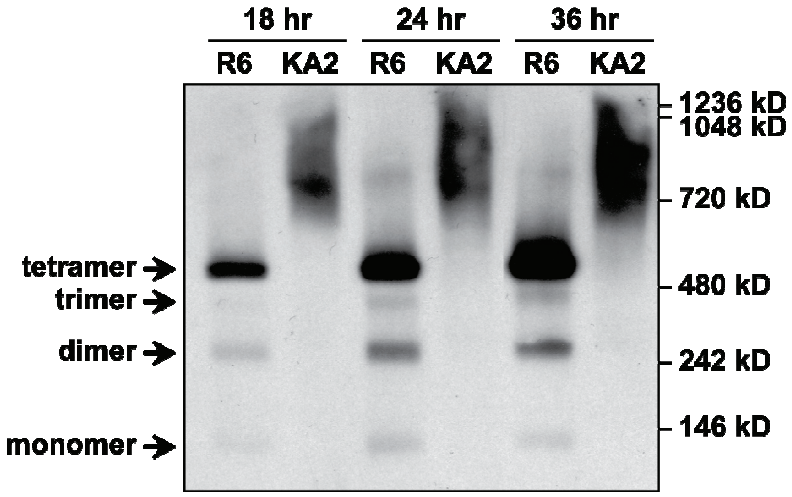

Figure 4.2: Homomeric KA2 receptors did not form tetramers.

A, Myc-GluR6a and myc-KA2 proteins from COS-7 cells were collected at several time points after transfection as indicated, separated by non-denaturing PAGE and Western blotting. Myc-KA2 proteins were aggregated to oligomers with larger molecular weights than tetramers of myc-GluR6a proteins from 18-36 hour post-transfection, whereas tetramers, trimers, dimers, and monomers of myc-GluR6a receptors were detected at 18 hours after transfection.

whether this alteration plays a role in the expression of functional heteromeric KARs at the plasma membrane. Similarly, we aim to compare the rate and the efficiency of oligomerization between different subunit compositions. These future studies will contribute to an understanding of how receptor stoichiometry regulates the folding and selective assembly of neuronal KARs at different synapses, which in turn modulate the trafficking and targeting of KARs.

In conclusion, these trafficking determinants and mechanisms for controlling kainate receptor biosynthesis are likely involved in the regulation of proper expression and targeting of distinct kainate receptors to diverse synaptic and non-synaptic sites. The present results combined with future studies will yield a more comprehensive

understanding of how cellular mechanisms regulate heterogenous expression and polarized distribution of kainate receptors, which modulate synaptic activity in the central nervous system.

REFERENCES

Alberts B, Johnson A, Lewis J, Raff M, Roberts K and Walter P (2002) *Molecular Biology of The Cell*. Garland Science, New York.

Appenzeller-Herzog C and Hauri HP (2006) The ER-Golgi intermediate compartment (ERGIC): in search of its identity and function. *J Cell Sci* **119**:2173-2183.

Armstrong N and Gouaux E (2000) Mechanisms for activation and antagonism of an AMPA-sensitive glutamate receptor: crystal structures of the GluR2 ligand binding core. *Neuron* **28**:165-181.

Armstrong N, Sun Y, Chen GQ and Gouaux E (1998) Structure of a glutamate-receptor ligand-binding core in complex with kainate. *Nature* **395**:913-917.

Ayalon G and Stern-Bach Y (2001) Functional assembly of AMPA and kainate receptors is mediated by several discrete protein-protein interactions. *Neuron* **31**:103-113.

Banker GA and Cowan WM (1977) Rat hippocampal neurons in dispersed cell culture. *Brain Res* **126**:397-342.

Bettler B, Egebjerg J, Sharma G, Pecht G, Hermans-Borgmeyer I, Moll C, Stevens CF and Heinemann S (1992) Cloning of a putative glutamate receptor: a low affinity kainate-binding subunit. *Neuron* **8**:257-265.

Braga MF, Aroniadou-Anderjaska V and Li H (2004) The physiological role of kainate receptors in the amygdala. *Mol. Neurobiol.* **30**:127-141.

Bredt DS and Nicoll RA (2003) AMPA receptor trafficking at excitatory synapses. *Neuron* **40**:361-379.

Brock C, Boudier L, Maurel D, Blahos J and Pin JP (2005) Assembly-dependent Surface Targeting of the Heterodimeric GABAB Receptor Is Controlled by COPI, But Not 14-3-3. *Mol. Biol. Cell* **16**:5572-5578.

Castillo PE, Malenka RC and Nicoll RA (1997) Kainate receptors mediate a slow postsynaptic current in hippocampal CA3 neurons. *Nature* **388**:182-186.

Chittajallu R, Vignes M, Dev KK, Barnes JM, Collingridge GL and Henley JM (1996) Regulation of glutamate release by presynaptic kainate receptors in the hippocampus. *Nature* **379**:78-81.

Clarke VR, Ballyk BA, Hoo KH, Mandelzys A, Pellizzari A, Bath CP, Thomas J, Sharpe EF, Davies CH, Ornstein PL, Schoepp DD, Kamboj RK, Collingridge GL, Lodge D and Bleakman D (1997) A hippocampal GluR5 kainate receptor regulating inhibitory synaptic transmission. *Nature* **389**:599-603.

Coblitz B, Wu M, Shikano S and Li M (2006) C-terminal binding: an expanded repertoire and function of 14-3-3 proteins. *FEBS Lett* **580**:1531-1535.

Coleman SK, Moykkynen T, Cai C, von Ossowski L, Kuismanen E, Korpi ER and Keinanen K (2006) Isoform-specific early trafficking of AMPA receptor flip and flop variants. *J Neurosci* **26**:11220-11229.

Collingridge GL, Isaac JT and Wang YT (2004) Receptor trafficking and synaptic plasticity. *Nat Rev Neurosci* **5**:952-962.

Conn PJ and Pin JP (1997) Pharmacology and functions of metabotropic glutamate receptors. *Annu Rev Pharmacol Toxicol* **37**:205-237.

Contractor A, Swanson G and Heinemann SF (2001) Kainate receptors are involved in short- and long-term plasticity at mossy fiber synapses in the hippocampus. *Neuron* **29**:209-216.

Cossart R, Esclapez M, Hirsch JC, Bernard C and Ben-Ari Y (1998) GluR5 kainate receptor activation in interneurons increases tonic inhibition of pyramidal cells. *Nat Neurosci* **1**:470-478.

Coussen F, Normand E, Marchal C, Costet P, Choquet D, Lambert M, Mege RM and Mulle C (2002) Recruitment of the kainate receptor subunit glutamate receptor 6 by cadherin/catenin complexes. *J. Neurosci.* **22**:6426-6436.

Coussen F, Perrais D, Jaskolski F, Sachidhanandam S, Normand E, Bockaert J, Marin P and Mulle C (2005) Coassembly of Two GluR6 Kainate Receptor Splice Variants within a Functional Protein Complex. *Neuron* **47**:555-566.

Cui C and Mayer ML (1999) Heteromeric kainate receptors formed by the coassembly of GluR5, GluR6, and GluR7. *J Neurosci* **19**:8281-8291.

Delaney AJ and Jahr CE (2002) Kainate receptors differentially regulate release at two parallel fiber synapses. *Neuron* **36**:475-482.

Derkach VA, Oh MC, Guire ES and Soderling TR (2007) Regulatory mechanisms of AMPA receptors in synaptic plasticity. *Nat Rev Neurosci* **8**:101-113.

DeVries SH and Schwartz EA (1999) Kainate receptors mediate synaptic transmission between cones and 'Off' bipolar cells in a mammalian retina. *Nature* **397**:157-160.

Dingledine R, Borges K, Bowie D and Traynelis SF (1999) The glutamate receptor ion channels. *Pharmacol Rev* **51**:7-61.

Dougherty MK and Morrison DK (2004) Unlocking the code of 14-3-3. *J. Cell Sci.* **117**:1875-1884.

Duden R (2003) ER-to-Golgi transport: COP I and COP II function (Review). *Mol. Membr. Biol.* **20**:197-207.

Egebjerg J, Bettler B, Hermans-Borgmeyer I and Heinemann S (1991) Cloning of a cDNA for a glutamate receptor subunit activated by kainate but not AMPA. *Nature* **351**:745-748.

Fleck MW (2006) Glutamate receptors and endoplasmic reticulum quality control: looking beneath the surface. *Neuroscientist* **12**:232-244.

Fleck MW, Cornell E and Mah SJ (2003) Amino-acid residues involved in glutamate receptor 6 kainate receptor gating and desensitization. *J. Neurosci.* **23**:1219-1227.

Garcia EP, Mehta S, Blair LA, Wells DG, Shang J, Fukushima T, Fallon JR, Garner CC and Marshall J (1998) SAP90 binds and clusters kainate receptors causing incomplete desensitization. *Neuron* **21**:727-739.

Gassmann M, Haller C, Stoll Y, Aziz SA, Biermann B, Mosbacher J, Kaupmann K and Bettler B (2005) The RXR-type endoplasmic reticulum-retention/retrieval signal of GABAB1 requires distant spacing from the membrane to function. *Mol Pharmacol* **68**:137-144.

Greger IH, Akamine P, Khatri L and Ziff EB (2006) Developmentally regulated, combinatorial RNA processing modulates AMPA receptor biogenesis. *Neuron* **51**:85-97.

Greger IH and Esteban JA (2007) AMPA receptor biogenesis and trafficking. *Curr Opin Neurobiol*.

Greger IH, Khatri L, Kong X and Ziff EB (2003) AMPA receptor tetramerization is mediated by Q/R editing. *Neuron* **40**:763-774.

Greger IH, Khatri L and Ziff EB (2002) RNA editing at arg607 controls AMPA receptor exit from the endoplasmic reticulum. *Neuron* **34**:759-772.

Grunwald ME and Kaplan JM (2003) Mutations in the ligand-binding and pore domains control exit of glutamate receptors from the endoplasmic reticulum in C. elegans. *Neuropharmacology* **45**:768-776.

Guo Q, Penman M, Trigatti BL and Krieger M (1996) A single point mutation in epsilon-COP results in temperature-sensitive, lethal defects in membrane transport in a Chinese hamster ovary cell mutant. *J Biol Chem* **271**:11191-11196.

Guo Q, Vasile E and Krieger M (1994) Disruptions in Golgi structure and membrane traffic in a conditional lethal mammalian cell mutant are corrected by epsilon-COP. *J Cell Biol* **125**:1213-1224.

Herb A, Burnashev N, Werner P, Sakmann B, Wisden W and Seeburg PH (1992) The KA-2 subunit of excitatory amino acid receptors shows widespread expression in brain and forms ion channels with distantly related subunits. *Neuron* **8**:775-785.

Hermans E and Challiss RA (2001) Structural, signalling and regulatory properties of the group I metabotropic glutamate receptors: prototypic family C G-protein-coupled receptors. *Biochem J* **359**:465-484.

Hirbec H, Francis JC, Lauri SE, Braithwaite SP, Coussen F, Mulle C, Dev KK, Coutinho V, Meyer G, Isaac JT, Collingridge GL and Henley JM (2003) Rapid and differential regulation of AMPA and kainate receptors at hippocampal mossy fibre synapses by PICK1 and GRIP. *Neuron* **37**:625-638.

Huettner JE (2003) Kainate receptors and synaptic transmission. *Prog. Neurobiol.* **70**:387-407.

Jaskolski F, Coussen F and Mulle C (2005a) Subcellular localization and trafficking of kainate receptors. *Trends Pharmacol. Sci.* **26**:20-26.

Jaskolski F, Coussen F, Nagarajan N, Normand E, Rosenmund C and Mulle C (2004) Subunit composition and alternative splicing regulate membrane delivery of kainate receptors. *J. Neurosci.* **24**:2506-2515.

Jaskolski F, Normand E, Mulle C and Coussen F (2005b) Differential trafficking of GluR7 kainate receptor subunit splice variants. *J Biol Chem* **280**:22968-22976.

Jeanclos EM, Lin L, Treuil MW, Rao J, DeCoster MA and Anand R (2001) The chaperone protein 14-3-3eta interacts with the nicotinic acetylcholine receptor alpha 4 subunit. Evidence for a dynamic role in subunit stabilization. *J. Biol. Chem.* **276**:28281-28290.

Jin R and Gouaux E (2003) Probing the function, conformational plasticity, and dimer-dimer contacts of the GluR2 ligand-binding core: studies of 5-substituted willardiines and GluR2 S1S2 in the crystal. *Biochemistry* **42**:5201-5213.

Jones MV and Westbrook GL (1996) The impact of receptor desensitization on fast synaptic transmission. *Trends Neurosci* **19**:96-101.

Keller SH, Lindstrom J, Ellisman M and Taylor P (2001) Adjacent basic amino acid residues recognized by the COP I complex and ubiquitination govern endoplasmic reticulum to cell surface trafficking of the nicotinic acetylcholine receptor alpha-Subunit. *J. Biol. Chem.* **276**:18384-18391.

Kennedy MJ and Ehlers MD (2006) Organelles and trafficking machinery for postsynaptic plasticity. *Annu Rev Neurosci* **29**:325-362.

Khalil H, Brunet A, Saba I, Terra R, Sekaly RP and Thibodeau J (2003) The MHC class II beta chain cytoplasmic tail overcomes the invariant chain p35-encoded endoplasmic reticulum retention signal. *Int Immunol* **15**:1249-1263.

Kim E and Sheng M (2004) PDZ domain proteins of synapses. *Nat Rev Neurosci* **5**:771-781.

Kohler M, Burnashev N, Sakmann B and Seeburg PH (1993) Determinants of Ca2+ permeability in both TM1 and TM2 of high affinity kainate receptor channels: diversity by RNA editing. *Neuron* **10**:491-500.

Kuismanen E and Saraste J (1989) Low temperature-induced transport blocks as tools to manipulate membrane traffic. *Methods Cell Biol* **32**:257-274.

Lee MC, Miller EA, Goldberg J, Orci L and Schekman R (2004) Bi-directional protein transport between the ER and Golgi. *Annu. Rev. Cell Dev. Biol.* **20**:87-123.

Lerma J (2003) Roles and rules of kainate receptors in synaptic transmission. *Nat. Rev. Neurosci.* **4**:481-495.

Lerma J, Paternain AV, Rodriguez-Moreno A and Lopez-Garcia JC (2001) Molecular physiology of kainate receptors. *Physiol. Rev.* **81**:971-998.

Lowe M and Kreis TE (1998) Regulation of membrane traffic in animal cells by COPI. *Biochim Biophys Acta* **1404**:53-66.

Madden DR (2002) The structure and function of glutamate receptor ion channels. *Nat Rev Neurosci* **3**:91-101.

Mah SJ, Cornell E, Mitchell NA and Fleck MW (2005) Glutamate receptor trafficking: endoplasmic reticulum quality control involves ligand binding and receptor function. *J. Neurosci.* **25**:2215-2225.

Margeta-Mitrovic M, Jan YN and Jan LY (2000) A trafficking checkpoint controls GABA(B) receptor heterodimerization. *Neuron* **27**:97-106.

Masters SC and Fu H (2001) 14-3-3 proteins mediate an essential anti-apoptotic signal. *J Biol Chem* **276**:45193-45200.

Mayer ML and Armstrong N (2004) Structure and function of glutamate receptor ion channels. *Annu. Rev. Physiol.* **66**:161-181.

Mayer ML, Ghosal A, Dolman NP and Jane DE (2006) Crystal structures of the kainate receptor GluR5 ligand binding core dimer with novel GluR5-selective antagonists. *J Neurosci* **26**:2852-2861.

McMahon HT and Mills IG (2004) COP and clathrin-coated vesicle budding: different pathways, common approaches. *Curr. Opin. Cell Biol.* **16**:379-391.

Mehta S, Wu H, Garner CC and Marshall J (2001) Molecular mechanisms regulating the differential association of kainate receptor subunits with SAP90/PSD-95 and SAP97. *J. Biol. Chem.* **276**:16092-16099.

Melyan Z, Lancaster B and Wheal HV (2004) Metabotropic regulation of intrinsic excitability by synaptic activation of kainate receptors. *J Neurosci* **24**:4530-4534.

Michelsen K, Yuan H and Schwappach B (2005) Hide and run. *EMBO Rep.* **6**:717-722.

Mu Y, Otsuka T, Horton AC, Scott DB and Ehlers MD (2003) Activity-dependent mRNA splicing controls ER export and synaptic delivery of NMDA receptors. *Neuron* **40**:581-594.

Nasu-Nishimura Y, Hurtado D, Braud S, Tang TT, Isaac JT and Roche KW (2006) Identification of an endoplasmic reticulum-retention motif in an intracellular loop of the kainate receptor subunit KA2. *J Neurosci* **26**:7014-7021.

Nufer O and Hauri HP (2003) ER export: call 14-3-3. *Curr Biol* **13**:R391-393.

O'Kelly I, Butler MH, Zilberberg N and Goldstein SA (2002) Forward transport. 14-3-3 binding overcomes retention in endoplasmic reticulum by dibasic signals. *Cell* **111**:577-588.

Obenauer JC, Cantley LC and Yaffe MB (2003) Scansite 2.0: Proteome-wide prediction of cell signaling interactions using short sequence motifs. *Nucleic Acids Res.* **31**:3635-3641.

Partin KM, Fleck MW and Mayer ML (1996) AMPA receptor flip/flop mutants affecting deactivation, desensitization, and modulation by cyclothiazide, aniracetam, and thiocyanate. *J Neurosci* **16**:6634-6647.

Paternain AV, Herrera MT, Nieto MA and Lerma J (2000) GluR5 and GluR6 kainate receptor subunits coexist in hippocampal neurons and coassemble to form functional receptors. *J. Neurosci.* **20**:196-205.

Perez-Otano I and Ehlers MD (2005) Homeostatic plasticity and NMDA receptor trafficking. *Trends Neurosci* **28**:229-238.

Pinheiro P and Mulle C (2006) Kainate receptors. *Cell Tissue Res* **326**:457-482.

Priel A, Selak S, Lerma J and Stern-Bach Y (2006) Block of kainate receptor desensitization uncovers a key trafficking checkpoint. *Neuron* **52**:1037-1046.

Rajan S, Preisig-Muller R, Wischmeyer E, Nehring R, Hanley PJ, Renigunta V, Musset B, Schlichthorl G, Derst C, Karschin A and Daut J (2002) Interaction with 14-3-3 proteins promotes functional expression of the potassium channels TASK-1 and TASK-3. *J. Physiol.* **545**:13-26.

Ren Z, Riley NJ, Garcia EP, Sanders JM, Swanson GT and Marshall J (2003a) Multiple trafficking signals regulate kainate receptor KA2 subunit surface expression. *J. Neurosci.* **23**:6608-6616.

Ren Z, Riley NJ, Needleman LA, Sanders JM, Swanson GT and Marshall J (2003b) Cell surface expression of GluR5 kainate receptors is regulated by an endoplasmic reticulum retention signal. *J. Biol. Chem.* **278**:52700-52709.

Renard A, Crepel F and Audinat E (1995) Evidence for two types of non-NMDA receptors in rat cerebellar Purkinje cells maintained in slice cultures. *Neuropharmacology* **34**:335-346.

Rodriguez-Moreno A, Herreras O and Lerma J (1997) Kainate receptors presynaptically downregulate GABAergic inhibition in the rat hippocampus. *Neuron* **19**:893-901.

Rozas JL, Paternain AV and Lerma J (2003) Noncanonical signaling by ionotropic kainate receptors. *Neuron* **39**:543-553.

Rubio ME and Wenthold RJ (1999) Calnexin and the immunoglobulin binding protein (BiP) coimmunoprecipitate with AMPA receptors. *J Neurochem* **73**:942-948.

Schagger H, Cramer WA and von Jagow G (1994) Analysis of molecular masses and oligomeric states of protein complexes by blue native electrophoresis and isolation of membrane protein complexes by two-dimensional native electrophoresis. *Anal Biochem* **217**:220-230.

Schiffer HH, Swanson GT and Heinemann SF (1997) Rat GluR7 and a carboxy-terminal splice variant, GluR7b, are functional kainate receptor subunits with a low sensitivity to glutamate. *Neuron* **19**:1141-1146.

Schmitz D, Mellor J and Nicoll RA (2001) Presynaptic kainate receptor mediation of frequency facilitation at hippocampal mossy fiber synapses. *Science* **291**:1972-1976.

Schoepfer R, Monyer H, Sommer B, Wisden W, Sprengel R, Kuner T, Lomeli H, Herb A, Kohler M, Burnashev N and et al. (1994) Molecular biology of glutamate receptors. *Prog Neurobiol* **42**:353-357.

Scott DB, Blanpied TA, Swanson GT, Zhang C and Ehlers MD (2001) An NMDA receptor ER retention signal regulated by phosphorylation and alternative splicing. *J. Neurosci.* **21**:3063-3072.

Shi S, Hayashi Y, Esteban JA and Malinow R (2001) Subunit-specific rules governing AMPA receptor trafficking to synapses in hippocampal pyramidal neurons. *Cell* **105**:331-343.

Sommer B, Burnashev N, Verdoorn TA, Keinanen K, Sakmann B and Seeburg PH (1992) A glutamate receptor channel with high affinity for domoate and kainate. *Embo J* **11**:1651-1656.

Standley S, Roche KW, McCallum J, Sans N and Wenthold RJ (2000) PDZ domain suppression of an ER retention signal in NMDA receptor NR1 splice variants. *Neuron* **28**:887-898.

Stern-Bach Y, Russo S, Neuman M and Rosenmund C (1998) A point mutation in the glutamate binding site blocks desensitization of AMPA receptors. *Neuron* **21**:907-918.

Storrie B, Pepperkok R and Nilsson T (2000) Breaking the COPI monopoly on Golgi recycling. *Trends Cell Biol* **10**:385-391.

Sun Y, Olson R, Horning M, Armstrong N, Mayer M and Gouaux E (2002) Mechanism of glutamate receptor desensitization. *Nature* **417**:245-253.

Swanson GT, Gereau RWt, Green T and Heinemann SF (1997) Identification of amino acid residues that control functional behavior in GluR5 and GluR6 kainate receptors. *Neuron* **19**:913-926.

Tygesen CK, Rasmussen JS, Jones SV, Hansen A, Hansen K and Andersen PH (1994) Stable expression of a functional GluR6 homomeric glutamate receptor channel in mammalian cells. *Proc Natl Acad Sci U S A* **91**:13018-13022.

Valluru L, Xu J, Zhu Y, Yan S, Contractor A and Swanson GT (2005) Ligand binding is a critical requirement for plasma membrane expression of heteromeric kainate receptors. *J. Biol. Chem.* **280**:6085-6093.

van Hemert MJ, Steensma HY and van Heusden GP (2001) 14-3-3 proteins: key regulators of cell division, signalling and apoptosis. *Bioessays* **23**:936-946.

Vandenberghe W, Nicoll RA and Bredt DS (2005) Interaction with the unfolded protein response reveals a role for stargazin in biosynthetic AMPA receptor transport. *J Neurosci* **25**:1095-1102.

Werner P, Voigt M, Keinanen K, Wisden W and Seeburg PH (1991) Cloning of a putative high-affinity kainate receptor expressed predominantly in hippocampal CA3 cells. *Nature* **351**:742-744.

Weston MC, Gertler C, Mayer ML and Rosenmund C (2006a) Interdomain interactions in AMPA and kainate receptors regulate affinity for glutamate. *J Neurosci* **26**:7650-7658.

Weston MC, Schuck P, Ghosal A, Rosenmund C and Mayer ML (2006b) Conformational restriction blocks glutamate receptor desensitization. *Nat Struct Mol Biol* **13**:1120-1127.

Yaffe MB (2002) How do 14-3-3 proteins work?-- Gatekeeper phosphorylation and the molecular anvil hypothesis. *FEBS Lett.* **513**:53-57.

Yan S, Sanders JM, Xu J, Zhu Y, Contractor A and Swanson GT (2004) A C-terminal determinant of GluR6 kainate receptor trafficking. *J. Neurosci.* **24**:679-691.

Yelshansky MV, Sobolevsky AI, Jatzke C and Wollmuth LP (2004) Block of AMPA receptor desensitization by a point mutation outside the ligand-binding domain. *J Neurosci* **24**:4728-4736.

Yuan H, Michelsen K and Schwappach B (2003) 14-3-3 dimers probe the assembly status of multimeric membrane proteins. *Curr. Biol.* **13**:638-646.

Zerangue N, Schwappach B, Jan YN and Jan LY (1999) A new ER trafficking signal regulates the subunit stoichiometry of plasma membrane K(ATP) channels. *Neuron* **22**:537-548.

Zhang Y, Nayeem N, Nanao MH and Green T (2006) Interface interactions modulating desensitization of the kainate-selective ionotropic glutamate receptor subunit GluR6. *J Neurosci* **26**:10033-10042.

Vita

Pornpun Vivithanaporn was born on April 2, 1979 at Bangkok, Thailand to Wirod and Leelawadee Vivithanaporn. She grew up in Bangkok and came to the USA on August, 2002 to begin her Ph.D. study at the University of Texas Medical Branch.

In 2006, Pornpun received the George Palmer Saunders II Memorial Scholarship.

Education

B.Sc. in Pharmaceutical Sciences (magna cum laude), May 2001
Chulalongkorn University, Bangkok, Thailand

Professional experiences

Instructor at Department of Pharmacology and Toxicology, 2001-2002, Mahidol University, Bangkok, Thailand

Research trainee at Medicinal Plant Research Institute, summer 2000, Ministry of Public Health, Nontheburee, Thailand

Publications

Vivithanaporn P, Yan S, Swanson GT (2006) Intracellular trafficking of KA2 kainate receptors mediated by interactions with coatomer protein complex I (COPI) and 14-3-3 chaperone systems. *J Biol Chem* **281**: 15475-15484.

Abstracts

Vivithanaporn P, Swanson GT (2005) Retention of KA2 kainate receptor subunits by the COPI chaperone system. Society for Neuroscience 35th annual meeting.

Vivithanaporn P, Swanson, GT (2005) Role of chaperone proteins in KA2 kainate receptor trafficking. American Society of Cell Biology 45th annual meeting.

Vivithanaporn P, Marszalec W, Swanson GT (2006) Intracellular retention of GluR6a kainate Receptors by a Point Mutation outside the Ligand-binding Domain. American Society of Cell Biology 46th annual meeting.

Vivithanaporn P, Lash LL, Marszalec W, Swanson GT (2007) Biosynthesis of GluR6a kainate receptors engages the extracellular transduction linker at multiple stages. Society for Neuroscience 37th annual meeting.

Permanent address: 641 Soi Ratchadanivet 17, Huay Khwang, Bangkok, Thailand 10320

This dissertation was typed by Pornpun Vivithanaporn.